MSc Thesis

Trajectory optimization to minimize the environmental impact of departing and arriving aircraft

AE5310: Thesis Control and Operations

L.H. van Dam

Delft University of Technology

TU Delft

MSc Thesis

Trajectory optimization to minimize the environmental impact of departing and arriving aircraft

by

L.H. van Dam

to obtain the degree of
Master of Science in Aerospace Engineering at the Delft University of Technology,
to be defended publicly on Friday November 18, 2022.

Studentnumber:	4601777
Supervisor:	Dr. J. Sun
Chair:	Prof. dr. ir. J.M. Hoekstra
Institution:	Delft University of Technology
Date:	4 November 2022

Cover Image: Aircraft Flying in the Sunset by Gerhard Gellinger

TU Delft

Preface

Dear reader,

I present my thesis titled “Trajectory optimization to minimize the environmental impact of departing and arriving aircraft”. My research entails implementing a genetic algorithm to reduce the climate and air quality costs of an aircraft’s climb and descent flight phases. I have chosen this thesis topic because it combines optimization with sustainability in the aviation industry. Additionally, it required me to use the knowledge and experience obtained during the bachelor and master courses and projects.

I sincerely hope another student or researcher is inspired to build on this research. A lot is to be explored before the optimization can be implemented in real life. One could, for instance, include the cruise phase or aircraft separation in the established optimization program. I encourage others to follow any of my recommendations such that the high-potential strategy of optimizing aircraft trajectories for an environmental objective can one day be implemented.

I have grown tremendously during the past six years at the Delft University of Technology. I vividly remember walking into the first lecture of the Faculty of Aerospace Engineering as an unknowing 17-year-old. I am glad I have developed myself extensively besides the challenging bachelor’s and master’s programs. The icing on the cake of my extracurricular activities is my full-time board year at the VSV ’Leonardo da Vinci’. I have had the privilege to connect with and learn from many inspiring people, and I got an insight into what the aerospace industry offers. Now, full of knowledge and experience, I look forward to proudly call myself a Delft Aerospace Engineer.

All of this was only possible with the presence and help of others. I want to thank my friends, family and peers generously. This thesis has challenged me in many ways, and at times, I doubted if I could finish it all in time. I am glad to be surrounded by people that support and encourage me to keep striving.

My supervisor Dr. Junzi Sun deserves a massive thank you, as well. I enjoyed our meetings full of discussions, and Junzi happily answered all my questions. I have learned a lot about programming and optimization techniques from Junzi. He shared enthusiasm about the topic, which has motivated me immensely throughout the past ten months. Also, I would like to thank Prof. dr. ir. Jacco Hoekstra for his feedback and critical questions during the milestone meetings.

Lastly, I want to thank you, the reader: enjoy reading about this exciting topic.

L.H. van Dam
Delft, 4 November 2022

Contents

List of Abbreviations

Abbreviation	Definition
ARTP	Absolute Regional Temperature Change Potential
ATC	Air Traffic Control
CCO	Continuous Climb Operations
CDA	Continuous Descent Approach
CDO	Continuous Descent Operations
CO	Carbon Monoxide
CO_2	Carbon Dioxide
CP	Control Point
CRS	Coordinate Reference System
D	Deliverable
DC	Direct Collocation
DOC	Direct Operating Cost
EASA	European Union Aviation Safety Agency
FL	Flight Level
GA	Genetic Algorithm
GWP	Global Warming Potential
GTP	Global Temperature Potential
H_2O	Water Vapor
HC	Hydrocarbon
ICAO	International Civil Aviation Organization
ICRAT	International Conference on Research in Air Traffic Management
ILS	Instrument Landing System
ISSR	Ice SuperSaturated Regions
LCC	Lambert Conformal Conic
M	Meeting
MTOW	Maximum Take-Off Weight
NO_x	Nitrogren Oxides
OCP	Optimal Control Problem
OEW	Operational Empty Weight
OPD	Optimal Profile Descent
R	Report
RF	Radiative Forcing
SA	Simulated Annealing
SID	Standard Instrument Departures
SO_x	Sulfer Oxides
STAR	Standard Arrival Route
TMA	Terminal Maneuvering Area
WGS	World Geodetic System
WHO	World Health Organization

List of Symbols

Symbol	Definition	Unit
C_e	Total emission cost	[$]
C_x	Emission cost of species x	[$]
D	Drag	[N]
$\boldsymbol{f}$	Fitness array	-
ff	Fuel flow	[kg/s]
g_0	Gravitational acceleration	[m/s^2]
j	Index	-
L_{den}	Day-evening-night weighted sound pressure level	[dB]
m	Mass	[kg]
n_{dv}	Number of design variables	-
n_{node}	Number of nodes	-
n_p	Number of individuals	-
n_{pop}	Population size	-
p	Probability	-
T	Thrust	[N]
t	Time	[s]
V_h	Horizontal velocity	[m/s]
V_{TAS}	True airspeed	[m/s]
V_v	Vertical velocity	[m/s]
x	Horizontal position along x-axis	[m]
$\vec{x}$	Solution	-
y	Horizontal position along y-axis	[m]
z	Altitude	[m]
Δ_x	Difference in variable x	-
γ	Flight path angle	[°]

List of Figures

Part I

Scientific Paper

Trajectory optimization to minimize the environmental impact of departing and arriving aircraft

L.H. van Dam
Supervisors: Dr. J. Sun and Prof. dr. ir. J.M. Hoekstra

Control and Simulation, Faculty of Aerospace Engineering,
Delft University of Technology, The Netherlands

***Abstract*—The aviation industry faces the challenge of reducing its climate effects. This paper aims to determine whether optimizing flight trajectories can reduce the environmental impact of aircraft during the climb and descent phases. It addresses the research gap in sustainable flight trajectory optimization by combining state-of-the-art research on optimization techniques with research on aviation's climate effects. A genetic algorithm is created for the climb and descent phases to minimize the impact of gaseous emissions; the objective function entails the climate and air quality costs of the emission of carbon dioxide, carbon monoxide, nitrogen oxides, sulfur oxides, and water vapor. OpenAP is used to evaluate the emissions of aircraft. The optimization includes variable mass and speed, wind, departure and arrival procedures, and airspace constraints. The optimization considers both the vertical and horizontal flight paths simultaneously. The model was tested for more than 22,000 flights in June 2018 at Amsterdam Schiphol Airport. It has been found that an average reduction in environmental costs of 8.6% and 18.6% is achievable for departing and arriving flights, respectively. The reduction depends on the aircraft type, weather conditions, and whether the aircraft departs or arrives. The open-source optimization model can be used for further research, for instance, evaluating the reduction possibilities at different locations. The research shows that the aviation industry can reduce its environmental impact considerably by optimizing departing and arriving traffic trajectories.**

I. Introduction

Researchers expect that the global number of flights will increase in the coming years [1], while simultaneously, the aviation climate effects should be reduced [2]. The aviation industry negatively affects the global climate and the health of people and wildlife; aviation affects the environment in the broadest sense [3].

The industry's environmental impact can be reduced in several ways. Teoh and Khoo [4] suggest a few: aircraft itself could be designed more sustainably; a greener form of propulsion could be used; policies and regulations could be altered, such as introducing the Emission Trading Scheme [5]; and current aircraft operations can be improved. This paper explores the latter strategy through rerouting flights.

The topic of sustainability in the aviation industry has been on the rise in recent years. The research on sustainable flight trajectory optimization follows the same trend [6]. However, gaps in the research area still need to be addressed.

One of these gaps is the optimization of climb and descent operations for environmental impact. Many studies have been conducted on optimizing flight trajectories in the terminal maneuvering area (TMA), such as a study by Ma et al. [7]. However, most focus on minimizing the number of conflicts or delays in the TMA; only a few studies optimize the trajectories for an environmental objective [6]. Besides, procedures and regulations of air traffic control (ATC) complicate the optimization of the flight trajectories in the TMA. Efforts have been made to reduce the impact of aviation during climb and descent, employing so-called continuous climb and descent operations (CCO and CDO). These operations should have a limited impact on the conflicts and sequencing problems in the TMA [8]. However, these operations do not focus primarily on minimizing environmental effects. CDOs, for instance, are focused on maintaining an idle thrust setting [9].

Aircraft emit various gasses that affect the environment. These include carbon oxides (CO_x), nitrogen oxides (NO_x), sulfur oxides (SO_x), water vapor (H_2O), hydrocarbons (HC), soot particles, and others in smaller quantities [5, 10]. The sum of these emissions results in positive radiative forcing, meaning the emissions are warming the atmosphere [11].

The emission location is one factor that affects the amount and impact of the emitted gasses [12]. The different types have varying effects throughout a flight [13]. For example, CO has an effect primarily at low altitudes, whereas contrails form at cruise altitudes. Contrails have little impact during the climb and descent phases and, thus, are not further considered in this paper [14]. Rerouting aircraft does not mitigate the negative effect of soot particles; using greener fuels can achieve this [1]. Therefore, the analysis excludes soot particles.

Another climate effect is noise production. Even though it is considered a threat to human health [15], this study excludes it. The reason is that the noise modeling for the optimization is complex and beyond the scope of this research [6].

The focus of the proposed research is the environmental impact of emissions. Hammad et al. [6] found that the minimization of gaseous emissions was the objective in 20% of the studies regarding sustainable flight trajectory optimization.

Climate metrics are employed to evaluate the impact of the emissions. Climate metrics can be purely physical, for instance, through the weight of the emitted gasses or obtaining the global temperature change potential (GTP) [6, 16]. Monetary metrics can also be used for quantifying emissions. Grobler et al. [1] determined the environmental cost of aviation by translating GTP values into a currency. This metric is chosen because it reflects emissions' social and environmental effects; the cost established by the researchers combines health, welfare, and ecology. It should be noted that considerable uncertainty is present in quantifying aircraft emissions due to a lack of

knowledge of atmospheric processes [11, 17].

There are several numerical methods to choose from concerning the trajectory optimization problem. The techniques can be divided into optimal (such as direct methods and dynamic programming) and non-optimal (such as meta-heuristics). According to Simorgh et al. [17], the choice for one of the two categories is equally divided in the climate optimal trajectory planning studies scrutinized in their review paper. The best method for the problem at hand depends on the objective, constraints, and other variables one wishes to include [17].

According to Hammad et al. [6], a direct method and a genetic algorithm (GA) are frequently used solution techniques in sustainable trajectory optimization for aircraft. A direct method often provides a more accurate solution to the problem at hand than a GA. A direct method's complexity is a drawback, leading to time-consuming and computationally heavy optimization programs. Besides, a GA is considered a global search technique [18], whereas direct methods have a chance of getting trapped in the local optimum [17]. Because of these findings and the popularity of the GA as a meta-heuristic, this study adopts this solution technique.

Several studies employ a GA: Yamashita et al. [19] create one in AirTraf 2.0 to optimize for various objectives, and Patrón and Botez [20] also employ a GA, minimizing the operating costs. Both papers optimize the cruise phase in lateral and vertical directions considering the wind. These studies, among others, are used to establish a GA for this research.

This paper aims to determine whether optimizing flight trajectories can reduce the environmental impact of aircraft during the climb and descent phases. An open-source GA is created to minimize the impact of gaseous emissions. It is desired that the model includes variable mass and speed, wind, departure and arrival procedures, and airspace constraints. The optimization is to consider both the vertical and horizontal flight paths simultaneously. The research aims to bridge the sustainable air traffic management gap by reducing the environmental footprint within the climb and descent phases.

This article has thus far presented an introduction to the research topic and provided background knowledge. The theory and methodology applicable to the research are described in section II. It is followed by section III, in which the research case study is explained. Sections IV and V present the case study results and discussion, respectively. Section VI concludes the article, and provides recommendations, as well. Finally, Appendices A, B, C, D, and E provide additional information.

II. Methodology

A. Genetic Algorithm

The genetic algorithm is based on the natural evolution process. The iterative process is visualized in Figure 1. At first, the model generates a random set (generation) of possible solutions (individuals). It then determines each individual's fitness (objective function). The model assigns individuals to be parents depending on the chosen selection method. The parents will reproduce and generate children, creating new solutions. The model randomly alters parts of some solutions (mutation) to decrease the likelihood of getting trapped in a local optimum. After that, the model evaluates new individuals' fitness and repeats the selection, crossover, mutation, and fitness evaluation process. Whenever the GA meets a stopping criterion, it terminates. [20, 21]

The individuals should be defined numerically so that the steps of the GA can be taken. This definition can be done in several ways: Yamashita et al. [21] utilize control points and basis splines to formulate solutions; Patrón and Botez [20] use a three-dimensional grid consisting of waypoints. The formulation of a solution in this paper is inspired by the latter. It implements a value-encoded genetic algorithm. An individual is defined to have a fixed number of connected nodes (n_{node}) forming a trajectory. The aircraft's position in a coordinate reference system at each node is defined in the horizontal (x and y) and vertical (z) planes. Besides, the velocity profile is defined per individual by a single value for the calibrated airspeed (V_{CAS}) and one for the Mach number (M). Figure 2 visualizes the definition. It displays the origin (node 0), two arbitrary adjacent nodes (nodes j and $j+1$), and the final node (node n_{node}).

The fitness of each solution is calculated to evaluate the solutions quantitatively. As discussed in section I, the climate

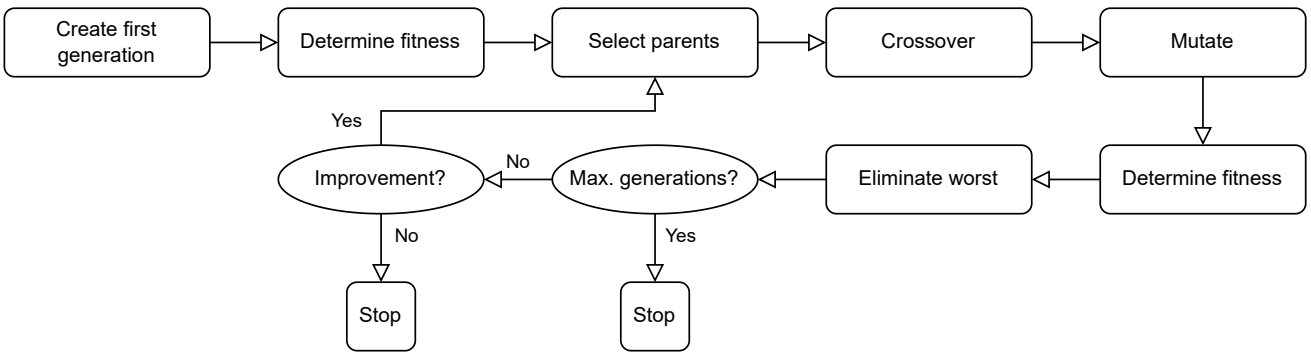

Fig. 1. Flow diagram of the created genetic algorithm. The rectangular blocks represent functions in the model. The oval blocks represent the stopping criteria.

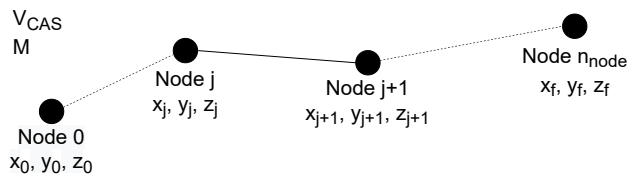

Fig. 2. Visualization of the definition of a single solution in the GA. The position (x, y, and z) is defined at each node. Additionally, a value for V_{CAS} and M is set.

metric chosen for this is the climate and air quality costs established by Grobler et al. [1]. These costs differ per flight phase because the emission's effect depends on the altitude [12]; below 3,000 ft, the "Landing and take-off" costs are used, and above that threshold, the "En route" costs are in place. Table I presents the costs. Grobler et al. [1] found different costs per region for air quality. This study uses the costs for Europe. The cost with a 3% discount rate applied by the researchers is chosen. The individual's fitness is found by summing the costs of each emission along its trajectory.

As further described in subsection II-D, the optimization includes constraints. Individuals are "punished" for violating a constraint through a penalty function. The penalties are given in percentages of the individual's fitness and differ per constraint; high-priority constraints have more considerable penalties than low-priority ones. Equation 1 provides the relation between the pseudo-fitness (f_p) and the fitness (f). In the equation, i represents the index of the individual. The pseudo-fitness is found by adding the product of the fitness and the summed penalty factors (p) to the fitness. Tables III, IV, and V overview the constraints and the penalties assigned if violated. It is discussed further in subsection II-D.

$$f_{p_i} = \left(1 + \sum (p_i)\right) \cdot f_i \tag{1}$$

The GA chooses pairs of parents for each iteration based on the roulette wheel selection method. Yamashita et al. [21] also use this methodology. Depending on the individual's pseudo-fitness, it is assigned a probability; a high-scoring individual in terms of pseudo-fitness has a higher chance of being selected for the crossover. The probability is calculated using Equation 2. The pseudo-fitness of all individuals in a generation is represented by $\boldsymbol{f_p}$, and P_i represents the individual's probability of breeding. The original formula is for a maximization problem and has been taken from an article by Blickle and Tiele [22]. The formula is rewritten to apply to a minimization problem.

$$P_i = \frac{\max(\boldsymbol{f_p}) - f_{p_i}}{\max(\boldsymbol{f_p}) - \min(\boldsymbol{f_p})} \tag{2}$$

A linear crossover has been chosen because it is effective for value-encoded GAs. Each parent pair (p_1 and p_2) produces three children (c_1, c_2, and c_3). The children's values of x, y, and z at all nodes and the values of V_{CAS} and M are found using the parents' values at the corresponding nodes according to Equation 3. These formulae are applied to each value at all nodes separately.

$$\begin{aligned} c_1 &= 0.5 \cdot p_1 + 0.5 \cdot p_2 \\ c_2 &= 1.5 \cdot p_1 - 0.5 \cdot p_2 \\ c_3 &= -0.5 \cdot p_1 + 1.5 \cdot p_2 \end{aligned} \tag{3}$$

Figure 3 visualizes the crossover of a single value; it shows the x value at node j for the parents (black dots) and the children (white dots). The children's values are found using Equation 3.

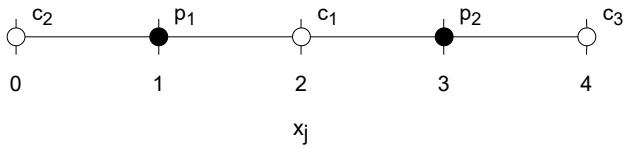

Fig. 3. Visualization of the linear crossover of a single value (x_j) of an individual's node. It shows the values of x_j of the parents (p_1 and p_2) in black and the children's (c_1, c_2, and c_3) values in white. The latter values are found using Equation 3.

Mutations occur in the production of new individuals in a GA. A mutation probability (p_m) is specified and determines the number of mutated nodes. The states at the first and final nodes are not mutated such that they adhere to the boundary constraints defined in subsection II-D. The values at the chosen nodes are mutated according to a normal distribution. Each state is assigned a specific value for the standard deviation (σ). These values are tuned for the case study described in section III. The tuning is described at the end of this subsection.

To determine which individuals enter the next generation, all parents and children, after the mutation, are evaluated on their pseudo-fitness. The best n_{ind} (number of individuals in

TABLE I. Climate, air quality and total costs of gaseous emission by aviation as found by Grobler et al. [1] for the landing and take-off (below 3,000 ft) and en route (above 3,000 ft) phases. The costs with a 3% discount rate are chosen [1]. The costs are given in monetary values per tonne of emitted gas. The air quality costs are for Europe only.

	Landing and Take-Off			En Route		
	Climate	**Air Quality**	***Total***	**Climate**	**Air Quality**	***Total***
CO_2	45	N/A	*45*	45	N/A	*45*
CO	N/A	1,100	*1,100*	N/A	270	*270*
NO_x	-590	67,000	*66,410*	-940	31,000	*30,060*
H_2O	N/A	N/A	*0*	2.8	N/A	*2.8*
SO_x	-2,600	52,000	*49,400*	-20,000	42,000	*22,000*

a generation) solutions comprise the next generation, after which the process is repeated until the maximum number of generations (250) is reached or when the fitness of the best solution is stagnated over a number of generations (20).

The settings of the genetic algorithm, such as n_{node}, n_{ind}, p_m, and σ, greatly affect the workings of the optimization. The settings presented in Table II are chosen by evaluating the results of various optimizations.

TABLE II. The values set for the various GA variables.

Variable	p_m	σ_{xy}	σ_z	σ_{CAS}	σ_M	n_{ind}	n_{node}
Value	0.1	50	10	1	0.01	100	50

Twenty flights with varying destinations, aircraft types, and routes have been chosen. Appendix A provides more information on these flights. These flights have been optimized seventeen times with varying settings for the GA. In Figure 4, the resulting mean reduction in cost, when compared to the actual flight, is plotted against the average number of constraints violated per flight. A trade-off has been made between the resulting cost reduction, violation of constraints, and computation time. Based on this, an appropriate setting for the parameters is in the lower left corner of Figure 4. The optimization with the least number of constraint violations and a relatively good score on fitness has been chosen for the case study presented in section III. Figure 4 indicates it as an orange star.

Figure 5 displays the mean cost difference in percentages between the actual and optimized trajectory against the number of generations. A spread in the form of 95% confidence is also provided. It can be seen that between 100 and 150 generations, the convergence stagnates. The exact number differs per flight and run. Thus, the maximum number of generations is set to 250.

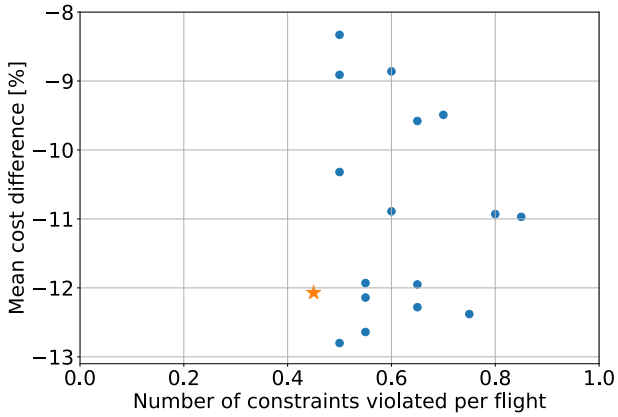

Fig. 4. The results of seventeen runs with varying parameter settings expressed in the number of constraints violated per flight and the mean reduction in cost. Each dot represents a run. The orange star represents the run with the chosen parameter setting. Table II provides the settings. The same twenty flights are considered for each run. See Appendix A for more information on the flights.

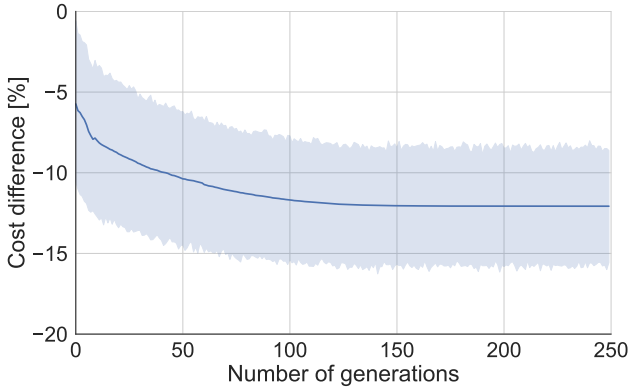

Fig. 5. The mean relative cost difference between the optimized and actual trajectory over the number of generations. The 95% confidence interval is given as a blue shade. The chosen parameter settings provided in Table II are used for the twenty flights of the tuning process. See Appendix A for more information on the flights.

B. Aircraft Model and Flight Dynamics

This study uses OpenAP for computations concerning aircraft performance. It constitutes Python packages through which, for example, it computes the aircraft's forces and fuel usage. Also, OpenAP includes aircraft data and provides information on emissions [23]. OpenAP does not comprise all emitted gasses described previously, such as hydrocarbons. Thus, the evaluation of climate and air quality costs is limited to CO_2, CO, NO_x, SO_x, and H_2O.

A point mass model with four degrees of freedom describes the dynamics of an aircraft in OpenAP [23]. The available aircraft types in the module are the most used commercial aircraft. According to Sun and Dedoussi [24, p. 8], OpenAP can be used "for around 94% of flights in European airspaces". This is assumed sufficient for this study to demonstrate how a reduction in aviation's environmental footprint in the climb and descent phases can be achieved. The model uses the default engine available in OpenAP.

Furthermore, several assumptions on flight dynamics are made. The true airspeed (V_{TAS}) is assumed to be parallel to the ground. For departing aircraft, the velocity profile consists of a constant acceleration at 0.1 m/s^2 from the initial velocity until the aircraft reaches a constant V_{CAS}. The aircraft maintains this constant velocity until it reaches crossover altitude. It then switches over to a constant M. This velocity profile is assumed because it is considered a standard operational procedure. The model calculates the thrust according to the climb phase calculations in OpenAP.

Arriving aircraft first maintain a constant M until they reach crossover altitude. Then the setting is switched to a constant V_{CAS}. The thrust is calculated using the idle descent setting in OpenAP. This setting corresponds to the CDO concept [8].

C. SID, STAR, and Restricted Airspace

Aircraft must follow set routes when leaving or approaching an airport: Standard Instrument Departures (SIDs) and Standard

Arrival Routes (STARs). The route consists of several waypoints that aircraft should fly over. Besides, ATC may impose constraints on velocity and altitude at these positions. The SIDs and STARs ensure that the ATC has an increased overview of the air traffic surrounding the airport.

In the optimization, trajectories should adhere to these procedures and constraints to keep them realistic. Aircraft should fly past the SID or STAR waypoints within a radius of 5 nm. The calibrated airspeed below flight level (FL) 100 cannot exceed 250 kts. Additionally, the altitude at the initial approach fix (IAF) – the final waypoint of a STAR – is constrained between FL70 and FL100. For departing and arriving aircraft, the trajectory can follow any route from the final waypoint to the final position. The model excludes ATC interventions, such as vectoring and holding patterns. The first generation in the GA consists of n_{ind} mutated versions of the to-be-followed SID or STAR.

Additionally, airspace can be considered a restricted area (RA) for aircraft. The model includes these areas and penalizes solutions for passing through restricted airspace. The model implements restricted airspace in the shape of beams and cylinders.

D. Constraints

Typically, a trajectory optimization problem includes three types of constraints: dynamic, boundary, and path constraints. The constraints imposed on the model are listed in Tables III, IV, and V and further explained in this subsection. The penalty factors given in the tables are based on the priority of each constraint; more considerable penalties are assigned to constraints with a higher priority.

Dynamic constraints ensure that aircraft remain within the flight envelope [13]. Dynamic constraints are imposed on the flight path angle (γ), velocity (V_{CAS}, M, and V_s, the vertical velocity), forces, acceleration, and mass. The values of the constraints depend on the selected aircraft, and OpenAP contains this information. Table III overviews the constraints. Equations 4 and 5 provide a detailed version of the total energy and force constraints. The thrust is represented by T, the drag by D, the mass by m, the gravitational acceleration by g, and the acceleration by a. These constraints are included to make sure that the aircraft can generate the necessary power for the desired climb, descent or acceleration [25].

$$\frac{T_{max} - D}{m} - \frac{g \cdot V_s}{V_{TAS}} - a > 0 \tag{4}$$

$$T - m \cdot g \cdot \sin\gamma - D < 0 \tag{5}$$

The boundary constraints specify the values of variables on the boundaries – the initial and final values. These are in place for the position and mass. The initial mass is determined to be 90% of the maximum take-off weight (MTOW) for departing aircraft and 80% of the maximum landing weight (MLW) for arriving aircraft. These values are based on empirical knowledge and applied to all aircraft used in the case study. Table IV lists the boundary constraints. MTOW and MLW can be taken from OpenAP and depend on the aircraft type.

TABLE III. Dynamic constraints imposed on the flight path. The flight type "D" describes departure aircraft, whereas "A" describes arrival aircraft. OpenAP provides the maximum operating velocity (VMO), maximum operating Mach number (MMO), and maximum value for V_s per aircraft type.

Variable	Flight Type	Lower	Upper	Penalty
V_{CAS}	D & A	0	VMO	3%
M	D & A	0	MMO	3%
$\Delta\phi$	D & A	-	90°	17%
$\Delta\gamma$	D & A	-	5°	17%
V_s	D & A	-	Max.	17%
Total Energy	D	0	-	10%
Force	A	-	0	10%

TABLE IV. Boundary constraints imposed on the flight path. The operational empty weight (OEW), MTOW, and MLW can be found in OpenAP and are aircraft-dependent.

Variable	Flight Type	Initial	Final	Penalty
m	D	0.9MTOW	>OEW	5%
m	A	0.8MLW	>OEW	5%

The evaluated flight defines the boundary conditions for the position. Section III discusses this in more detail.

The path constraints are imposed on the aircraft states between the boundary points [13]. Table V presents the path constraints. The previously described SIDs, STARs, and restricted airspace impose constraints on the optimization. Also, the model constrains the vertical position between the airport's altitude and the aircraft's ceiling altitude. The model also limits each node's heading and flight path angle change.

TABLE V. Path constraints imposed on the flight trajectory. The airport and ceiling altitude can be found in OpenAP.

Variable	Flight Type	Lower	Upper	Penalty
z	D & A	Airport	Ceiling	5%
z at IAF	A	FL70	FL100	10%
V_{CAS} <FL100	D & A	0	250kts	17%
RA	D & A	-	-	25%
SID/STAR	D & A	-	-	25%

E. Wind

The inclusion of wind in the model only directly affects the aircraft's ground speed (GS). Equation 6 gives the relation between the wind ($\vec{u}$), ground speed, and true airspeed. The wind's velocity and direction are assumed to be constant throughout a flight.

$$\vec{GS} = \vec{V_{TAS}} + \vec{u} \tag{6}$$

III. Case Study

A case study is conducted to test the model's capabilities. Through the study, it can be determined whether it can minimize the environmental impact during the climb and descent phases through trajectory optimization.

A. Location

A comparison is made between the actual route's climate and air quality costs and the optimized trajectory's costs. The case study is conducted for a single airport, Amsterdam Schiphol Airport (EHAM), for June 2018. The search space around the airport is a square with sides of 500 km with EHAM as the center. The size is chosen such that most aircraft can complete an entire descent or climb within the search space.

B. Wind and Airspace Data

Data on the wind in June 2018 at and around EHAM is taken from the ERA5 hourly reanalysis model [26]. The wind considered in the analysis is from the hour at the start of the aircraft's trajectory within the search space. As mentioned in subsection II-E, the wind is assumed constant for the entire flight.

The information on the waypoints, SIDs, STARs and restricted airspace applicable at and around EHAM is available via the aeronautical information publication (AIP)[1]. The SIDs are taken from June 2017 [27], and the STARs from March 2018 [28]. Figure 6 shows the restricted airspace included in the optimization in red. Appendix B lists the names and locations of the included restricted airspace. The study does not consider all restricted airspace indicated by the AIPSection III-B, only the ones that can affect the trajectories are considered. This is done because the computation time increases with an increasing number of objects to check.

C. Flight Data

Real flight trajectory data are required and are obtained via traffic [29] from The OpenSky Network's historical database[2]. The data for June 8, 2018, is unavailable. Therefore, the model evaluates 29 days of flights. It only considers flights that depart or arrive at EHAM. The flights with aircraft that are unavailable in OpenAP are removed. The data are also filtered for duplicates, outliers, and missing points. Aircraft that climb, cruise, and descent within the search space are filtered. Flights with too few data points ($<n_{node}$) are not considered. Table VI lists the number of flights removed from the data per filter. Of the 34,608 flights available at first, the filters eliminated 7,002, leaving 27,606 (±80%) to be evaluated and optimized.

D. Route Identification

The model could not detect the SID or STAR of 4,946 flights of the remaining flights (±18%), as presented in Table VI. Possibly, the aircraft flew a trajectory that deviated, as ordered by ATC, from the route. These flights have been omitted. Otherwise, the optimization would be a free-route optimization between the airport and the search space boundary and can thus not be fairly compared with the actual flight.

The exclusion leaves 22,660 flights over 29 days for the model to evaluate. Appendix C provides more information on the distribution of the trajectories evaluated in the case study.

[1]https://eaip.lvnl.nl/2022-09-22-AIRAC/html/index-en-GB.html. Accessed on September 30, 2022.

[2]https://opensky-network.org. Accessed on September 29, 2022.

TABLE VI. The number of flights removed from the actual flight trajectory data per filter. Also, the number of flights is given of which the SID or STAR could not be identified.

Filter	#Flights	
Unavailable Aircraft	2,403	
Duplicates, Outliers and Missing Values	789	
Climb and Descent	3,659	
Minimum Data Points	151	+
Subtotal	*7,002*	
Unidentified SID/STAR	4,946	+
Total	*11,948*	

Figure 6 shows the actual and optimized trajectories of two example flights: EZY92DK-193 arriving at EHAM and following REKKEN 2A, and; AAL221-1155 departing from EHAM and following BERGI 3V via waypoint AMGOD. Both flights were flown on June 1, 2018. The waypoints of the SID and STAR are shown as green circles with a radius of 5 nm.

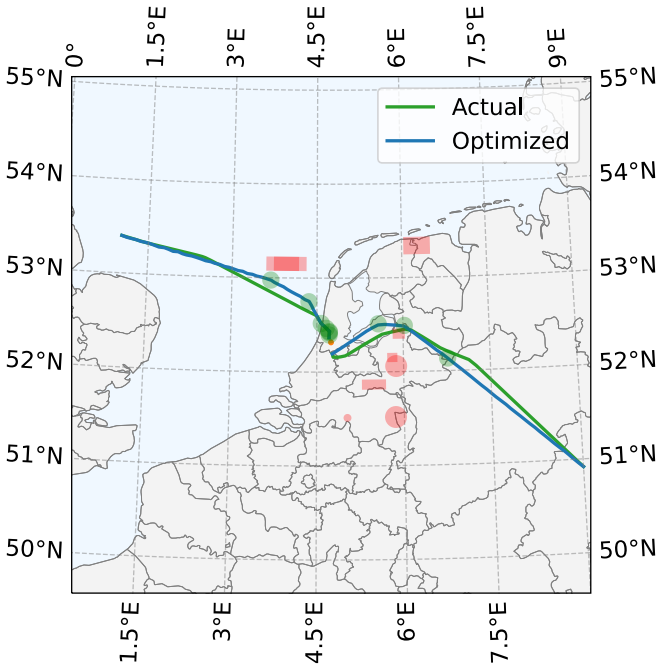

Fig. 6. The optimized and actual trajectories of two flights (AAL221-1155 and EZY92DK-193, flown on June 1. 2018) are displayed. The green circles represent the SID or STAR waypoints. The red areas represent the restricted airspace.

E. Trajectory Analysis and Optimization

For departing aircraft, the trajectory is analyzed from the first data point located 100 m above the runway to the point where the aircraft leaves the search space. This is decided to exclude the different velocity and acceleration profiles aircraft follow immediately after take-off.

For arriving aircraft, the trajectory is analyzed from the point where the aircraft enters the search space until the last data point over 1,500 ft above the runway. From this point on,

aircraft are to follow a fixed glide slope towards the runway; an optimization is not possible for this section as it would decrease the safety of operations [30].

For the actual flights, the methodology described in subsection II-A can be used to determine the cost of emissions. The model identifies which SID or STAR the aircraft followed. The initial guess for the GA is the trajectory through the waypoints defined by the SID or STAR, as explained in subsection II-C.

IV. Results

A. Air Traffic Control Interference

As discussed earlier, ATC may interfere during departure and arrival; aircraft may have to deviate from the SID or STAR they were meant to follow. To adhere to the ATC commands, pilots often level off the aircraft. While this helps limit collision risks, the level segments require an increase in thrust to keep a constant vertical position or velocity [9]. The level segments, in turn, result in aircraft using more fuel, causing an increase in emissions during climb and descent. These level-offs are also the reason why CDOs are employed [9].

The level-offs have been found in many flight trajectories analyzed. Figure 7 illustrates an example of the level segments. It shows the vertical path of the actual and optimized flight trajectories (KLM1990-802 on June 1, 2018). It can be seen that the optimized trajectory excludes level segments.

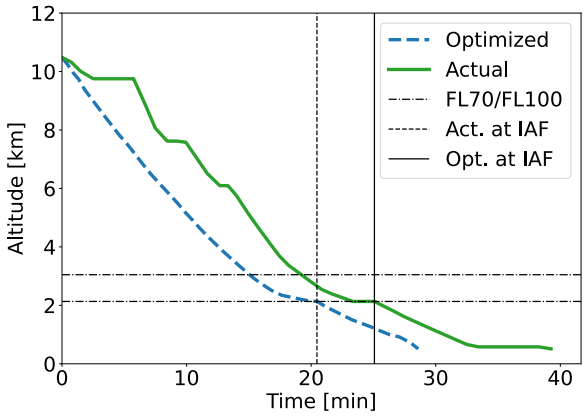

Fig. 7. The altitude profile of the actual and optimized trajectories of flight KLM1990-802 on June 1, 2018, descending to EHAM. The green line visualizes the actual flight path, showing various level-offs. The dashed blue line visualizes the optimized trajectory. The black lines indicate the moment a trajectory passes the IAF. As given in subsection II-C, an aircraft should be between FL70 and FL100 when crossing the IAF.

B. Climate and Air Quality Costs by Flight Type

The objective of the optimization is to minimize the flight's climate and air quality costs. The value found for the optimized routes is compared to those of the actual trajectories. The leftmost distribution of Figure 8 shows the difference as a percentage of the actual flight's cost. It also visualizes the resulting distance, time, and fuel relative differences to minimize the cost. All distributions have been split to visualize the difference between departure (left and blue) and arrival (right and orange) flights.

The model can reduce the climate and air quality costs on average by 8.6% and 18.6% for departing and arriving flights, respectively. The resulting mean reduction in the distance for arrival aircraft is 5.6%. For departing flights, an increase of 0.3% is found. The duration of departing aircraft is increased by 5.3% and decreased by 7.3% for arriving aircraft; departing aircraft use 3.3% less fuel, and arriving aircraft 12.9%.

Appendix D provides the distribution plots of the absolute differences of the four metrics when minimizing the climate and air quality costs. A distinction between the flight type and aircraft weight category is made.

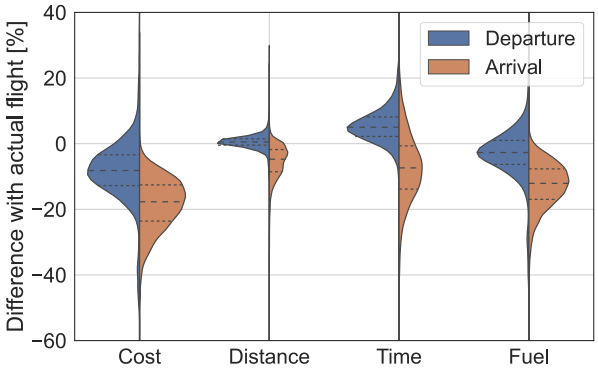

Fig. 8. Distribution plots for minimizing climate and air quality costs. The difference in percentages of the optimized trajectories compared to actual trajectories is given. The difference in other metrics, such as distance, time, and fuel usage, are also provided in percentages. A split has been made between departure and arrival flights.

C. Climate and Air Quality Costs by Weight Category

Figure 9 presents the difference in cost between the optimized and actual flight trajectories split by flight type and aircraft weight category.

Appendix E provides more information on the weight categories used. The case study data consists of 17,333 medium-weight and 5,308 heavy-weight aircraft. Appendix C provides more information on the distribution of the aircraft weight categories. Figure 9 does not present the "Light" category because only 19 flights belonged to it, which is considered unrepresentative. The A380 is the only aircraft comprising the category "Super". This aircraft is not present in the case study data.

For departing flights, the costs for medium-weight aircraft are reduced on average by 8.0% and 10.3% for heavy-weight aircraft. For arriving flights, the costs for medium-weight aircraft are reduced on average by 17.4% and 22.8% for heavy-weight aircraft.

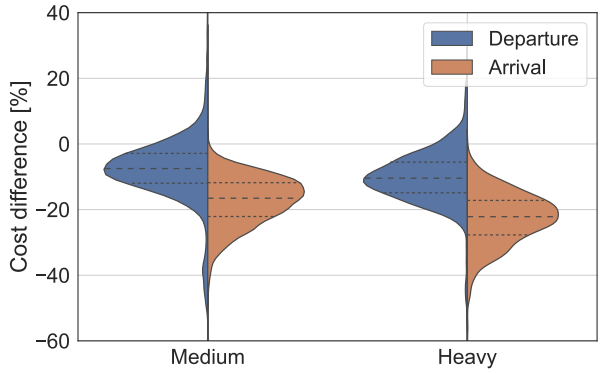

Fig. 9. Distribution plots of the relative difference in climate and air quality costs between the optimized and actual trajectories. The distributions are split for aircraft weight category and flight type.

V. Discussion

A. Verification

The model's outcome has been compared with studies that evaluate flights with similar conditions. A similar study is that of Hartjes and Visser [31]. A flight with identical position boundary conditions was set up with the same aircraft. The result was in the same order of magnitude as the most fuel-efficient flight by the researchers; the fuel usage found by the researchers came to 507.3 kg, whereas the GA came to 590.0 kg. The deviation from the optimal found by Hartjes and Visser could be due to missing information on the initial mass assumption and a different aircraft performance model used.

The case study outcome of the descent's fuel savings has also been compared to the findings of studies related to CDOs. Cao et al. [8] concluded that the average amount of fuel saved per flight is 147 kg, Dalmau [9] found a 10% reduction, and Clarke et al. [32] found 64 kg fuel saved. The established genetic algorithm in this paper achieved an average reduction in fuel usage of 136 kg, equivalent to 12.9%, for arriving flights. This reduction is in the same order of magnitude as [8] and [9]. The former researchers compare their results to other papers, as well. The 136 kg reduction is within the ballpark of those results. The large difference in the outcome of Clarke et al. [32] could be due to a smaller lateral distance in their research.

B. Effect of Minimization of Climate and Air Quality Costs

At first glance at Figure 8, one can deduce that a reduction in climate and air quality costs for both departure and arrival aircraft at EHAM is possible. A clear difference between the two flight types can be distinguished; the four metrics' relative difference between the actual and optimized flights is more considerable for arriving aircraft. For both flight types, minimizing the costs results in fuel reduction simultaneously. The fuel reduction is expected because a decrease in climate and air quality costs is related to fewer emissions related to fuel usage.

A difference is visible for the distance and time metrics. The distance covered by the actual and optimized trajectories for departing aircraft is nearly the same. However, the optimized departing flight duration is longer because the aircraft fly with a lower velocity than the actual flights.

For arrival aircraft, the distance and duration of the flight are both decreased. These findings are in line with research conducted on CDOs [33] and studies concerning the optimization of arrivals [34].

The difference between departing and arriving aircraft is assumed to be due to the difference in actual routes. ATC often applies vectoring to separate arriving aircraft and prevent conflicts. As the model does not consider these interferences in the optimization, a more significant reduction in the distance travelled is expected for arriving flights. Departing aircraft are naturally more separated; thus, the difference between the actual and optimized route's distances is lower than for arriving aircraft.

C. Effect of Aircraft Weight

Figure 9 indicates a difference between the two aircraft weight categories. In the left distribution – the medium-weight aircraft – the possible reduction in climate and air quality costs is lower than for heavy-weight aircraft. The relative difference for departure aircraft is nearly similar, whereas the room for improvement in the arrival of heavy aircraft is notably larger. The mass of an aircraft affects the fuel flow, which is related to the cost. This relation is thought to be the reason behind these differences.

D. Effect of Wind

The case study was run twice for all flights, once with and once without wind. The results of the optimization considering wind have been presented previously. If the model does not consider wind, the reduction is 0.3% smaller for departing aircraft, whereas the reduction is 0.3% larger for arriving flights. Only a slight difference is expected; the trajectory is to follow the identified SID or STAR and thus cannot deviate much from the defined route.

The reduction may be larger when a tailwind is applied to the aircraft. The reason is that the ground speed increases according to Equation 6 and, thus, the duration and total fuel usage decrease. However, for aircraft experiencing a headwind, the reverse is true. In the case study, aircraft come in from all directions and, therefore, some experience headwinds and others tailwinds, evening out the resulting cost reduction. This is another reason for the slight difference in the percentage reduction between including and excluding wind.

E. Constraint Violation

One can deduce from Figure 8 that for some trajectories, especially for departing aircraft, the costs are higher for the optimized trajectories; the relative difference is above 0%. The cost increase can be explained through the application of the

constraints. It was found that actual flights frequently violated imposed constraints. The actual trajectories often violated the constraints on the velocity below FL100, the altitude at IAF, the total energy and force, and the maximum absolute vertical velocity. The optimization model aims to violate as few constraints as possible. Therefore, the optimized route may violate fewer constraints than the actual flight but, in turn, has to fly a longer route or with another velocity and altitude profile.

Figure 6 shows an example: the actual trajectories of both flights only pass some waypoints. As the optimized route passes all waypoints, a longer route is expected, which could increase climate and air quality costs. Figure 8 displays this increase to inform the reader of the model's outcome.

The violation of constraints of the actual trajectories could be due to incorrect settings of the constraints, for instance, for the maximum vertical velocity. Concerning the velocity below FL100 and the altitude at IAF, the violation could be due to ATC commands. The ATC may order aircraft to fly faster or a more direct route when there is space to do so. The model is, however, not allowed to do this. Lastly, the total energy and force constraints violations could be related to the assumption of the mass and engine and OpenAP's thrust approximation. The initial mass assumption is considered crude. It affects the outcome of the total energy and force constraints, and this could thus be the reason for actual trajectories violating constraints.

Margins for the constraints could be specified to overcome incorrect assumptions or constraint settings. For example, a minor penalty could be assigned if the trajectory violates a constraint but is within the margin. This addition could improve the workings and reality of the GA.

F. Case Study Location

As stated in subsection III-D, the model did not identify a SID or STAR in approximately 18% of the evaluated flights. The inability to identify the route is due to a large amount of vectoring (and some holding patterns) applied at EHAM. The model did not evaluate these flights, so it found no estimate of the possible reduction of climate and air quality costs for them. The model potentially optimizes a larger portion of the flights at other airports, where ATC applies less vectoring.

Additionally, the case study excluded 3,659 flights because they included a climb and a descent phase. The model can only optimize the climb or the descent, so it does not evaluate these flights. It would be interesting to determine if reducing the climate and air quality costs are possible for these trajectories.

G. Operational Procedures

As described in subsection II-B, the specified velocity profile is an additional assumption. It was assumed to follow the current operational procedures concerning the velocity. A different outcome, and possibly a more considerable cost reduction, can be expected when the velocity is allowed to vary freely throughout the trajectory. Currently, a constant V_{CAS} and M, and also a constant a for departing aircraft, restricts the GA to a specific velocity profile for the trajectory.

Even though the aircraft follow the SIDs and STARs, the model does not consider aircraft separation; the optimization considers only a single flight. Therefore, the results may show a more optimistic reduction than possible in an actual situation. For future work, it is deemed beneficial to consider multiple aircraft in the model, ensuring that aircraft are separated.

H. Uncertainties

The absence of data on the mass of aircraft gives rise to uncertainties, as Sun and Dedoussi [24] concluded. This conclusion applies to this research as well. Additionally, the assumption of the default engine and the thrust approximation of OpenAP for idle descent can cause deviations from more accurate results [23].

The last uncertainty concerning the result is that of the climate metric used. The costs established by Grobler et al. [1] are exposed to large uncertainties. According to Simorgh et al. [17], this is because the knowledge of the processes in the atmosphere needs to be improved to quantify emitted gasses accurately. Additionally, the model does not consider several emissions, for instance, of hydrocarbons.

The effect of the assumptions and uncertainties could be evaluated using a sensitivity analysis. This could aid in the improvement of the model.

VI. Conclusion and Recommendations

This research aims to determine if reducing the climate effects of aircraft's climb and descent phases is attainable through trajectory optimization. A genetic algorithm is employed to optimize actual flight trajectories in the horizontal and vertical direction for aircraft climate and air quality costs. The optimized trajectory should follow the identified SID or STAR and adhere to additional constraints, such as velocity and altitude limits.

A case study has been conducted to test the model's capabilities and answer the research question. More than 22,000 actual aircraft trajectories arriving at and departing from Amsterdam Schiphol Airport are evaluated on their climate and air quality costs. The model optimizes each route and determines the relative difference between the costs, and other metrics, of the actual and optimized trajectories. The model can reduce the climate and air quality costs by 8.6% and 18.6% on average for departing and arriving flights. It is concluded that reducing environmental costs does not necessarily result in shorter flights in terms of time and distance. The fuel usage is reduced for most trajectories. The costs of heavy-weight aircraft trajectories can be reduced a few per cent more than those of medium-weight aircraft. The wind is shown to have a limited effect on reducing the costs because the identified SID or STAR constrains its path.

Several elements of the model may affect the possible reduction of environmental costs. These include the assumed velocity profile, the inability to evaluate flights that include both climb and descent, and the violation of constraints by actual flights. Additionally, uncertainties are present in the mass approximation, thrust calculation, and applied climate metric.

Based on the results, recommendations for future research are provided. Firstly, it would be interesting to omit the assumed velocity profile and let the velocity vary freely throughout the trajectory. One can improve the accuracy of the results by better approximating the mass of aircraft, for instance, by considering the flight length or the operating airline.

It could also be beneficial to perform a sensitivity analysis. Such an analysis could be done on the mass, the imposed constraints or the climate metric used.

The model can be more realistic by including ATC commands; the model could optimize for multiple aircraft and include conflict detection and aircraft separation. Besides, it would be interesting to evaluate if the optimization can achieve similar reductions at other airports. Comparing different regions and periods could aid in a deeper understanding of the possibility of limiting the environmental effects of aviation.

In future research, one can use the implementation of restricted airspace to redirect trajectories past areas restricted for noise purposes, among others.

The case study has demonstrated the possibility of reducing the anthropogenic effects of the aviation industry on the environment through trajectory optimization. An average reduction of 8.6% and 18.6% for the climate and air quality costs for departing and arriving flights at Amsterdam Schiphol Airport is achievable. Others can use the open-source GA to conduct further research to explore how to improve the reduction or to evaluate the possibilities at other locations[3].

References

[1] C. Grobler, P. Wolfe *et al.*, "Marginal climate and air quality costs of aviation emissions," *Environmental Research Letters*, vol. 14, no. 11, p. 114031, 11 2019.

[2] T. Ryley, S. Baumeister, and L. Coulter, "Climate change influences on aviation: A literature review," *Transport Policy*, vol. 92, pp. 55–64, 6 2020.

[3] S. Yim, G. Lee *et al.*, "Global, regional and local health impacts of civil aviation emissions," *Environmental Research Letters*, vol. 10, no. 3, p. 034001, 2 2015.

[4] L. Teoh and H. Khoo, "Green air transport system: An overview of issues, strategies and challenges," *KSCE Journal of Civil Engineering*, vol. 20, no. 3, pp. 1040–1052, 4 2016.

[5] EASA, "Updated analysis of the non-CO2 climate impacts of aviation and potential policy measures pursuant to EU Emissions Trading System Directive Article 30(4)," European Union Aviation Safety Agency, Tech. Rep. 1, 9 2020. [Online]. Available: https://www.easa.europa.eu

[6] A. Hammad, D. Rey *et al.*, "Mathematical optimization in enhancing the sustainability of aircraft trajectory: A review," *International Journal of Sustainable Transportation*, vol. 14, no. 6, pp. 413–436, 2020.

[7] J. Ma, D. Delahaye *et al.*, "Integrated optimization of terminal maneuvering area and airport," in *Sixth SESAR Innovation Days*, 11 2016, p. 8. [Online]. Available: https://www.sesarju.eu

[8] Y. Cao, L. Jin *et al.*, "Evaluation of fuel benefits depending on continuous descent approach procedures," *Air Traffic Control Quarterly*, vol. 22, no. 3, pp. 251–275, 7 2014.

[9] R. Dalmau, "Optimal trajectory management for aircraft descent operations subject to time constraints," Ph.D. dissertation, Technical University of Catalonia, 5 2019. [Online]. Available: https://www.tdx.cat

[10] G. Brasseur, M. Gupta *et al.*, "Impact of aviation on climate: FAA's Aviation Climate Change Research Initiative (ACCRI) Phase II," *Bulletin of the American Meteorological Society*, vol. 97, no. 4, pp. 561–583, 4 2016.

[11] D. Lee, D. Fahey *et al.*, "The contribution of global aviation to anthropogenic climate forcing for 2000 to 2018," *Atmospheric Environment*, vol. 244, p. 117834, 1 2021.

[3]Available via https://github.com/leannevandam/Thesis/tree/main/MyFiles.

[12] F. Quadros, M. Snellen, and I. Dedoussi, "Regional sensitivities of air quality and human health impacts to aviation emissions," *Environmental Research Letters*, vol. 15, no. 10, p. 105013, 10 2020.

[13] A. Gardi, R. Sabatini, and S. Ramasamy, "Multi-objective optimisation of aircraft flight trajectories in the ATM and avionics context," *Progress in Aerospace Sciences*, vol. 83, pp. 1–36, 5 2016.

[14] J. Fuglestvedt, K. Shine *et al.*, "Transport impacts on atmosphere and climate: Metrics," *Atmospheric Environment*, vol. 44, no. 37, pp. 4648–4677, 12 2010.

[15] *Environmental noise guidelines for the European Region*. WHO Regional office for Europe, 2018. [Online]. Available: https://www.euro.who.int

[16] M. Lund, B. Aamaas *et al.*, "Emission metrics for quantifying regional climate impacts of aviation," *Earth System Dynamics*, vol. 8, no. 3, pp. 547–563, 7 2017.

[17] A. Simorgh, M. Soler *et al.*, "A comprehensive survey on climate optimal aircraft trajectory planning," *Aerospace*, vol. 9, no. 3, p. 146, 3 2022.

[18] A. Rao, "A survey of numerical methods for optimal control," *Advances in the Astronautical Sciences*, vol. 135, p. 33, 1 2010.

[19] H. Yamashita, F. Yin *et al.*, "Newly developed aircraft routing options for air traffic simulation in the chemistry–climate model EMAC 2.53: AirTraf 2.0," *Geoscientific Model Development*, vol. 13, no. 10, pp. 4869–4890, 10 2020.

[20] R. Patrón and R. Botez, "Flight trajectory optimization through genetic algorithms for lateral and vertical integrated navigation," *Journal of Aerospace Information Systems*, vol. 12, no. 8, pp. 533–544, 8 2015.

[21] H. Yamashita, V. Grewe *et al.*, "Air traffic simulation in chemistry-climate model EMAC 2.41: AirTraf 1.0," *Geoscientific Model Development*, vol. 9, no. 9, pp. 3363–3392, 9 2016.

[22] T. Blickle and L. Thiele, "A comparison of selection schemes used in genetic algorithms," *Evolutionary Computation*, vol. 4, p. 67, 1996.

[23] J. Sun, J. Hoekstra, and J. Ellerbroek, "OpenAP: An open-source aircraft performance model for air transportation studies and simulations," *Aerospace*, vol. 7, no. 8, p. 104, 7 2020.

[24] J. Sun and I. Dedoussi, "Evaluation of aviation emissions and environmental costs in Europe using OpenSky and OpenAP," *Engineering Proceedings*, vol. 13, no. 1, p. 5, 12 2021.

[25] J. Sun, "OpenAP.top: open flight trajectory optimization for air transport and sustainability research," *Aerospace*, vol. 9, no. 7, p. 383, 7 2022.

[26] H. Hersbach, P. de Rosnay *et al.*, "Operational global reanalysis: progress, future directions and synergies with NWP," 2018, publisher: ECMWF.

[27] *Amsterdam Schiphol - Standard Departure Chart-Instrument - 22 Jun. 2017*, Air Traffic Control the Netherlands.

[28] *Amsterdam Schiphol - Standard Arrival Chart-Instrument - 29 Mar. 2018*, Air Traffic Control the Netherlands.

[29] X. Olive, "traffic, a toolbox for processing and analysing air traffic data," *Journal of Open Source Software*, vol. 4, p. 1518, 2019.

[30] M. Soler, A. Olivares *et al.*, "Framework for aircraft trajectory planning toward an efficient Air Traffic Management," *Journal of Aircraft*, vol. 49, no. 1, pp. 341–348, 1 2012.

[31] S. Hartjes and H. Visser, "Efficient trajectory parameterization for environmental optimization of departure flight paths using a genetic algorithm," *Proceedings of the Institution of Mechanical Engineers, Part G: Journal of Aerospace Engineering*, vol. 231, no. 6, pp. 1115–1123, 5 2017.

[32] J. Clarke, J. Brooks *et al.*, "Optimized profile descent arrivals at Los Angeles International Airport," *Journal of Aircraft*, vol. 50, no. 2, pp. 360–369, 3 2013.

[33] R. Dalmau and X. Prats, "How much fuel can be saved in a perfect flight?" in *Sixth International Conference on Research in Air Traffic Management*, 5 2014, p. 8. [Online]. Available: https://www.icrat.org/

[34] M. Zhang and A. Filippone, "Optimum problems in environmental emissions of aircraft arrivals," *Aerospace Science and Technology*, vol. 123, p. 107502, 4 2022.

Appendix

A. Distribution of Flights for Tuning

Figure 10 displays the distribution of flights evaluated in the tuning process described in subsection II-A. The trajectories are sorted by weight category and flight type. All trajectories were flown on June 1, 2018.

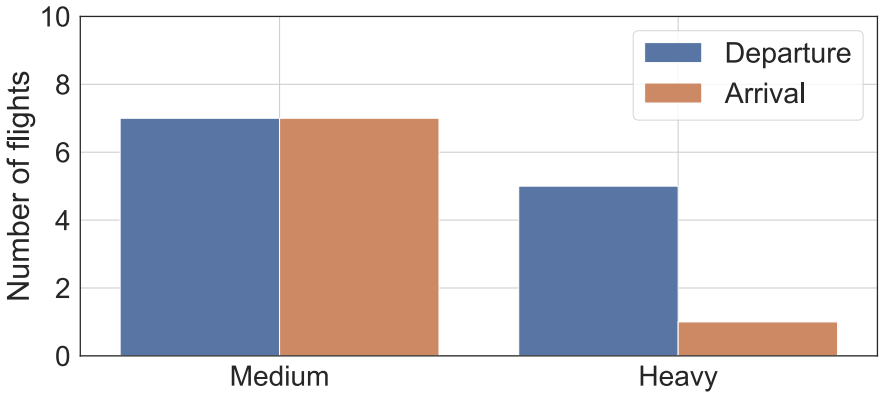

Fig. 10. A bar plot of the flights considered in the tuning of the GA. The trajectories are sorted by weight category and flight type.

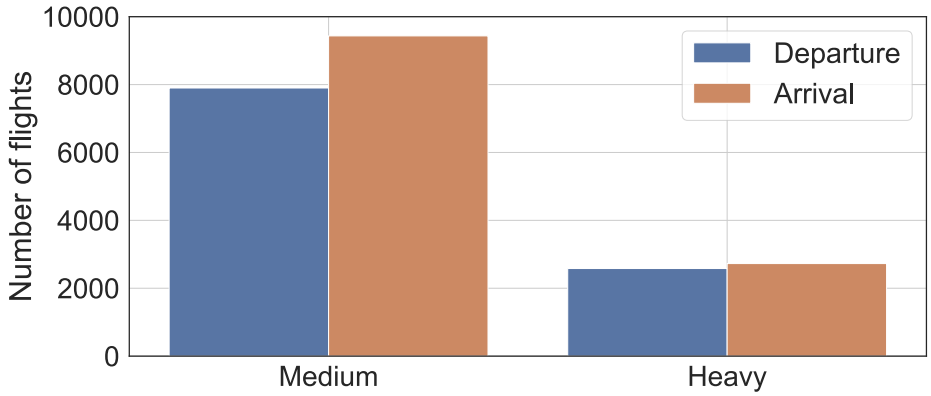

Fig. 11. A bar plot of the flights considered in the case study (after filtering and excluding unidentified SID or STAR flights). The trajectories are sorted by weight category and flight type.

B. Restricted Airspace

Tables VIII and IX provide the location and dimensions of the restricted airspace. The former table lists the areas shaped as boxes. The latter lists the areas shaped as cylinders. Figure 6 shows the restricted airspace as red areas.

C. Distribution of Flights for Case Study

Figure 11 displays the distribution of flights evaluated in the case study described in section III. The flights of which the model could not identify a SID or STAR, as described in subsection III-D, are filtered. Figure 11 excludes these flights. Also, the flights filtered as described in subsection III-C are not shown. The trajectories are sorted by weight category and flight type.

D. Results in Absolute Values

Figure 12 provides the absolute difference between the actual and optimized climate and air quality costs. Figures 13, 14, and 15 provide the absolute distance, time, and fuel difference between the actual and optimized trajectories. These are the metrics' resulting differences for minimizing the climate and air quality costs. The same conclusions can be drawn from these figures as from the relative distribution plots presented in section IV.

E. Aircraft Weight Categories

Table VII provides the aircraft weight categories specified by ICAO for wake turbulence[4].

TABLE VII. The aircraft weight categories. The category "Super" is not included. The minimum and maximum values are given in kg.

Category	Min.	Max.
Light	0	7,000
Medium	7,000	136,000
Heavy	136,000	-

[4]https://www.skybrary.aero/articles/icao-wake-turbulence-category. Accessed on October 27, 2022.

TABLE VIII. The considered restricted airspace location boundaries. These airspace are shaped like boxes. The table provides the minimum and maximum values for latitude, longitude, and altitude. MSL refers to mean sea level, and GND refers to ground.

Airspace	lat_{max}	lat_{min}	lon_{max}	lon_{min}	z_{min}	z_{max}
EHD41A, B, C	53°13′00″ N	53°05′00″ N	4°18′00″ E	3°37′00″ E	MSL	FL055
EHD41D	53°13′00″ N	53°05′00″ N	4°10′00″ E	3°45′00″ E	MSL	FL660
EHTRA72	51°54′38″ N	51°49′13″ N	5°40′44″ E	5°17′32″ E	GND	FL195
EHR3	52°27′00″ N	52°21′30″ N	6°01′00″ E	5°50′00″ E	GND	FL365
EHR2A	53°25′21″ N	53°15′17″ N	6°29′21″ E	6°02′44″ E	GND	FL195
EHR9	52°11′30″ N	52°06′40″ N	5°52′50″ E	5°44′00″ E	GND	5,900ft

TABLE IX. The considered restricted airspace location boundaries. These airspace are shaped like cylinders. The table provides the location of the circle centre, its radius, and the minimum and maximum altitude. GND refers to ground.

Airspace	lat_{centre}	lon_{centre}	r	z_{min}	z_{max}
EHTRA80	52°03′35″ N	5°52′19″ E	6.5nm	3,000ft	FL065
EHTSA1A	51°31′02″ N	5°51′20″ E	6.5nm	GND	FL195
EHTRA58	51°30′45″ N	5°01′40″ E	2nm	GND	FL245

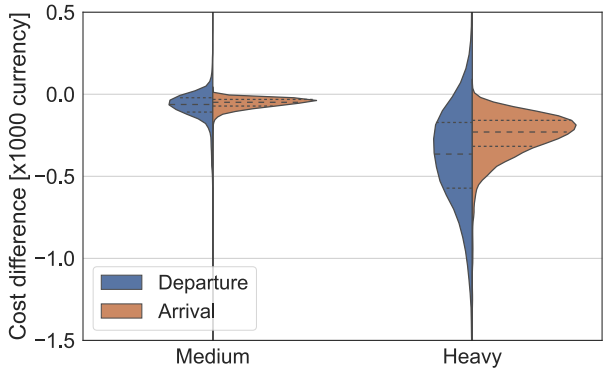

Fig. 12. Distribution plots of the absolute difference in climate and air quality costs between the optimized and actual trajectories. The differences are sorted by weight category and flight type.

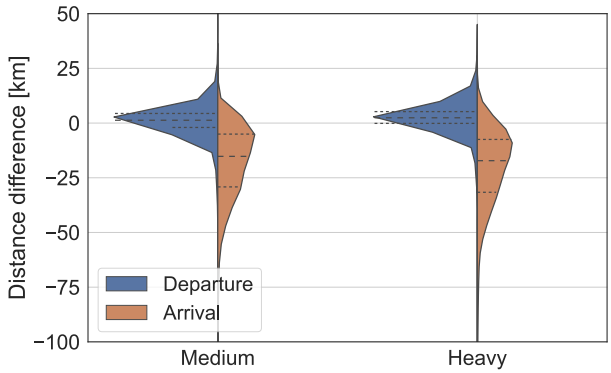

Fig. 13. Distribution plots of the absolute difference in distance between the optimized and actual trajectories. The objective was to minimize the environmental costs. The differences are sorted by weight category and flight type.

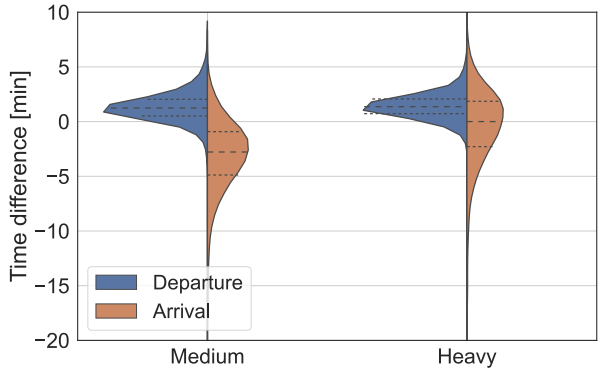

Fig. 14. Distribution plots of the absolute difference in time between the optimized and actual trajectories. The objective was to minimize the environmental costs. The differences are sorted by weight category and flight type.

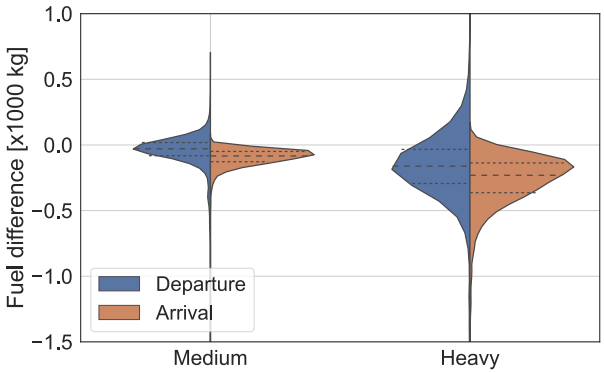

Fig. 15. Distribution plots of the absolute difference in fuel usage between the optimized and actual trajectories. The objective was to minimize the environmental costs. The differences are sorted by weight category and flight type.

Part II

Preliminary Thesis Report (Previously graded for AE4020)

Abstract

In this document, a research plan and preliminary results are provided for a master thesis. The proposed research aims to minimize the impact of aviation on climate, focusing on the climb and descent phase of the flight. There are multiple ways to achieve this. In this thesis, it is investigated whether the environmental footprint can be minimized by finding optimal flight trajectories. The climate impact in this study is defined as the emissions of aircraft, which will be quantified as a monetary metric. The optimization does not include the effect of contrails, because of the limited effect at lower altitudes, and also not the effects of noise, because of its complex nature.

The result of the thesis will be an open-source platform that allows others to optimize the flight trajectory for their needs. The method for the optimization has been chosen to be a genetic algorithm. A preliminary model has been made which aims to optimize a lateral trajectory for minimal emission costs. It is implemented in Python, and use is made of several software packages such as OpenAP. The basic model is nearly finished and will be improved first such that it can correctly find a near-optimal flight trajectory. It will then be extended to include optimization in the vertical direction, wind effects, varying velocity and mass, and regulations from ATC. These decisions have been made after a thorough literature study on sustainable aircraft trajectory optimization, which is described in more detail in this plan.

An experiment in the form of a case study will be conducted in the research. This will allow for a comparison between the current flight trajectories and the optimized ones. Through the case study, it can be determined how and by how much, the environmental footprint can be reduced by route alterations in the climb and descent phase – achieving the research objective.

1 Introduction

There is a need for the aviation industry to become less polluting. It is expected that the number of flights globally increases in the coming years [1], while simultaneously a reduction of the aviation climate effects should be achieved [2]. Not only does the aviation industry negatively affect the global climate, but the health of people and wildlife is also greatly impacted; aviation affects the environment in the broadest sense [3].

A reduction of the environmental impact of the industry can be achieved in several manners, a few are suggested by Teoh and Khoo [4]. Firstly, the aircraft itself could be designed more sustainably. For example, using a greener form of propulsion or increasing efficiency. Secondly, airlines could use the existing fleet of aircraft more effectively. Also, policies and regulations can be altered, such as introducing the Emission Trading Scheme [5]. Lastly, the routing of flights could be altered. The latter strategy will be explored in this project. In other transportation industries, this has been applied before. For example in road cargo transportation, in which a reduction of 25% could be achieved for the emission of carbon dioxide [6].

The topic of sustainability in the aviation industry has been on a rise in recent years. The research on the theory and application of sustainable flight trajectory optimization follows the same trend [7]. However, gaps in the research area remain, and several challenges have to be conquered.

One of these gaps is the optimization of the climb and descent operations for environmental impact. There are many studies conducted on the optimization of flight trajectories in the terminal maneuvering area (TMA) such as [8]. However, only in a few of these studies the trajectories are optimized for an environmental objective; most focus on minimizing the number of conflicts or delays in the TMA. Besides, the climb and descent phases of flight trajectories are subject to more procedures and regulations of air traffic control (ATC) than the cruise phase is. This complicates an optimization of the flight trajectories in the TMA. Efforts have been made to reduce the impact of aviation during climb and descent employing so-called continuous climb and descent operations (CCO and CDO). These operations should have a limited impact on the conflicts and sequencing problems in the TMA [9]. However, they focus mostly on optimizing the vertical and speed profile, and not on environmental effects. It is thought that through sustainable trajectory optimization in the TMA the environmental effects in the climb and descent phase can be further reduced.

Regarding the environmental effects related to aviation, such as the emission of CO_2 and non-CO_2 gasses, the available research is limited. For instance, the research on the effects of contrails on the environment is not far enough to implement a model of the emergence of contrails in trajectory optimization [10]. Also, there is a large uncertainty present in the quantification of the emissions of aircraft [11]. This is in part because aircraft emit the gasses in different proportions depending on position and altitude [12]. These uncertainties and the limited research on several environmental effects pose another challenge to the research; it is hard to accurately determine the environmental impact of a flight trajectory.

In this project, the goal is to determine whether the reduction of the environmental impact of aircraft during the climb and descent phase through an optimization of the flight trajectories can be achieved.

The main aim of the work is to create a program, that is accessible to others and is easily adjustable. It should be customizable to optimize flight trajectories for departures and approaches for different aircraft, locations, and conditions. If this is achieved, a wider public can be informed about the possibilities of trajectory alterations for lower environmental impact during climb and descent.

This preliminary report presents an extensive literature review, describes how the project will be completed and demonstrates the initial results of the performed optimization. First, in Chapter 2, the existing literature regarding the environmental effects of aviation, the methods for trajectory optimization, and the procedures for arrival and departure is reviewed. The gap in the research is to be identified from this, leading to the research question. This is discussed in Chapter 3 along with the objectives of the research. In Chapter 4, the research framework is provided and the planning in the form of a Gantt chart (presented in Appendix A) of the complete project is laid out. The theory applicable to the research and the methodology of the project are described in Chapter 5 and Chapter 6, respectively. This is followed by Chapter 7, in which the preliminary results and outcome are presented and discussed. The future plans for the model and the set-up of the experiment are presented in Chapter 8. The preliminary report is concluded in Chapter 9.

2

Literature Review

The proposed research in sustainable aircraft trajectory covers multiple disciplines, namely aviation environmental impact, trajectory optimization, and arrival and departure procedures for airports. It is of importance to know what the current state-of-the-art is in these fields. It should be known how and what methods are commonly used to develop a better understanding of the topic.

The literature was found through an extensive search in which multiple search engines were utilized. These include, among others, Scopus[1] and Web of Science[2]. Additionally, the proceedings from applicable conferences, like the International Conference on Research in Air Traffic Management (ICRAT)[3], have been explored. Several keywords were used in the searches in different combinations and using synonyms. These include *trajectory optimization*, *sustainable air transport*, *environmental impact*, *emission metric*, and *aviation climate effects* among others.

The available literature on the environmental effects of aviation is presented first. This is followed by Section 2.2, in which the existing literature in trajectory optimization is discussed. The state-of-the-art research on arrival and departure procedures are presented in Section 2.3. Lastly, in Section 2.4, a discussion is written on the literature concerning the proposed research project.

2.1. Environmental Effects of Aviation

It is well known that aviation negatively impacts the environment; Lee et al. [11] estimated that 5% of the worldwide radiative forcing (RF) by humans is brought about by the aviation industry. These effects are caused by, among others, the emission of gasses, the formation of contrails, and the production of noise. To determine a environment-optimal flight trajectory an understanding of those effects is required. Additionally, a metric to define the effects quantitatively is needed. Several studies explore these topics and also review articles exist, such as [5], that evaluate the available research. The state-of-the-art is presented in this section.

2.1.1. Emissions

The first environmental effect of aviation to be discussed is the emission of gasses. Aircraft emit various gasses which affect the environment. These include carbon dioxide (CO_2), carbon monoxide (CO), nitrogen oxides (NO_x), soot particles and other particulate matter, sulfur oxides (SO_x), water vapor (H_2O), hydrocarbons (HC), and others in smaller quantities [5, 13]. Not all of the emissions necessarily harm the climate. For instance, some forms of NO_x can contribute to the cooling of the environment, according to Lee et al. [11]. However, the researchers state that the sum of all emissions results in positive RF, thus warming up the atmosphere. RF is a method to quantify the impact of emitted gasses, which will be discussed more extensively at the end of this section.

[1] `https://www.scopus.com`. Accessed throughout the project.
[2] `https://www.webofscience.com`. Accessed throughout the project.
[3] `https://www.icrat.org`. Accessed on Feb. 15, 2022.

The contribution of non-CO_2 gasses to the environment by aviation should not be neglected, as Matthes et al. [14] also stipulate. Lee et al. [11] state that the contribution of non-CO_2 gasses to RF is two-thirds of the total amount. However, this distribution does not always hold. As mentioned by Lund et al. [15], this is because it depends on what timescale the effects are measured. For example, as stated in the article, the emission of CO_2 has a larger contribution in the longer timescales (in the order of decades). Whereas the contribution of CO_2 to the warming of the climate is considerably smaller in the short term [16].

The timescale on which the emissions are calculated is not the only variable that affects the amount of emitted gasses. The position and altitude at which the gasses are emitted also affect the impact [12]. In Figure 2.1 the impact of the types of environmental effects for each flight phase is visualized. It can be seen that not all emissions have an effect throughout the complete flight [17].

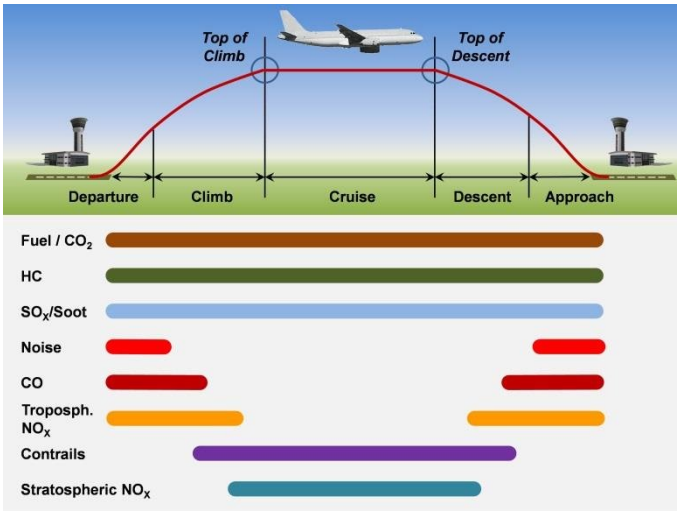

Figure 2.1: Emitted species by aircraft per flight phase. The image is taken from [17, p. 5].

Matthes et al. [14] determined that flying at a lower altitude results in a reduction of the total positive RF, even though the emissions of CO_2 are slightly increased. Lund et al. [15] concluded that there is a difference in temperature change at different latitude bands due to aviation emissions. The authors determined that the difference in global warming potential (GWP) and global temperature change potential (GTP) at the different latitude bands can be factor two. The GWP and GTP are both metrics to quantify the effect, and will be discussed below. It should be noted that in [12, 14, 15] the formation of contrails is included. This brings uncertainty to the exact dependency of position and altitude on emissions. The research on the effect of contrails is discussed in the following subsection.

Uncertainties also arise in calculating the environmental impact of flights due to the limited understanding in climate science according to Simorgh et al. [18]. The authors state that the knowledge on the processes in the atmosphere are insufficient to accurately quantify emitted gasses. Lee et al. [11] also touch upon this. They discuss the lack of knowledge on knowing which substance contributes what amount due to the unknown exact evolution of species. This is related to the (unknown) differences of emissions among different timescales [11].

Additionally, the absence of data on the mass of aircraft, according to Sun and Dedoussi [19], gives rise to uncertainties. As they discuss, the performance of an aircraft, and thereby the amount of emitted gasses, depends on the mass of the aircraft. Information on the mass of the aircraft is often kept to air operators themselves [19]. It is not mandatory to inform ATC how much the aircraft weights. This all results in uncertainties in determining the amount of emitted gasses of a flight.

The gaseous emissions do not only affect the atmospheric temperature, the health of humans and wildlife is also affected. Yim et al. [3] estimate that approximately 16,000 premature deaths occur annually due to the emitted gasses by aviation. The researchers state that a quarter is caused by emissions of aircraft during the climb and descent phases. The population in proximity to airports experiences an increased risk of lung and heart disease [20]. The share of health effects in climb and

descent phases is even larger in Europe and North America because of the high density of high-volume airports in these regions [3].

2.1.2. Contrails

The second environmental effect is condensation trails, better known as contrails. Contrails are not directly emitted by aircraft; the clouds are formed behind an airplane using the emitted gasses when flying in ice supersaturated regions (ISSR) [21]. The effect of contrails is, as for the emission of gasses, dependent on the location and altitude of emergence; contrails do not have the same environmental impact at each position. According to Fuglestvedt et al. [10], 98% of the contribution of contrails to the total RF is caused by contrails formed at an altitude between 8 and 12 km. This is supported in the report [5] by European Union Aviation Safety Agency (EASA). Fuglestvedt et al. [10, p. 4666] also state that "most of this [contribution] is within the latitude band 30° N to 90° N".

Lee et al. [11] note that it is hard to quantify the impact of contrails. The researchers mention that this is because it is not always known whether the contrail has a positive or negative effect. It depends on whether it is day or night and what the life cycle of the contrail is. However, it is estimated in the research by Lee et al. that they have a net, large positive RF; overall, contrails warm up the atmosphere.

2.1.3. Noise

The last environmental effect discussed in this plan is noise. Noise is considered to be a threat to the health of humans. Numerous studies have been performed in which the relationship between health implications and aircraft noise has been determined. According to the World Health Organization (WHO) [22], environmental noise can not only affect the hearing abilities of people but also more severe effects can occur due to long-term exposure. One of these is heart disease, as discussed by Sparrow et al. [23]. The latter study also concludes that the cognitive abilities of children who are subject to noise from aviation are lower, as well as their performance on standardized examinations. Additionally, the study discusses the negative effect on the sleep of people as a decrease in the quality of sleep can have negative effects on their health. These findings are supported by the research of Stansfeld and Clark [24]. It is estimated that in Europe 1.2 million people are subject to increased noise levels at night due to aviation [22].

2.1.4. Quantifying Environmental Effects

The impact of the discussed effects should be quantified to compute an environment-optimal flight trajectory. This is where climate or emission metrics come into play. Grewe and Dahlmann [25, p. 373] define climate metrics as "calculation rules, used to translate emissions in terms of kg per year to an impact parameter on a common scale which is relevant to climate change". They also emphasize that the choice of the metric should be made carefully. The reason being that there is a wide variety of climate metrics to be used. Each covers a different emission scenario over another time scale for different climate indices.

One of the easiest ways to express the environmental impact is the mass of the emitted gasses. Another method, described in previous subsections, is RF. It expresses the effect on the environment as change due to each species in radiation [11]. However, both metrics do not immediately show the effect of each species on the climate [25]. This can be achieved with GWP. It entails the total change in radiation values over a certain time interval. GWP can be found by determining the RF over a specified time interval. GWP100, the GWP for a time horizon of a hundred years, is a metric that is used often in literature [5]. Closely related to the GWP is the GTP. The GTP translates the RF values to a change in temperature, directly conveying an effect on the environment [25]. Both GTP and GWP can be expressed as an absolute value or relative to CO_2 (a CO_2 equivalent metric) [18]. Whereas GTP and GWP indicate the climate effects globally, other metrics focus on regional effects, such as the absolute regional temperature change potential (ARTP) [15].

These metrics are purely physical. Monetary metrics can also be used for the quantification of emissions. Grobler et al. [1] determined the cost of aviation by translating GTP values to US dollars. The total cost of aviation emissions by the researchers combines multiple facets, namely health, welfare, and ecology. The monetary metric of [1] displays both the social and environmental effect of emissions and/or contrails. Whereas the discussed metrics in the previous paragraph only represent the environ-

mental effect. The optimization study of Tian et al. [26] uses the green direct operating cost, which adds an environmental cost component to the direct operating cost (DOC). The environmental cost is determined using the cost index of each species.

The effect of noise is not considered in the previously discussed metrics. According to the noise guidelines of the WHO [22], the widely used metrics to quantify noise pollution are L_{den} (day-evening-night-weighted sound pressure level) and L_{night} (equivalent continuous sound pressure level at night). However, the WHO reports that these metrics may not apply to aviation. This is because health implications caused by aircraft noise are often related to the number of events and not to an average noise level over a period of time. This is in line with the article by Sparrow et al. [23]. The authors stress the necessity of finding a more adequate metric for aircraft noise. They also state that the noise metrics can be monetary, but that this is currently not developed sufficiently to be used.

Each of the discussed metrics suffers from large uncertainties due to limited available knowledge of several effects on different timescales as discussed in Section 2.1.1. The EASA [5] states, regarding the monetary metrics, that there is no agreement in the literature on which costs is the best for the quantification of the environmental impact. This is also true for the physical metrics; a study on which metric is optimal for the quantification of the emissions has not been conducted to the author's best knowledge. However, Matthes et al. [16] studied the robustness of their flight trajectory optimization. They found that for all the metrics used the impact on the environment of the optimal solution was indeed reduced. Nonetheless, the different metrics resulted in a different reduction in percentages.

2.1.5. Mitigating Environmental Effects

There are ways to mitigate the effect of the emissions. As mentioned in Chapter 1, altering routes is one of those strategies. This is in part because the position of emitted gasses affects the impact they have on the environment [12]. For instance, concerning contrails, the consensus on the reduction of its formation is to avoid ISSRs [5] or to lower the cruise altitude [18]. Additionally, the velocity profile and vertical and/or lateral path can be adjusted to achieve the mitigation of other aviation pollutants [18].

The alteration of routes to reduce the amount of emitted gasses is not necessarily shortening the route or minimizing the use of fuel [27]. As mentioned by Simorgh et al. [18], several studies exist that demonstrate that to achieve a reduction in contrails and/or emissions a slight increase in fuel usage and time is required.

Not all emissions can be reduced through finding a climate-optimal flight trajectory. The emission of soot particles cannot be directly reduced by flying alternative routes; soot's impact on the climate can be mitigated through the use of greener fuels [1].

The effect of noise mitigation strategies to overcome the negative effects has been studied by the WHO. One strategy is to limit the noise produced by aircraft [23]. This is in line with the mitigation of soot. Other strategies are more relevant to this research, such as the alteration of the ground path of flights to regions where fewer people are affected. Also, adjustments can be made to the vertical profile of flights [22]. These so-called CCOs and CDOs are discussed in Section 2.3. It can be hard to implement these strategies in flight trajectory optimization, because the weather can affect the propagation of noise. This makes noise levels difficult to model accurately, and therefore, many researchers assume a static atmosphere in which noise does not propagate [7].

2.2. Methods for Trajectory Optimization

In this section, the methods available for trajectory optimization are discussed. There is a wide variety of formulations, objective functions, and solution methods used in the literature. Additionally, the optimization problem requires the definition of constraints and variables.

To the author's best knowledge, only two survey articles exist that critically review the literature on sustainable aircraft trajectory optimization. Hammad et al. [7] review the available literature published between 2000 and 2016, and the article of Simorgh et al. [18] also includes the literature up to and including 2021. Using these references, and other literature, the most common and applicable options used in the existing research are presented below.

2.2.1. Objective Function

To perform optimization, an objective function should be defined to quantify what the optimal solution is. Hammad et al. [7] discuss that there are many objective functions chosen for sustainable aircraft trajectory optimization. As is explained by Hammad et al., these can be environmentally focused, such as the GTP or monetary metrics for emissions, but can also be economic or social. Economic objective functions can for example be the cost of fuel usage (as in [28]) or the DOC (as in [29]). Social objective functions focus on the impact on affected people. For example, the sound exposure level is social. It is part of the objective function in [30].

According to Hammad et al. [7], one-third of the environmental objectives in the reviewed studies include noise, which can be categorized both as environmental and social. Optimizing aircraft trajectories for noise is especially done in the vicinity of airports [31]; the departure and arrival phases of flights affect more people than the cruise phase, as the latter is often over non-populated areas. When noise is implemented in a trajectory optimization, use is often made of the Aviation Environmental Design Tool [7]. However, it can be difficult to use a noise metric as an objective function. This is because noise propagation is highly affected by atmospheric conditions, and therefore hard to model [7]. Besides, the metrics for noise are not adequate for aviation as discussed before [23].

Optimization problems can be solved for a single objective, but also for multiple simultaneously. According to Corlu et al. [6], more and more research in transportation optimization includes multi-objective functions. The multiple factors of the objective function could be combined into a single objective, or use could be made of weights for each factor. With the latter method, a Pareto curve could be utilized to evaluate the choice of weights [6]. The Pareto curve can be created for two or more objectives combined into one objective function. This, however, creates the challenge of determining what the desired weight distribution is. The combination of multiple objectives is for instance done by Visser and Hartjes [30]. The researchers find the most optimal route to minimize the weighted combination of noise levels, emissions, and DOC.

2.2.2. Problem Formulation and Solution Methods

For sustainable trajectory optimization, Rao [32] states that numerical methods are required to find an optimal solution due to the complexity of the problems. There are several options to choose from concerning the formulation of the trajectory optimization problem. Which method is best for the problem at hand depends on the objective, constraints, and other variables one wishes to include [18]. Additionally, it depends on the time available for the implementation of the method [32].

In Figure 2.2, the existent methods for finding an optimal trajectory are sorted in categories [17]. The trajectory optimization can be formulated as an optimal control problem (OCP) or using alternative formulations. In Figure 2.3, the techniques in the category ”alternative formulations” in Figure 2.2 are given. These techniques are non-optimal; the solutions approach the optimal value. Simorgh et al. [18] identified that the optimization problem is formulated as an OCP in approximately half of the studies included in the research. The remaining studies opt for a non-optimal approach.

The solution methods found in the literature for OCP include dynamic programming, indirect methods (e.g. indirect shooting and gradient-based methods), and direct methods (e.g. direct collocation (DC) and direct multiple shooting). The direct method is chosen in the majority of the studies formulating the problem as an OCP [7, 18]. This is because, the indirect methods require more complex expressions to be solved, and are inefficient when nonlinear constraints are imposed [18]. According to Hammad et al. [7], DC is the most efficient solution method when formulating the sustainable trajectory problem as an OCP.

An alternative to solving the problem as an OCP, is employing meta-heuristics. According to Simorgh et al. [18], meta-heuristics are used in 30% of the studies using non-optimal control. As mentioned in [6], for meta-heuristics, the most utilized solution methods are genetic algorithms (GA) and simulated annealing (SA). Other methods exist for solving optimization problems using meta-heuristics, such as particle swarm optimization [32]. However, these methods are not used in any of the sustainable trajectory optimization studies included in [7], and thus not further explored.

In the review by Hammad et al. [7], the GA method is used in 23% of all included studies. A GA is based on the theory of evolution; populations of solutions are created by mutating the individuals and

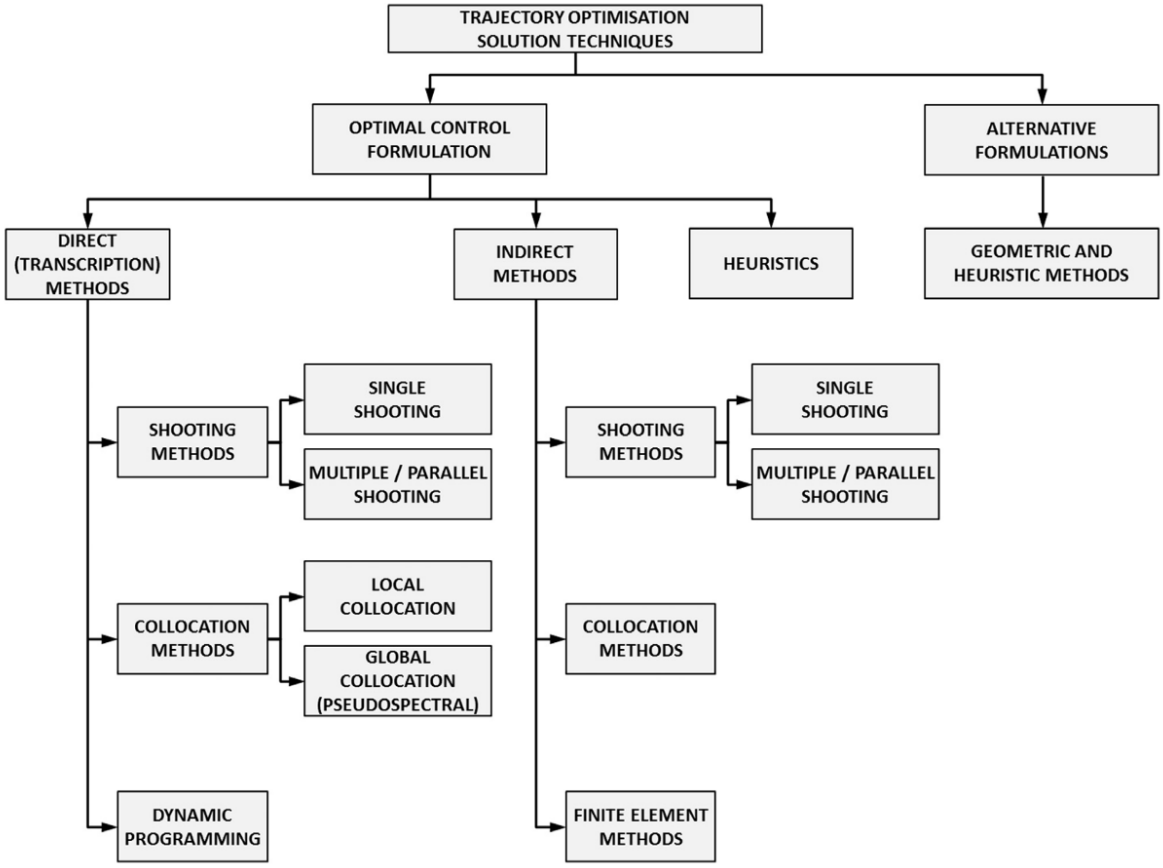

Figure 2.2: Tree displaying the solution techniques used for trajectory optimization. The image is taken from [17, p. 11].

letting the best (in GA terminology: fittest) solution survive, eventually finding a near-optimal solution [32]. For instance, Yamashita et al [28] employ a GA in AirTraf 2.0 and Patrón and Botez [29] do so as well. The remaining studies in [7] use SA, which is based on the physical theory of internal energy [32]. SA has been used by Zhou et al. [33] in the optimization in the TMA of the arrival and departure routes.

As mentioned earlier, the choice of method is related to the components that make up the optimization problem. There are several differences between the OCP and non-optimal methods which should be considered before choosing.

As Simorgh et al. [18] discuss, the DC method can be more time-consuming and computationally heavier. This is because GAs, in general, require fewer calculations than the DC method, as they do not have to find derivatives of functions [29]. The complexity of the DC method is one of the reasons why meta-heuristics are opted for in optimizations concerning a large number of flights [18]. The complexity of the DC method is why meta-heuristic algorithms are generally found to be more intuitive and easier to implement [18]. However, the DC method is generally more accurate than meta-heuristics are [18].

Another limitation of the OCP methodologies is the chance of getting trapped in a local optimality [18]. Whereas a GA, as well as SA, is considered to be a global search technique [32]. This is because the mathematical programming techniques are deterministic, and heuristic approaches are performed using stochastics [32]. This is the reason why Ma et al. [8] adopted the SA method; the researchers wanted to steer away from getting stuck in local optimality. In GAs, global optimality is achieved because the creation and mutation of children are stochastic [17]. Besides, the most optimal solutions are not the only ones to reproduce, lesser qualified ones also do. As Patrón and Botez [29, p. 538] state ”they bring diversity to the population”. Meta-heuristics are therefore considered to better be able find the global solution than direct methods [18].

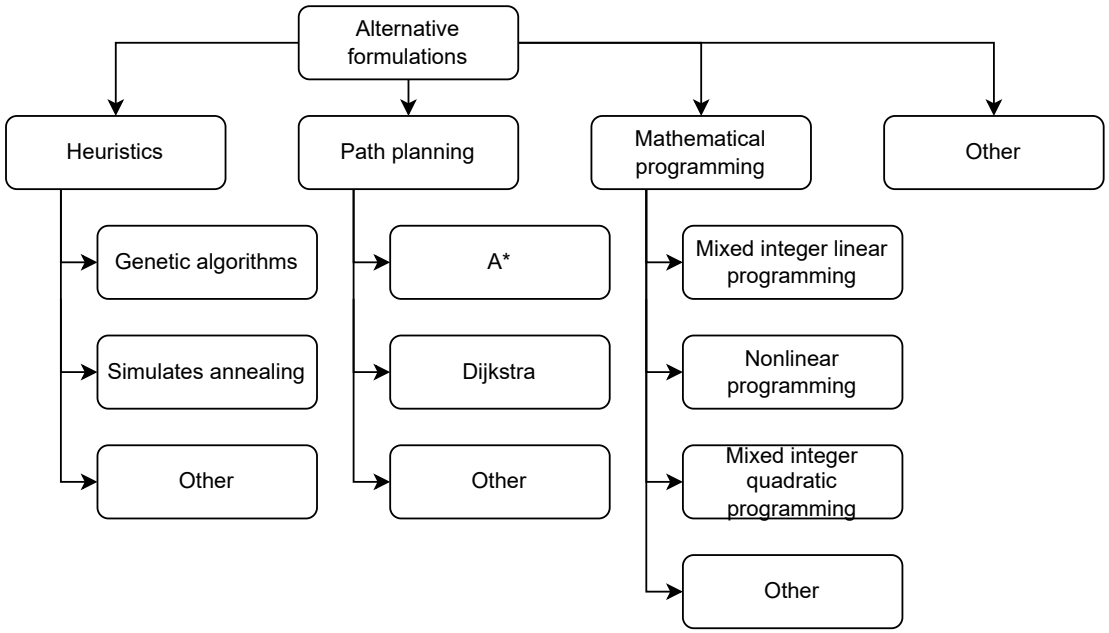

Figure 2.3: Tree displaying the non-optimal solution techniques ("alternative formulations" in Figure 2.2) used for trajectory optimization.

2.2.3. Path, Constraints, Variables, and Conditions

For the trajectory optimization problem, it should also be defined what is to be optimized. The complete flight can be optimized, or it could be optimized for just a phase. Tian et al. [26], for example, optimize the flight trajectory for the cruise phase only. This is also done by Yamashita et al. [28], Patrón and Botez [29], and Franco et al. [34]. However, according to Hammad et al. [7], more than half of the studies included in the review find a path for the descent or climb phase. For example, Dalmau [35] focuses the research on the descent phase. Others study the trajectory across multiple phases, such as Visser and Hartjes [30].

The path to be optimized can be in one, two, or all three dimensions. The optimization tool TOMATO, described by Rosenow et al. [36], optimizes a trajectory for the lateral path first, and then optimizes the vertical path. This results in a three-dimensional trajectory. In this research, the altitude of the aircraft is allowed to vary freely. Others constrain it to an (optimal) altitude or only allow step changes, as is done in [29]. The combination of lateral and vertical paths in the optimization problem will enlarge it. Therefore, its complexity is also increased. Several studies reviewed by Hammad et al. [7] opt for a three-dimensional trajectory.

Various constraints are included in the studies of flight trajectory optimization. For example, path constraints can be implemented, as is done in the study of Franco et al. [34]. Airways are defined in their optimization algorithm, which limits the solution space. This constrains the problem to a certain geographical position or region. These constraints can be imposed by ATC or are used to avoid certain regions. For example, ISSRs can be avoided to limit the environmental impact of contrails [5]. The alternative is to omit any airspace constraints, assuming free airspace. In the tool AirTraf, described in [28], this is done.

The research by Visser and Hartjes [30] allows for the inclusion of other forms of regulations imposed by ATC. The authors implement dynamic constraints on speed and altitude for certain waypoints. In the optimization of Visser and Hartjes, the aircraft's speed is allowed to vary, provided that it does not neglect the constraints of ATC. In an optimization study, the aircraft's speed can also be set to a constant value as done by Patrón and Botez [29]. Whether path constraints are implemented depends on the aim of the research. The decision of a variable or a constant speed, however, depends on which flight phase is optimized. In cruise flight, the speed can be assumed to be constant. In a climb,

however, the speed should vary to take off and climb to the desired altitude.

Another factor that can be defined as a constant or a variable is the mass of the aircraft. The optimization in [29] applies a variable mass. This is to be expected for the studies that determine optimal trajectories for the cruise phase because a large amount of fuel is used. This impacts the mass of the aircraft heavily, and thus the (environmental) performance of the flight. However, during descent, this may be less applicable because there is only a slight change in mass due to fuel consumption. The descent operations will be discussed in more detail in Section 2.3.

Besides, different assumptions of the conditions of the atmosphere, in particular, that of wind, are adopted in the literature. Making use of the wind, or at least limiting the amount of headwind, can reduce the environmental footprint of a flight. This is because a lower thrust setting can be used to reach the same ground speed compared to flying against the wind [17]. Some studies include wind in trajectory optimization. For instance, Park and Clarke [37] study the impact of wind on optimal vertical trajectories. The AirTraf model described by Yamashita et al. [28] and the optimization by Patrón and Botez [29] include wind as well. Even though the wind has an inevitable effect on the emissions and noise propagation of flights [38], a static atmosphere is often assumed [7]. Both in studies that exclude and include wind. In the latter case, data on the wind conditions are taken at a moment in time and remain fixed for the duration of the flight trajectory [34].

Many different combinations of the previously discussed variables and constraints are possible and have been studied in the available literature; the aim of the study dictates the choice of the available options.

2.3. Arrival and Departure Procedures

The procedures for arrival and departure typically employed at most airports are to ensure the maximum capacity of its facilities [39]. This is to accommodate the increased numbers of air travel. It can be achieved by tactical interventions from ATC to space and sequence departing and arriving aircraft.

The current procedures typically employed are discussed in Section 2.3.1. In Section 2.3.2, the procedures designed for fuel saving and noise abatement are discussed. The CCO and CDO concepts are discussed in this section.

2.3.1. Standard Arrival Routes and Standard Instrument Departures

Often, aircraft are to follow set routes when leaving or approaching an airport. These are so-called Standard Arrival Routes (STARs) and Standard Instrument Departures (SIDs). As Dalmau [35] discusses, these routes are designed to allow different types of aircraft, ranging in weight and size, to follow one of the available procedures.

The route consists of several waypoints that should be flown over. Also, constraints on speed and altitude are imposed at these positions. The SID/STARs ensure that the ATC has an increased overview of the air traffic surrounding the airport. As the aircraft follow the procedure, ATC may still dictate alternative routes to the pilots. These interventions include vectoring for example [39]. To adhere to the ATC commands pilots often level off the aircraft. While this is helpful to limit risks of collision, the level segments require an increase in thrust to keep a constant vertical position and/or velocity [35]. This in turn results in an increased amount of fuel to be used, causing an increase in emissions during climb and descent. Besides, the level-off leads to an increase in noise annoyance [39].

2.3.2. Fuel Saving and Noise Abatement Procedures

There are several procedures designed that aim at reducing the usage of fuel and the production of noise in the TMA. The ICAO [40] has studied noise abatement procedures in a review study and divided the procedures into three categories: ground management, spatial management, and flight procedures. The review focuses on reducing noise but is assumed to have similar effects on fuel usage and emissions.

As the International Civil Aviation Organization (ICAO) [40] stated, spatial management procedures include among others (noise) preferred arrival and departure routes and flight track dispersion. The flight procedures include among others CDO and NADP according to the study. CDO is the concept

considered to have a prominent effect on minimizing environmental impact; the implementation of CDO is said to lead to an approximate fuel saving of 10% [35]. A similar concept exists for the climb phase, namely the CCO. A reduction of the fuel usage is not the only advantage of CDOs and CCOs, the duration of the flight is also decreased [41]. This is beneficial to the airline operators, also. The principles and additional (dis)advantages of continuous operations will be further explored in this section to find opportunities to improve the thesis research.

Continuous Climb Operations
According to ICAO [42], the phase in which the aircraft ascents to the optimal altitude requires the largest flow of fuel. For jet engined aircraft, the efficiency of the fuel usage increases as it climbs [42]. It is, therefore, beneficial to climb to the optimal altitude as quickly as possible [41]. The path that should be followed during this climb to ensure a CCO is continuous.

CCO is achieved by lowering the rate of ascent with increasing altitude according to Soler et al. [43]. Dalmau and Prats [41] state that the optimal setting for thrust must be kept throughout the climb to fly at fuel-optimal velocity. The optimal thrust setting changes during the climb due to a decrease in mass. However, adjusting the setting would deviate the velocity from its fuel-optimal. Thus, as Dalmau and Prats [41, p. 6] state "the excess thrust [is used] to slowly climb the aircraft.". The continuous nature of the proposed climb operations allows for a reduction in fuel usage, emitted gasses and noise [42]. The reduction in climb rate throughout the phase also eliminates the need for a sudden transition to the cruise phase [43].

The altitude to which the aircraft should climb and at what rate it climbs optimally depends on the specifications of the aircraft. As ICAO [42, p. A-1-1] states it depends on "the aircraft type and mass as well on the meteorological conditions of the day.". This results in a large variation of optimal flight paths for aircraft in the climb phase [42]. This poses a challenge for the ATC concerning the separation of aircraft. If the ATC has to interfere and a CCO is not completed, a reduction in environmental effects can still be achieved [42]. However, as expected, the effect is of a lesser extent.

Continuous Descent Operations
As mentioned before, the interventions of ATC often require pilots to level off the aircraft at a certain altitude, adjusting the throttle setting. The CDO concept, as the name suggests, requires the aircraft to perform a continuous descent [9]. This is achieved by keeping the throttle to the idle setting from the altitude at which the descent is started until "the interception of the instrumental landing system (ILS) glide slope" [35, p. 3]. After the interception, the conventional flight path is followed because a CDO profile is too steep to be considered safe enough [43].

A descent in which a CDO is performed is shown in Figure 2.4 as the blue, continuous line. The black line illustrates a conventional descent in which the lightning bolts show the moments in which thrust is used.
As Dalmau [35] discusses in his dissertation, a CDO is not defined by no level-offs in the descent, but by remaining an idle thrust setting. The vertical profile of a CDO can show level-offs. When the thrust setting is kept to idle, the level-off will only result in a decelerating effect, according to Dalmau.

It should be noted that the term CDO is sometimes used interchangeably in the literature with continuous descent approach (CDA) and optimized profile descent (OPD) [9, 39]. However, an OPD is not the same as a CDO. It is a procedure enabling CDOs, or as Dalmau [35, p. 7] states, "[it] is a procedure, normally associated with a published STAR, designed to allow maximum practical use of CDOs".

The continuous movement in a CDO eliminates the need to adjust the throttle setting, and thus limits the use of fuel, exhaust emissions, and noise production [9]. The average amount of fuel saved per flight has been studied in various studies and ranges from 23 to 64 kg [9, 39]. The exact amount of fuel saved depends among others on the aircraft size and weight and the ATC commands given to an aircraft [9]. Another benefit of a CDO is that the aircraft can continue the cruise phase at an optimal altitude in terms of fuel usage for a longer time [35].

As with CCOs, there are several drawbacks to the employment of CDOs. Firstly, a decrease in capacity and throughput of airspace and/or airport is expected, according to Dalmau [35]. The researcher states that this is according to the variation in optimal flight paths for different aircraft; the path of a CDO depends on the type of the aircraft, its state, and the environmental conditions. This results in more

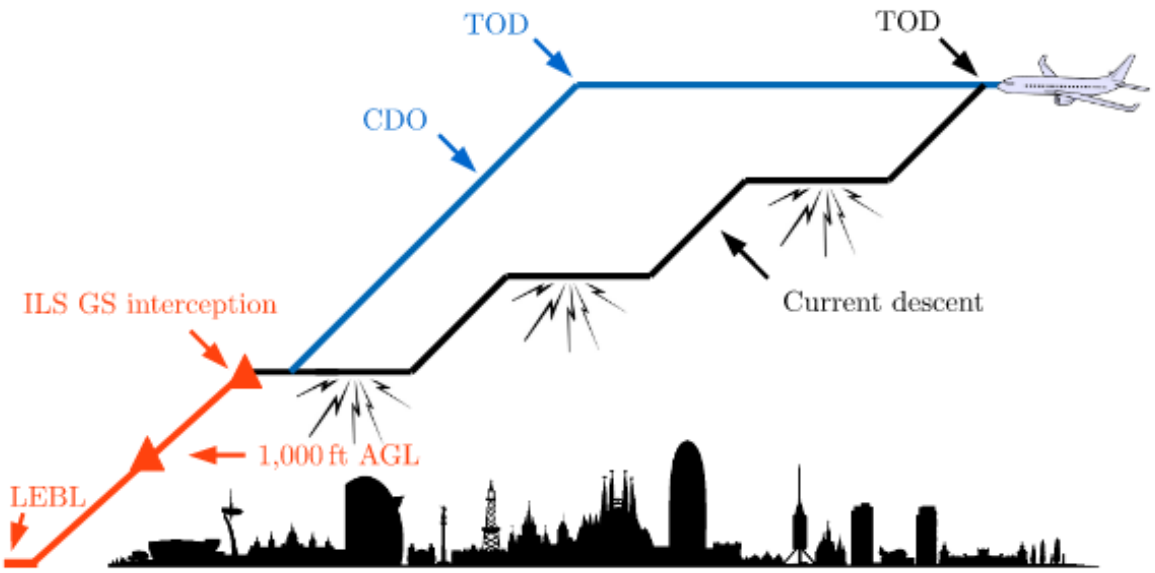

Figure 2.4: A conventional descent (black line) and a CDO (blue line) flight path are visualized. The lightning bolts represent a change in thrust setting. The image is taken from [35, p. 2].

uncertainties and a decreased predictability for the ATC [9]. The ATC may need to interfere with the optimal flight, and as it is hard to maneuver with the thrust settings at idle, the CDO most likely has to be aborted [35]. But, as Dalmau [35] mentions, a CDO, like a CCO, that is aborted already has environmental benefits.

Besides, one study by White et al. [44] showed that for a small area underneath the flight path of an aircraft an increased annoyance of noise can be expected. The CDO, however, does reduce noise levels in all other areas surrounding the aircraft, according to the study.

Another challenge is the implementation of CDOs; as stated in the ICAO review [40, p. 1]: ”procedures must be developed, tested and evaluated for benefits and ATC impacts, approved and accepted by the airport and the ANSP, and adopted by the airlines and other airport users.”. This should, however, not hold back the development of more environmentally friendly procedures.

2.4. Conclusions of Literature Review

The three research disciplines in which the literature review is conducted are brought together in this section. Firstly, the focus of the proposed research will be on the environmental impact of emissions only. Soot particles are excluded from the analysis because the negative effect can be mitigated through the use of greener fuels [1]. The formation of contrails is not included, because contrails are approximately 98% of the time formed at higher altitudes (from 8 to 12 km), thus having little impact in the climb and descent phase [10]. The reason for the exclusion of noise is that the implementation of a noise model in the optimization is beyond the scope of this project due to its complex character.

The metric for the environmental effect, which is the objective function of the optimization problem, has not been decided upon yet. Although, there is a tendency toward the monetary metric of Grobler et al. [1] because it encompasses not only the climate but also the social and health costs due to emissions. The choice of the metric is not critical to the proposed research, because a change in the objective function should not require much time or energy.

Because of the popularity of the GA as a meta-heuristics approach and because of its intuitiveness, this solution technique is to be adopted. There is enough available literature to develop a sufficient understanding to complete the project. For example, Gardi et al. [17] present the theory of multi-objective trajectory optimization along with methods to implement different objectives, variables, and conditions. The chosen method is explained in more detail in Chapter 5.

The research focuses on the climb and descent phases of the flight. Thus, the vertical and horizontal flight paths of aircraft are to be optimized because both vary greatly during the phases. It is recognized

that the amount of emitted gasses in the cruise phase of flights is considerably larger than during climb and descent phases. However, there remains an opportunity for the reduction of emissions in the latter phases, which should be explored.

The SIDs and STARs discussed in Section 2.3 are implemented in the research as well. To keep the study realistic, the procedures are to be followed and constraints should be met. ATC interventions to prevent conflicts for instance are not included in the model. The flight path is not optimized to be a CCO/CDO. However, the resulting vertical flight profile and course of the thrust setting of the optimization should closely represent a CCO/CDO. This is expected because they are procedures that reduce the environmental impact of the climb and descent of aircraft. If the flight path represents a CCO/CDO, an additional benefit of the study is that the noise is indirectly limited as well.

The state-of-the-art research on optimization techniques for flight trajectories is combined with the research on the climate effects of aviation to optimize flights for minimal environmental impact. An aircraft trajectory optimization will be performed for the climb and descent phases to minimize the impact of gaseous emissions through a genetic algorithm including a variable mass, variable speed, wind, and airspace constraints. To the author's best knowledge, a study with these conditions has not been conducted previously. The research will bridge the research gap in the field of sustainable air traffic management on environmental footprint within the climb and descent phases.

3

Research Question and Objectives

In this section, the research question is stated first. It can be found in Section 3.1, in which the sub-questions are included, as well. This is followed by a section on the objectives of the research.

3.1. Research (Sub-)Question(s)

The importance of reducing the anthropogenic climate effects of the aviation industry is recognized by many. It is necessary to limit the negative consequences on the environment and health of living beings. It has been identified in the previous chapter, however, that there is limited research conducted on the reduction of environmental impact of flights in the climb and descent phase through trajectory optimization. Therefore, the research question that will be answered in the proposed thesis project is:

> How can flight trajectories be optimized to minimize the environmental impact of aviation during the climb and descent phase?

The research question is constituted of three main elements: environmental impact, flight trajectory, and optimization. These should be further researched to formulate an answer to the research question. To facilitate this, sub-questions have been formed for each element. These should be answered first, as the answers to the sub-questions form the answer to the main question. The sub-questions can be found in the list below.

1. Environmental impact:
   (a) What environmental effects of aviation should be considered in the research?
   (b) What is an adequate metric to quantify the environmental impact of aviation?
   (c) How can the metric be used as an objective function?
2. Flight trajectory:
   (a) In which dimension(s) should the flight trajectory be optimized?
   (b) How can wind be implemented in the optimization model?
   (c) How can variable speed be implemented in the optimization model?
   (d) How can variable mass be implemented in the optimization model be achieved?
   (e) How can the regulations of ATC be implemented in the optimization model?
3. Optimization:
   (a) How should the flight trajectory optimization problem be formulated?
   (b) Which solution method should be used for the optimization?
   (c) Which aerodynamic model should be used for the flight dynamics of the aircraft?
   (d) How can the optimization method and model be verified?
   (e) How can the optimization method and model be validated?

3.2. Research Objectives

The aim of the project reflects the current challenge to limit the environmental impacts induced by humans, specifically the impacts of aviation. There are different strategies to limit the impact of aviation on the environment. Trajectory optimization could potentially be adopted in a shorter amount of time than for instance implementing newly designed, more sustainable aircraft [18]. Additionally, as mentioned by Hammad et al. [7], the number of studies on the topic has increased in the last years. Thus, the objective of the thesis project is described in the following sentence.

> To investigate the reduction of the environmental impact of aircraft during the climb and descent phases by means of optimizing the flight trajectory for an environmental, multi-objective function.

Several other objectives should be accomplished to achieve the main objective of the project. This includes an appropriate quantification of the environmental impact of aviation during the climb and descent phases. This can be achieved by identifying the critical environmental effects of aviation and choosing an appropriate metric. Besides, the creation of useful results for different settings and variables in the model should be realized. Such that the effect of different factors on the reduction of environmental impact can be determined. This can be achieved by creating an easily customizable optimization model. Lastly, this model should be available on an open platform that can be accessed by interested parties. When all objectives are met, the research on sustainable flight trajectory optimization is elevated.

4

Research Approach

This chapter is devoted to the research framework and planning. In Section 4.1, the steps to be taken in the project are described and visualized. A schedule for these tasks is also made, a brief explanation of this is given in Section 4.2. The schedule in the form of a Gantt chart is presented in Appendix A.

4.1. Research Framework

The research project is divided into four phases: the literature study, model development, experiment, and documentation and wrap-up. Each phase is composed of different tasks which are connected. The research framework is visualized in Figure 4.1.

The first phase of the project is the literature study. This entails completing the associated courses, searching for literature, reviewing the studies, and determining the research question and objective. Also, it is determined which environmental metrics and optimization methods can be used. These tasks have been completed concurrently, as reviewing literature lead to the search for more applicable literature, which resulted in several iterations. Also, the courses have been completed concurrently, as they were a guide to the literature study process.

During the second phase, the models will be developed. Two different methods will be used to optimize the flight trajectories, thus two models will be created and verified. This has started in the second half of the literature phase. This way, the gathered knowledge on the problem at hand could be immediately applied and tested. First, a dummy model has been generated which forms the basis. This model will be extended after this report is finished to include wind and variable speed. This phase includes iterations, as the development of models is prone to mistakes, and requires debugging.

The third phase, focusing on the experiment and the results, will start near the end of the development phase when the models are verified and validated. A case study will be conducted. A sensitivity analysis may also be executed in this phase. Before the results can be gathered, the case should be well defined, and data should be gathered and prepared. This phase includes the analysis of the results, as well.

The fourth phase of the project is its wrap-up and documentation. This phase runs throughout the whole project and is to be completed in parallel to the other phases. Writing throughout the process ensures that delays due to documenting are kept to a minimum. The phase includes tasks such as documenting and reporting, preparing for meetings and presentations, and implementing feedback from others.

4.2. Project Planning

To achieve the objective and answer the research question in the available time of nine months, a schedule has been created. It is in the form of a Gantt chart and is presented in Appendix A. The several phases discussed in the previous section are represented by different colors in the Gantt chart. The literature phase and the months leading up to this report are not included as these have been completed. The red lines around dates visualize the deadlines of the project plan, preliminary study, and thesis. The deadlines of the Control & Simulation department (preliminary report/meeting) have been included instead of the general milestones (literature study report and mid-term report/meeting).

Three letters can be found in the planning: ‘D’ represents a deliverable, ‘M’ a meeting, and ‘R’ a report. The week numbers on the top rows indicate the week of the thesis project. The holidays are indicated as ’Holiday’ in the same row and do not count towards the number of weeks. The literature study phase has been completed and the model development phase is half completed, as can be seen in the Gannt chart.

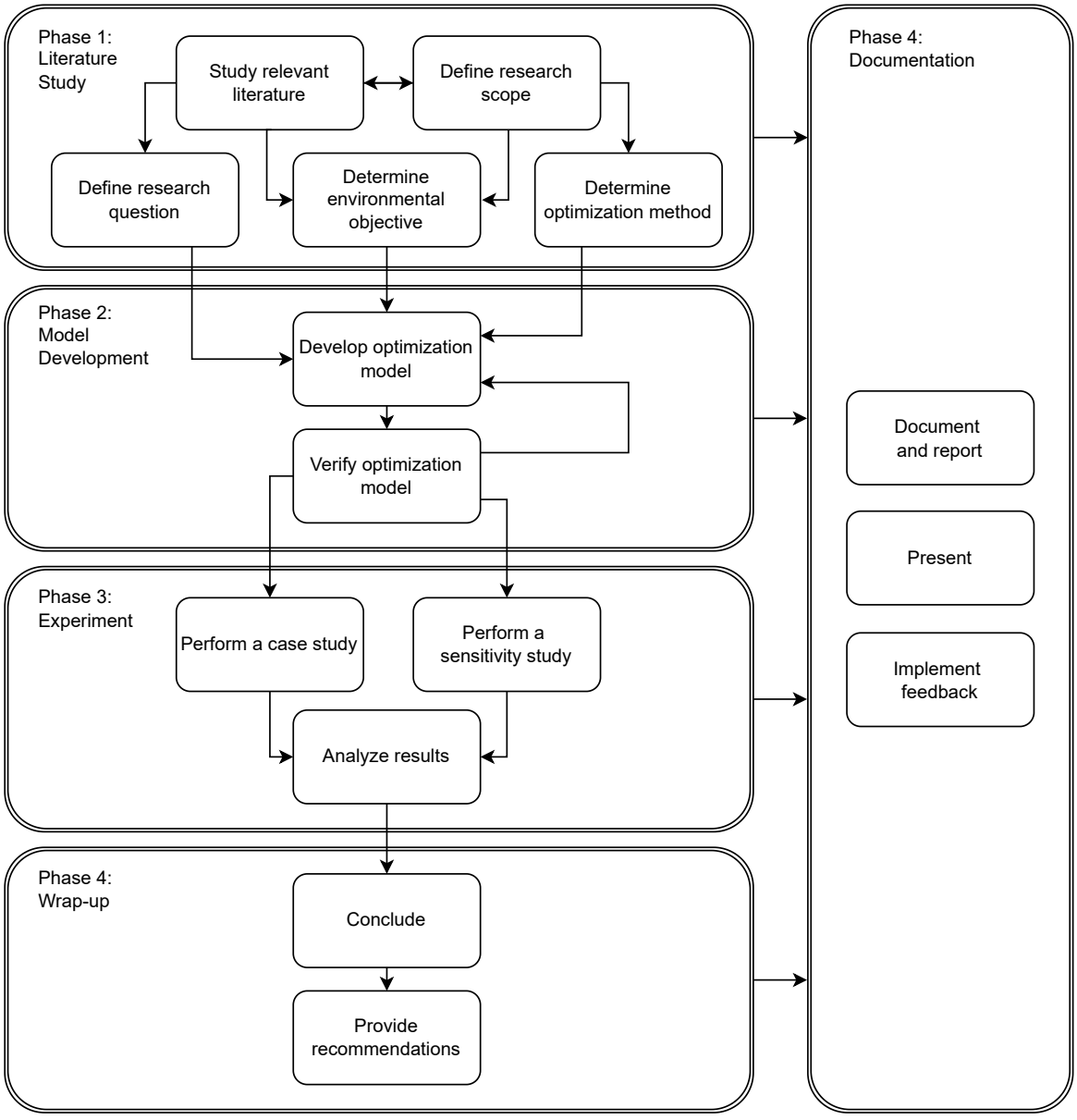

Figure 4.1: Research framework of the thesis project.

5

Theory

The theoretical framework of the problem will be established in this chapter. The studies mentioned in Chapter 2 can be used for this. Most studies describe the applied methodology in detail. In the papers, detailed information on possible problem formulations, solution methods, constraints, and variables are given for multi-objective trajectory optimization.

The aircraft dynamics used in the research are discussed first, in Section 5.1. This is followed by Section 5.2, in which the theory of genetic algorithms in flight trajectory optimization. The different methodologies to set up a GA are discussed. It also includes theory on the constraints that can be included in the model.

5.1. Flight Dynamics

In trajectory optimization, the aircraft dynamic equations are often simplified [18]. The aircraft point-mass model is used in many cases. It does not describe the motion of flight in full detail but is considered sufficient for calculations regarding trajectory optimization [35]. The optimization algorithms often require many computations and can be complex. The simplification of the aircraft dynamics aids in the reduction of the number of computations [17, 18].

The point-mass model describes the flight dynamics in three axes. The forces are assumed to act on the center of gravity [35]. Thus, in the model, the rotational dynamics can be eliminated [17]. In Equations 5.1 through 5.5, the applicable equations are described.

$$\dot{x} = V_{TAS} \cdot \cos(\gamma) \tag{5.1}$$

$$\dot{y} = V_{TAS} \cdot \cos(\gamma) \tag{5.2}$$

$$\dot{z} = V_{TAS} \cdot \sin(\gamma) \tag{5.3}$$

$$\dot{V_{TAS}} = \frac{T - D}{m} - g_0 \cdot \sin(\gamma) \tag{5.4}$$

$$\dot{m} = -ff \tag{5.5}$$

The three positional vectors are x, y, and z (the altitude). V_{TAS} represents the true airspeed, γ is the flight path angle, T is the thrust, D is the drag, m is the mass of the aircraft, g_0 is the gravitational acceleration, and ff is the fuel flow.

If the wind is to be included in the model, the components of the wind speed can simply be added to Equations 5.1, 5.2, and 5.3 [35].

5.2. Genetic Algorithm

The genetic algorithm is based on the evolution theory of Darwin, as the name suggests. The solving algorithm is a repeating process. At first, it generates a random set of possible solutions, referred to as a generation of individuals. Each individual's fitness is then evaluated, which can be defined in different manners and can be seen as the objective function. Depending on the chosen selection method, a particular selection is made of the individuals who are appointed as parents. The parents will reproduce and generate children, creating new solutions to the optimality problem. Part of some solutions are randomly altered, so-called mutation, to decrease the likelihood of getting trapped in a local optimum. The new individuals are thereafter evaluated on their fitness, and the process of selection, crossover, mutation, and fitness evaluation is repeated. The iteration is brought to a halt whenever a stopping criterion is met. [29, 45]

The theory behind the steps taken in the genetic algorithm will be further explained in the following sections. In Section 5.2.1, the different formulations of individuals, also referred to as solutions, are presented. The section thereafter discusses the evolution process. In Section 5.2.3, the variables of a GA are briefly discussed. The final section, Section 5.2.4, presents the implementation of constraints in the trajectory optimization problem.

5.2.1. Solution Formulation

The solutions – flight trajectories – should be defined numerically so that the steps of the GA can be taken. This can be done in different ways; Yamashita et al. [45] utilize control points (CP) and B-splines (basis splines) to formulate solutions. Patrón and Botez [29] use a three-dimensional grid that consists of waypoints. Other formulations are also possible.

In the 3D grid method by Patrón and Botez [29], waypoints are defined. In Figure 5.1, an example of a grid is given. As can be seen, the grid surrounds the predefined flight route (dashed, blue line in Figure 5.1). In the horizontal plane, multiple routes are created on both sides of the predefined route. In the vertical plane, trajectories are stacked on top of each other and separated by a certain distance. Along these trajectories, waypoints are defined at determined intervals. The flight can only be altered to adjacent waypoints. [29]

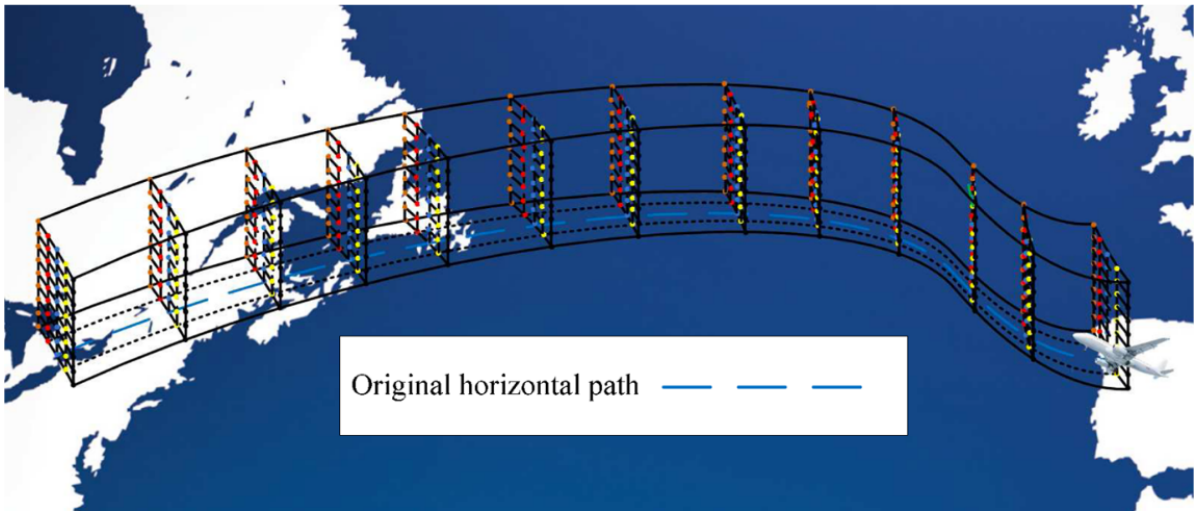

Figure 5.1: A 3D grid method to formulate solutions to the trajectory optimization problem. The dashed, blue line represents the original path. In the lateral direction, two paths are added in parallel. In the vertical direction, multiple paths are stacked on top of each other. The image is taken from [29, p. 538].

Yamashita et al. [45] utilize control points, in the vertical and horizontal planes, spread out between the destination and arrival airport. A solution is defined as a vector that consists of a number of design variables, n_{dv}. The design variables are indexed by j and are allowed to vary between the lower and upper boundaries. The design variables in [45] are the control points. The definitions are provided by the authors in Equations 5.6, 5.7, and 5.8 [45].

$$\vec{x} = (x_1, x_2, \cdots, x_{n_{\text{dv}}})^T \tag{5.6}$$

$$j = 1, 2, \cdots, n_{\text{dv}} \tag{5.7}$$

$$\left[x_j^{\text{l}}, x_j^{\text{u}}\right] \tag{5.8}$$

In Figure 5.2, the CPs in the horizontal plane are displayed as black dots within the dashed rectangles. Each pair of CPs (three in Figure 5.2) forms a position: the odd CPs represent longitudes and the even latitudes. The CPs are allowed to vary within the dashed rectangles (the boundaries), of which the center is located on the great circle route (thin, black line in Figure 5.2) between the airports. The boxes are spread out evenly. The width and length of the boxes are defined as 10% and 30%, respectively, of the difference in longitude of the airports. The flight trajectory (thick, black line in Figure 5.2) "is represented by a B-spline curve (third-order) with the three CPs as locations [...] and then any arbitrary number of waypoints is generated along the trajectory", as the authors state [45, p. 3375].

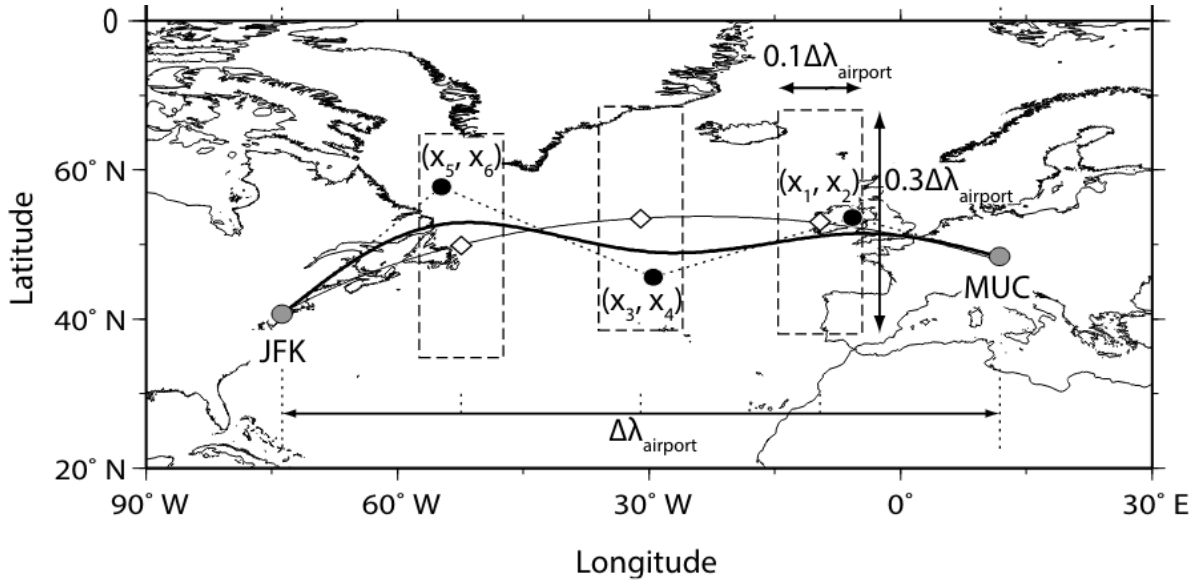

Figure 5.2: The control point methodology to formulate a solution to the trajectory optimization problem. The horizontal plane of an exemplary route is visualized. The filled dots are the control points, each made up of two values: the longitude and the latitude. The values can vary within the dashed rectangle around it. These rectangles are spaced equally along the great circle route, shown as the thin line. The thicker line illustrates the solution, which is a B-spline created between the CPs. This image is taken from [45, p. 3375].

The CPs in the vertical plane are represented by black dots in Figure 5.3 and define the altitude. The figure displays the vertical path of the flight trajectory in Figure 5.2. The boundaries of the CPs are Flight Level (FL) 290 and FL410; the boundaries hold the same value for all the vertical control points in the study of Yamashita et al. [45]. Like in the horizontal plane, the control points are allowed to vary between these boundaries. The position in terms of the longitude of each vertical CP is predetermined; the CPs are spread out evenly between the airports. Again, a B-spline curve determines the flight path.

5.2.2. Evolution

As mentioned before, the GA is started with a first generation. This is followed by a fitness test, the selection, crossover, and mutation, which are repeated until a stopping criterion is met. All steps of the algorithm are discussed in this section.

First Generation

The first generation is randomly established. It consists of n_p individuals. In [45], each individual is composed of the same number of design variables, as defined in Equation 5.6. The values of these design variables are chosen randomly but are chosen between their own lower and upper boundaries.

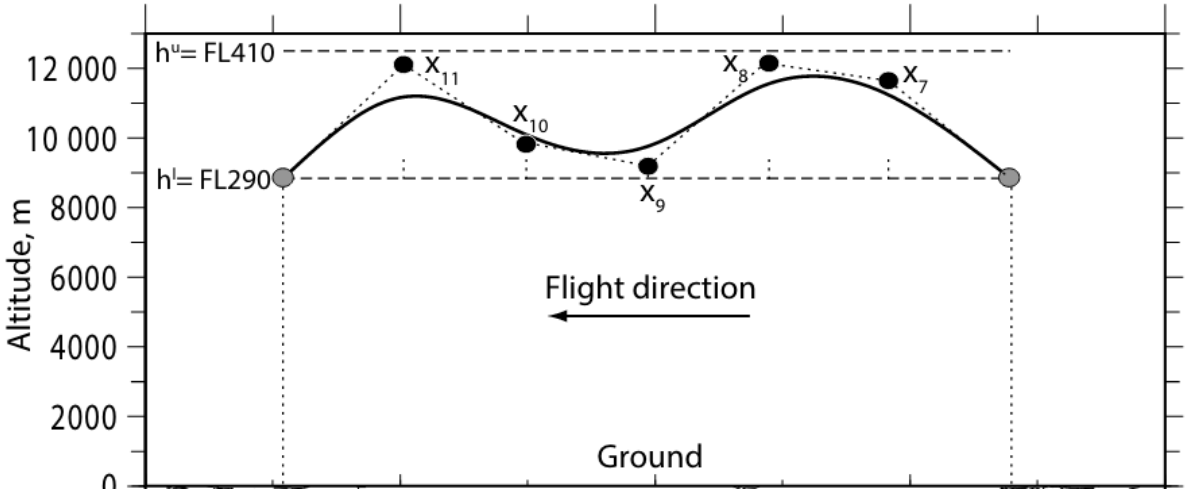

Figure 5.3: The control point methodology to formulate a solution to the trajectory optimization problem. The vertical plane of an exemplary route is visualized. As in Figure 5.2, the filled dots are the control points. In the vertical plane, each is made up of one value, the altitude. The values can vary between the dashed lines. The thicker line illustrates the solution, which is a B-spline created between the CPs. This image is taken from [45, p. 3375].

In [29], the solutions do not necessarily have the same number of waypoints. The first generation is established randomly and consecutive waypoints should be adjacent to one another.

Fitness
To evaluate the solutions quantatively, the so-called fitness of each is calculated. In trajectory optimization, it is better known as the objective function. It can be defined differently, as explained in Chapter 2, and it depends on the aim of the research. In the study of Yamashita et al. [45], the objective function is to minimize the flight time. Thus, the fitness of a solution is determined by the time it takes an aircraft to fly that specific route. Patrón and Botez [29] use the flight cost as the fitness of a solution. In theory, all metrics discussed in Section 2.1.4 can be used as the objective function.

Selection
Several methodologies exist for the selection of parents among the individuals, as Patrón and Botez [29] describe. They explain briefly the four methods listed below. Do note that more methods exist as GAs are widely used in other disciplines, as well.

- Uniform: each individual is equal and all can create children.
- Rank: a rank is made based on the fitness, and only the best solutions are entered into the mating pool.
- Roulette wheel: higher scoring individuals get a larger chance of being chosen as a parent. Solutions that have low fitness still have a chance.
- Tournament: individuals are not allowed to crossover when they lose in a battle between each other.

In [29], the tournament selection method is used. Yamashita et al. [45] utilize the roulette wheel method. Patrón and Botez [29] discuss also the advantages and disadvantages of the methods. They state that the roulette wheel method is beneficial as it does not get stuck quickly in local optima. However, according to them, it is not so fast in finding the optimal solution. The tournament method converges sooner.

Crossover
From the mating pool, parents are randomly chosen based on the determined probability to form children. Each pair of parents will create two children, such that the size of the population remains constant throughout the generations. The thought behind the selection and crossover steps is the principle of the strongest survives. This should lead to stronger individuals each generation, and eventually result in the most optimal solution [29].

Again, several methods exist to perform this step. Patrón and Botez [29, p. 539] take ”one-half of one individual and combining it with a half from another individual”. This was opted for because of the use of the grid method; choosing another method would result in the violation of the requirement that each consecutive waypoint is adjacent.

Yamashita et al. [45] opt for the ’Blend crossover operator’, which is explained in more detail in their paper.

Mutation
As in the natural process of evolution, mutations occur in the production of new individuals in a GA. This is done to limit the risk of converging to a local optimum instead of the global optimum [45]. The mutation of the individuals is effective for reducing this risk because when solutions are randomly altered a larger spectrum of trajectories is explored.

Yamashita et al. [45] use a polynomial mutation operator, which selects the solutions that are to be mutated based on a certain probability function. The method is described in more detail in their article.

Patrón and Botez [29] apply a different method. The researchers replace solutions instead of altering several values in the solution. The least performing individuals in terms of fitness are replaced with random solutions, which are created similarly to the first generation. The authors do not mention the reason for this, but it probably has to do with the choice of the grid method. The route can only be altered to adjacent waypoints. Changing a single value in the solution violates this. In the study by Yamashita et al. [45], the choice of values of the control points do not depend on each other, and thus can be altered randomly.

Iteration
The evolution process (fitness, selection, crossover, and mutation) repeats itself until a stopping criterion is met. The principal ’survival of the fittest’ is applied, and thus it is assumed that the individuals of each generation are better than the preceding generations. A stopping criterion could be to stop when a certain number of generations has been made or when the solution has not improved over a number of consecutive generations. [29, 45]

5.2.3. Settings
Several parameters can be adjusted in the algorithm which can influence the outcome and efficiency of the optimization model. These include the number of control points or grid size, the size of the population, the selection method, the crossover rate, the mutation rate, and the stopping criteria. According to Patrón and Botez [29, p. 538], a strategy to apply for the size of the population is that it should ”represent a small percentage of all the possible solutions.”. The authors warn the reader with adding control points, as the number of potential solutions will increase exponentially. A trade-off should be done during the research between the parameters to optimize the accuracy and computation time [45].

5.2.4. Constraints
Typically, there are three types of constraints imposed within a trajectory optimization problem. These are dynamic, boundary, and path constraints. The constraints can be categorized into equality and non-equality constraints.

Dynamic constraints are imposed to ensure that the solutions are feasible in terms of the aircraft’s state [17]. For example, the velocity should be large enough to prevent stalling but not exceed the maximum velocity. Also, the path angle should lie between its lower and upper boundary value; it should stay realistic. The mass of the aircraft and altitude are typically constrained as well.

Boundary constraints specify the values of variables on the boundaries - the initial and final values. These constraints are typically equality constraints [18]. Simorgh et al. [18, p. 7] provide several examples: ”the geographical location of origin and destination, initial mass, and initial speed are some equality boundary constraints that are usually considered”.

Path constraints are imposed on the states of the aircraft between the boundary points [17]. For instance, aircraft should adhere to the regulations of ATC when performing a SID/STAR. At predetermined waypoints, the velocity and altitude are constrained [17].

In GAs, the constraints can be implemented as penalty functions [46]. If a solution violates any of the constraints, a penalty score is added to the fitness. This decreases its likelihood of becoming a parent. The consequence is that the solutions are not only selected based on the objective function but also on whether they comply with the constraints. Nanakorn and Meesomklin [46] describe a method to implement penalties effectively. Other methods exist as well.

6

Methodology

The next step in the research is the creation of the basic optimization. This will encompass the steps of a GA as described in the previous chapter. The model will not yet include wind, variable mass, variable speed, and airspace constraints. To develop the basic model, it should be understood how the chosen software functions.

The software that is used in the basic model is described in Section 6.1. The creation and implementation of the basic model are set out in Section 6.2. This is followed by Section 6.3, in which the first steps toward the verification and validation of the trajectory optimization are presented.

6.1. Software

The basic model that is created for trajectory optimization is programmed in Python. For the model, use is made of multiple open-source packages in Python, namely NumPy [47], Matplotlib [48], OpenAP [49], and Proj [50].

NumPy is used because it facilitates fast computations with multidimensional arrays. As is explained in the following section, almost all computations can be vectorized using NumPy. This allows the GA to compute faster than when using ordinary Python lists or dictionaries.

Matplotlib is used to visualize the model's results. It allows the user to more easily look over what is achieved with the code. The visualizations will be extended with Cartopy [51] in the future. This is discussed in Section 8.2.4.

OpenAP constitutes packages for Python through which, for example, the thrust settings and fuel usage can be computed for an aircraft flying a certain route. Also, model data are included in which information is available among others on emissions [49]. The dynamics of an aircraft are described as a point mass model with four degrees of freedom [49]. The difference with the flight dynamics presented in Section 5.1 is the rotational axis for the roll of the aircraft. For the computation of the emitted gasses using the performance in terms of fuel flow, this should not be problematic.

In other research, for computations concerning aircraft's performance, use is sometimes made of BADA [17]. OpenAP is chosen because it approximates the performance of an aircraft better during climb phases [49]. Besides, OpenAP is readily available.

Proj is a package that allows for easy transformation between different coordinate reference systems (CRSs) [50]. It is used in this model to transform from a World Geodetic System (WGS) '84 projection to coordinates in the Lambert Conformal Conic projection (LCC). The latter is often used in aviation[1]. The LCC CRS is easier to use in the computations of this model.

There can be several drawbacks to the usage of the chosen software. The available aircraft types in OpenAP are limited; data are only available for turbofan engines [49]. However, the available aircraft types are the most used commercial aircraft. According to Sun and Dedoussi [19, p. 8], OpenAP can

[1] `https://proj.org`. Visited on Apr. 14, 2022.

be used ”for around 94% of flights in European airspaces.”. For this project, it should be sufficient to demonstrate how a reduction in the environmental footprint of commercial aviation can be achieved.

Additionally, there may be a shortage of computing power on the available laptop. If during the development phase, it is found that this is the case, an alternative computer with more computing power can be looked for at the Faculty of Aerospace Engineering in Delft.

6.2. Implementation

The implementation of the theory discussed in the previous section is implemented in the model. Neither the definition of Yamashita et al. [45] nor of Patrón and Botez [29] is adopted. The best practices of the theories are taken, and adjustments are made to the theories to fit this research.

The implementation of each step discussed in Section 5.2 is explained in detail in this section. The same structure is followed.

6.2.1. Solution Formulation

Each individual is defined by four states at a predetermined number of nodes, n_{node}. The shape of each individual is 4 by n_{node}. The four states are the positional variables (x, y, and z) and the difference in time between two consecutive nodes (Δt). The nodes are spread at an equal distance between one another between the origin and destination of the trajectory. A baseline solution is given in Figure 6.1. The number of nodes defines the resolution of the solution; the more nodes are used, the larger the resolution of the trajectory. Due to this definition – each individual having the same array shape – vectorization of the computations can be used.

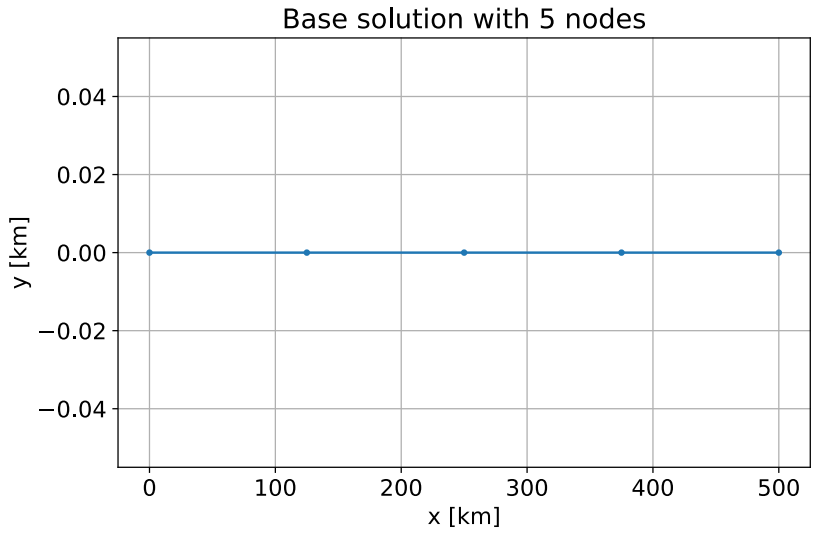

Figure 6.1: The solution formulation is visualized for a trajectory with 5 nodes. The origin of the route is at $(0, 0)$ and the destination at $(500, 0)$.

The search space should also be formulated before the GA is started. As the research focuses on the climb and descent phases, one airport is taken as the center. Using a back-of-the-envelope calculation, a distance of $500km$ was found to be the horizontal distance covered by an aircraft from the runway to the initial cruise altitude. If an aircraft were to climb $30,000ft$ at a climb rate of $1000fpm$, it would take $0.5h$ to climb. Assuming the aircraft flies at a velocity of $900km/h$, the horizontal distance covered is $450km$. An additional margin of $50km$ has been assumed. This results in the $500km$ stated before.

The Proj Python package [50] is used to transform between different CRSs. The information available for navigational purposes in OpenAP requires the location information in WGS ’84. It is, however, considered easier to work with x- and y-axes. Thus, after the information is extracted, the CRS WGS ’84 is transformed to LCC. This CRS is applicable to the research and should be sufficient in terms of accuracy for the search space.

Ideally, a circular, horizontal search space is defined around this airport. However, it is easier to implement a rectangular search space around the origin and destination in the code. The search space is not limited to the space between the origin and destination as it is possible that an aircraft has to fly in opposite direction first. This is for instance the case when an aircraft takes off and the wind blows from the opposite direction of the destination.

The vertical search space is defined by a rectangle as well. The lowest airport in the world is taken as the minimum value for the altitude. This is Bar Yehuda Airport, which lies $386m$ below sea level[2]. The upper boundary of the search space is defined by the initial cruise altitude. This value depends on the aircraft type and can be obtained from OpenAP.

6.2.2. First Generation

The first generation is created randomly. To do so, a baseline is made between the origin and destination. It is a straight line split into equal-length segments between n_{node} nodes. To create n_{pop} random individuals in the first generation, the nodes are randomly varied. Only the values of the first and final nodes remain the same as the baseline. This is because these nodes represent the origin and destination, respectively.

In the x- and y-direction, each node can take on a value that is between $500km$ below and $500km$ above the baseline value. It is done according to a uniform distribution. An example with 5 individuals is provided in Figure 6.2. Currently, the values of z and Δt are kept constant. This way, a simple optimization can be performed and verified. In the expansion of the model, these values will be randomly altered as well for the first generation. This is discussed in Section 8.1.

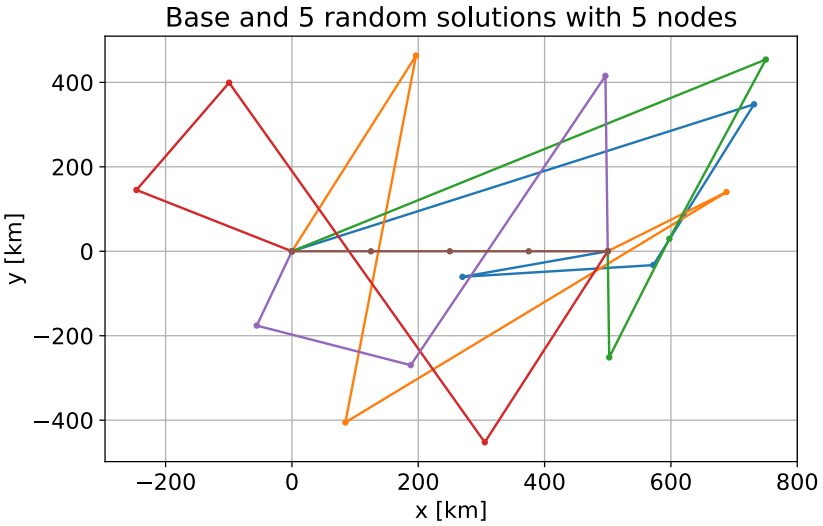

Figure 6.2: The base and 5 randomly generated individuals are visualized for a trajectory with 5 nodes. The origin of the route is at $(0, 0)$ and the destination at $(500, 0)$.

6.2.3. Fitness Evaluation

When all individuals are defined, the fitness of each should be found. The objective function is defined as the cost of emissions of the trajectory. The emission costs of [1] are used for this. The monetary metric can be computed by determining the amount of emitted gasses using the fuel flow. The latter value can be determined using the OpenAP package. As input, it requires the mass of the aircraft, the true airspeed, the altitude, and the flight path angle. The latter two are already known, as these partly define the solutions. The former two have to be calculated using the known states.

[2] `https://en.wikipedia.org/wiki/List_of_lowest_airports`. Accessed on Apr. 11, 2022.

The true airspeed can be found through Equation 6.1. The horizontal velocity (V_h) and vertical velocity (V_v) are found through Equations 6.2 and 6.3, respectively. They are found by dividing the traveled distance between two nodes by the covered time. The definition of the traveled distances can be found in Equation 6.4.

$$V_{TAS} = \sqrt{V_h^2 + V_v^2} \tag{6.1}$$

$$V_h = \frac{\sqrt{\Delta x^2 + \Delta y^2}}{\Delta t} \tag{6.2}$$

$$V_v = \frac{\Delta z}{\Delta t} \tag{6.3}$$

$$\begin{aligned} \Delta x &= x_i - x_{i-1} \\ \Delta y &= y_i - y_{i-1} \\ \Delta z &= z_i - z_{i-1} \\ \Delta t &= t_i - t_{i-1} \end{aligned} \tag{6.4}$$

The flight path angle is defined as the angle between the horizontal line through the aircraft's center of gravity and the velocity vector. Equation 6.5 defines the flight path angle.

$$\gamma = \text{arctan}\left(\frac{V_v}{V_h}\right) \tag{6.5}$$

As described in Equation 5.5, the difference between the mass at two consecutive nodes is the amount of fuel burned. The mass can be calculated in an iterative manner. It is described in Equation 6.6. Currently, the initial value of the mass is defined as 80% of the maximum take-off weight (MTOW). For the extension of the model, another value may be used.

The fuel flow of the aircraft at the first node is found using the aircraft's conditions at that moment. It is assumed that these are constant for the segment between two consecutive nodes. The fuel flow is then multiplied by the time it takes the aircraft to travel to the next node. This is subtracted from the mass at the first of two nodes, and the mass at the second node is then found. These steps are repeated to find the fuel flow and mass at all nodes.

$$m_i = m_{i-1} - ff_{i-1}\left(m, V_{TAS}, z, \gamma\right) \cdot \Delta t_i \tag{6.6}$$

Once all the states and the fuel flow are determined at all nodes, the 'emission flow' can be calculated. It is found with the use of OpenAP as well. Again, several inputs are required. These depend upon the emitted species and include the fuel flow, true airspeed, and altitude. The resulting value is the mass of emission per second. Thus, to find the total emitted mass of each species, each has to be multiplied by Δt. These masses are multiplied by the emission costs determined by Grobler et al. [1]. Ultimately, the emission cost of each segment is summed. The formula for the total emission cost (C_e) can be found in Equation 6.7. Each C represents a cost, and each m the mass of the specific species.

$$C_e = \sum_{n=1}^{n_{node}} \left(\Delta t \cdot \left(C_{CO2} \cdot m_{CO2} + C_{H2O} \cdot m_{H2O} + C_{NOX} \cdot m_{NOX} + C_{CO} \cdot m_{CO} + C_{HC} \cdot m_{HC}\right)\right) \tag{6.7}$$

These emission costs are different throughout the flight; the cost has another value in climb than in cruise. This has not yet been accounted for but will be done at a later time to ensure a more accurate result. Another limitation exists concerning the emission cost. Not all emitted gasses can be found using OpenAP, such as black carbon. According to Sun and Dedoussi [19, p. 8] this culminates to "17% of aviation's societal costs.".

6.2.4. Selection

The fitness values are used to evaluate the individuals. It depends upon their score what the probability is that they are selected to be a parent in the crossover phase. To minimize the environmental impact of the flight, the fitness should be as low as possible. The selection method that is chosen is the roulette wheel method. It is also known as the fitness proportionate selection method. As discussed in Section 5.2, higher-scoring individuals have a larger chance of being chosen as a parent. However, the lower-scoring solutions also have a slight chance. The probability is found using Equation 6.8. The array of the fitness values of each individual in a generation is noted as $\boldsymbol{f}$.

$$p_i = \frac{\max(\boldsymbol{f}) - f_i}{\max(\boldsymbol{f}) - \min(\boldsymbol{f})} \tag{6.8}$$

The original formula is for a maximization problem and has been taken from an article by Blickle and Tiele [52]. The formula is rewritten to be applicable for a minimization problem. Besides, the probability selection array is normalized after Equation 6.8 is applied to all nodes.

Using the calculated probability of each individual, the parents are chosen. The number of parents is equal to the population size, n_{pop}. As two parents are required to produce two children, n_{pop} can only be an even number. Pairs of parents are generated randomly according to the probability distribution. The parents in a pair cannot be the same individual. Additionally, pairs of parents are required to be unique in the complete set of pairs. Otherwise, identical offspring are created in the crossover step.

6.2.5. Crossover

Children are made through the crossover of the parent pairs. The four states (x, y, z, and Δt) of each parent are split in half. The first child is made up of the first half of the first parent and the second half of the second parent. The second child is made up of the other halves; it consists of the first half of the second parent and the second half of the first parent. In this manner, the number of children equals n_{pop}. The process is visualized in Figure 6.3. A parent pair and its offspring are shown in Figure 6.3a and Figure 6.3b, respectively.

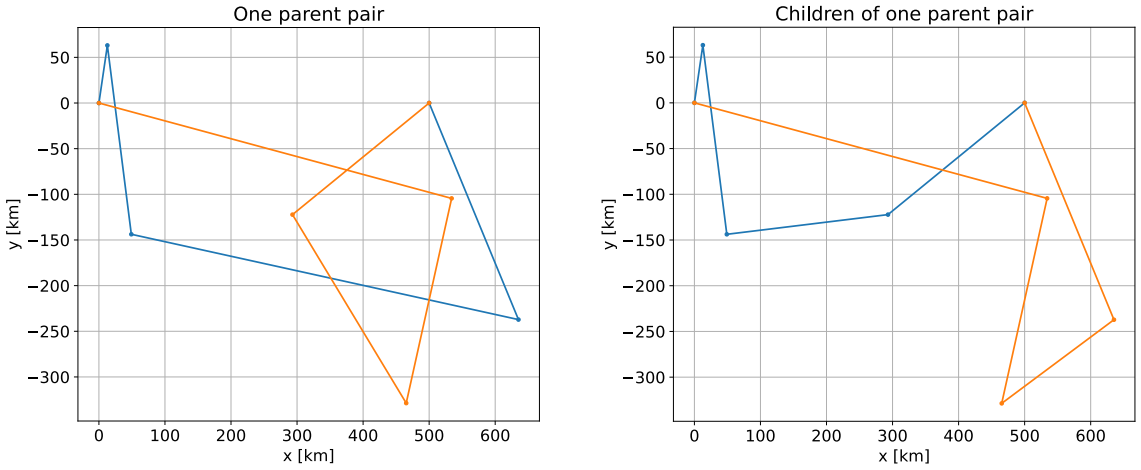

(a) Two individuals selected to reproduce together.

(b) The offspring of the parents shown in Figure 6.3a.

Figure 6.3: A parent pair and its offspring are presented. On the left, the parents can be seen. The right figure shows the offspring. The solutions consist of 5 nodes. The parents are split at node 3, the middle. The origin of the route is at $(0, 0)$ and the destination at $(500, 0)$.

6.2.6. Mutation

To prevent the algorithm from getting trapped in a local optimum, mutations take place in the states of the newly created children. In the complete model, each value in an individual is varied according to a normal distribution. The value of the standard deviation depends on the state. It will be reduced over

the course of the process according to a mutation rate. This will result in smaller deviations from the trajectories over time.

Currently, the standard deviation is kept constant. Also, only the values of x and y are allowed to change. This has been done so that a simple case with constant altitude and velocity can first be evaluated. The implementation of a variable standard deviation is discussed in Section 8.1. The mutation process is visualized in Figure 6.4.

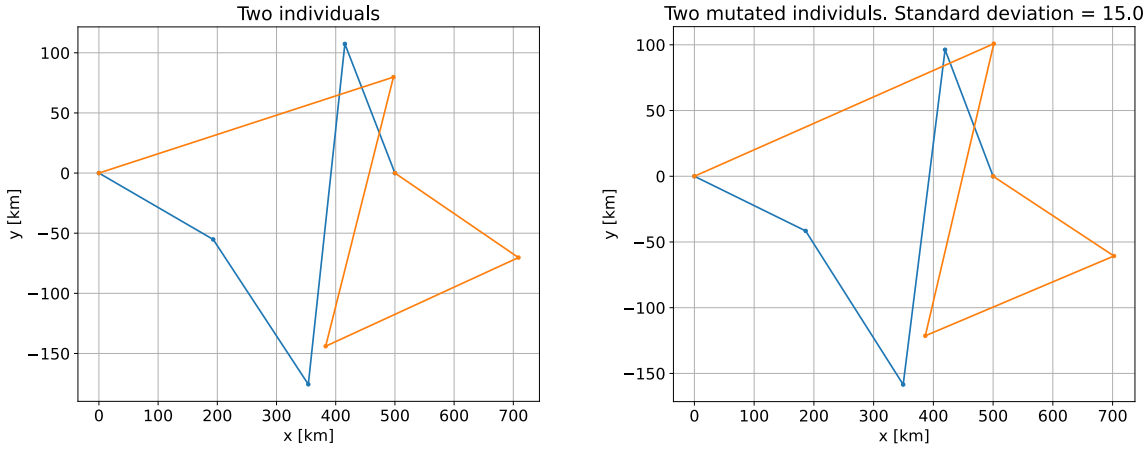

(a) Two individuals.

(b) The individuals shown in Figure 6.4a after mutation.

Figure 6.4: The process of mutation is visualized. On the left, the individuals can be seen before mutation. The right figure shows the same individuals after mutation. The solutions consist of 5 nodes. The mutation is according to a normal distribution with a standard deviation of 15. The origin of the route is at $(0, 0)$ and the destination at $(500, 0)$.

6.2.7. Elimination

The mutated children should be compared to their parents in terms of their fitness. The best n_{pop} individuals of the current generation (the parents) and the children will comprise the next generation. The others are eliminated. If this step is skipped and the children are simply adopted as the next generation, the best solution may be lost.

To find the fitness of each child, the fitness step (Section 6.2.3) is completed for these individuals. The fitness of the parents and children is evaluated and sorted. The best half of these individuals – the ones with the lowest fitness score – make up the next generation.

6.2.8. Iteration

The previously described steps are repeated: a probability distribution is made of the new generation, pairs of parents are selected, the crossover is completed, children are mutated, and the worst half of the parents and children are eliminated. The flow of the model is presented in Figure 6.5.

The iteration is continued as long as no stopping criterion is met. Currently, the stopping criterion is a maximum number of generations. In the extension of the model, a criterion will be added that will stop the process when the best solution does not improve over a number of generations. This is described in Section 8.1.

6.2.9. Constraints

As presented in Section 5.2.4, there are three types of constraints. The basic model is equipped with only one of these types, namely the boundary constraint. The trajectory optimization is forced to comply with the initial and final values of both x and y. All nodes in between are allowed to vary, except the first and last. The initial mass of the aircraft is also defined. It is set to 80% of the MTOW. No penalties are involved with these constraints. For each individual, the boundary conditions are complied with.

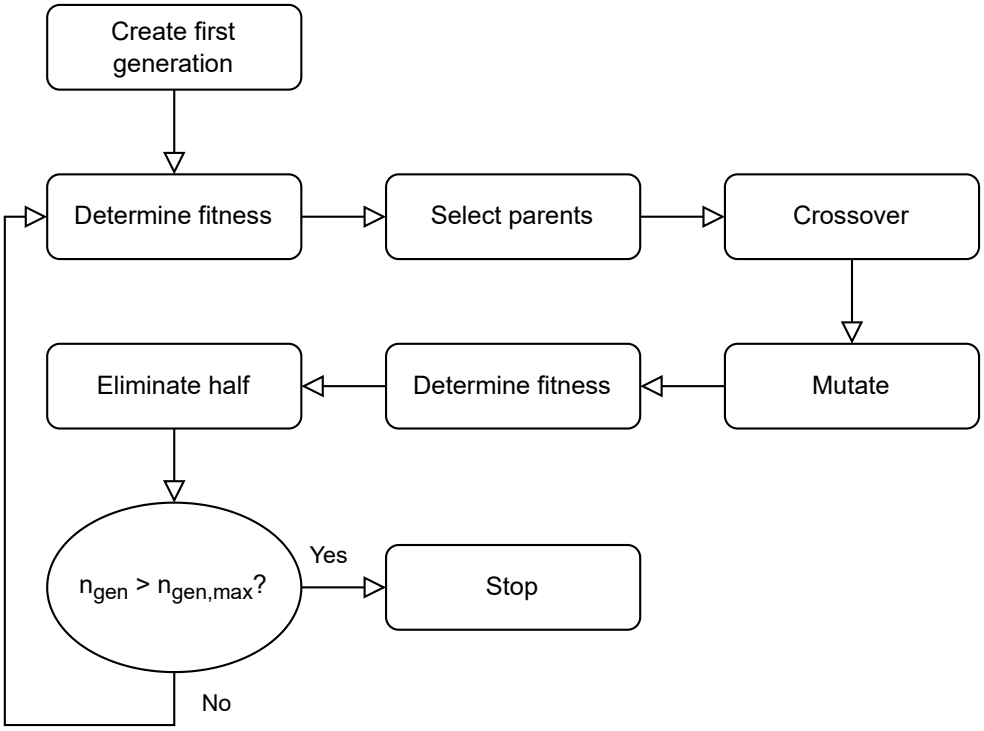

Figure 6.5: Flow diagram of the current genetic algorithm. The rectangular blocks represent functions in the model. The oval blocks represent the iteration conditions.

In theory, more constraints are imposed on the model. Both z and Δt are kept constant. These could be classified as boundary and path constraints as they force the values to remain constant. However, they are not specified as such.

In the extension of the model, additional constraints will be imposed. Path and dynamic constraints will also be included. These constraints are discussed in Section 8.1.6.

6.3. Verification and Validation

The verification and validation of the models and the results are of importance for the quality of the research. The basic model has been developed first. The model should be verifiable using a very simple case. It is a case that can also be optimized by hand. This is discussed in more detail in Chapter 7.

The functioning of the steps of the GA has been verified separately. Before the implementation of the next step, the results were analyzed. It was checked whether the outcome of the function in the code was in line with the expectation. The intermediate steps have been printed such that calculations could be checked by hand. Besides, the results were visualized in various figures. This aided the verification of the units.

Each time the model is expanded, it will be verified again. However, it might not be possible to verify it with a ‘simple case’ once there are too many variables. This is because the optimization problem will at some point become too large to calculate by hand.

An additional form of verification of the results is to compare the model’s outcome with those from earlier conducted research. This should include studies for which the developed models can be customized. For example, a case study that includes noise pollution would not be applicable.

The future plans concerning verification and validation are further discussed in Section 8.1.7.

7

Preliminary Results

This chapter presents the results of the basic model. This model is described in the previous chapter. The results and a brief explanation of them can be found in Section 7.1. A discussion on the outcome of the basic model is given in Section 7.2.

7.1. Results

The results are presented for a simple route between two points. The altitude and velocity are kept constant as discussed before. The objective function of the model is the cost of emissions. The best solution is the one with the shortest route. This is because the unit costs of emissions are constant; the fuel flow determines the total cost. The fuel flow is calculated using the mass, velocity, flight path angle, and altitude, as defined in OpenAP. The mass is the only variable of the fuel flow that differs per trajectory, which is in itself dependent on the fuel flow. The solution with the lowest usage of fuel is thus the one with the lowest cost of emissions. This is the solution that covers the shortest distance.

The origin of the trajectory is at $x = 0km$ and $y = 0km$. The destination is $500km$ to the East, so $x = 500km$ and $y = 0km$. The aircraft that is considered in the optimization is the Airbus 320. It is assumed to fly at a constant speed of $900km/h$ at a constant altitude of $11km$. The vertical speed is non-existent, thus the flight path angle is $0°$.

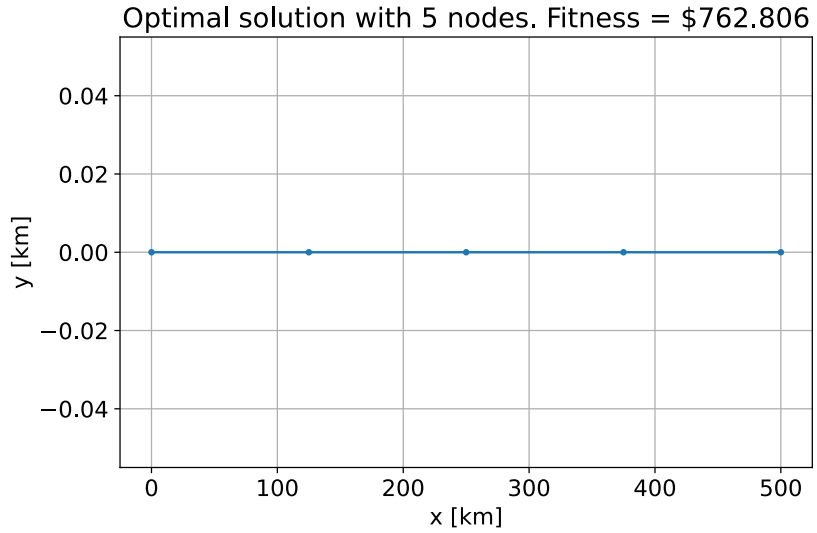

Figure 7.1: The optimal solution of the route. The solution consists of 5 nodes. The origin of the route is at $(0, 0)$ and the destination at $(500, 0)$. The fitness of the optimal solution: $C_e = \$762.806$.

The optimal outcome of this problem can easily be determined by hand and is the line from $(0, 0)$ to $(500, 0)$. All nodes should be placed along the x-axis. It is visualized in Figure 7.1. The values of y should converge to $0km$. The cost of emission (fitness) in this case is calculated to be $\$762.806$.

The settings that can be adjusted in the model are the number of nodes that define a solution; the size of the population; the number of generations allowed; and the standard deviation of the normal distribution in the mutation phase.

The model has been run for several different combinations of these settings. In Figure 7.2, the optimal and best solution after 1000 generations of an optimization for a trajectory consisting of 5 nodes is presented. A generation exists of 100 individuals. The standard deviation of the mutation is set to 15. This number has been chosen through trial and error. The fitness of the best solution is almost equal to that of the optimal solution. The difference is only $\$0.025$. The route is, however, at its maximum $1.4km$ away from the optimal route.

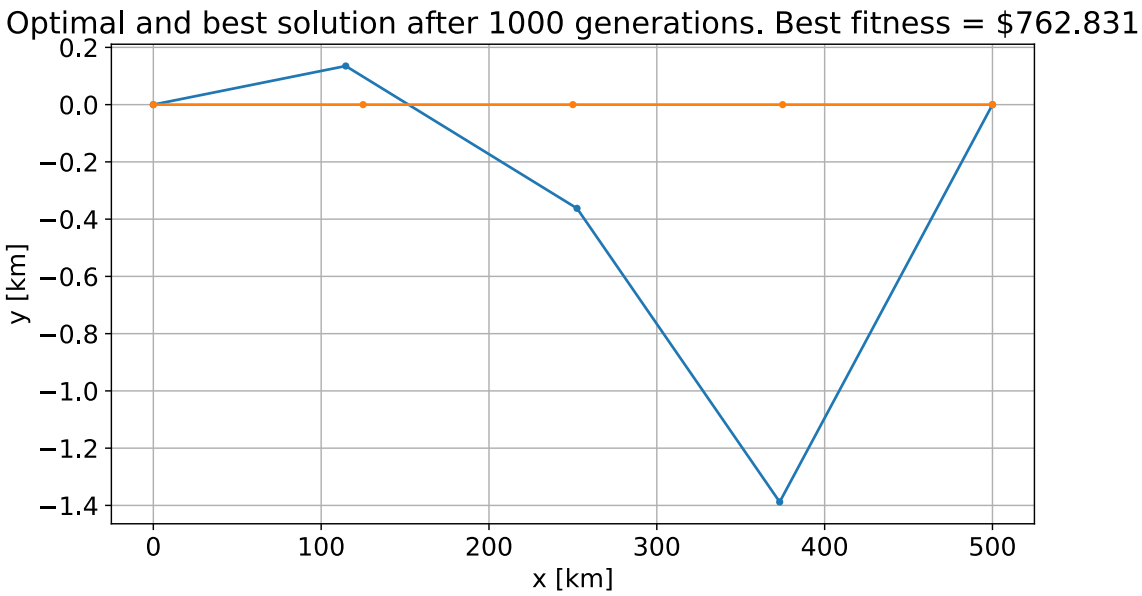

Figure 7.2: The optimal (orange) and best (blue) solutions of the final generation (1000) are presented. The solutions consist of 5 nodes. A generation consists of 100 individuals. The origin of the route is at $(0, 0)$ and the destination at $(500, 0)$. The standard deviation of the mutation is set to 15.The fitness of the best solution: $C_e = \$762.831$

In Figure 7.3, an optimization is run for trajectories with 10 nodes. The same number of individuals and generations has been used as in Figure 7.2. The value of the standard deviation has been increased to 30. This was also determined through trial and error. The resulting best solution has a fitness of $C_e = \$767.806$. The difference is larger than with fewer nodes; the difference with the optimal total cost is $\$5.000$. This difference seems small, but can be deceiving. Looking at Figure 7.3, the flight trajectory does not follow the x-axis at all.

Increasing the number of nodes leads to outcomes that are further from the optimal solution. In the optimization visualized in Figure 7.4, the number of nodes is 50. The resulting total cost of emissions is more than triple the optimal value.

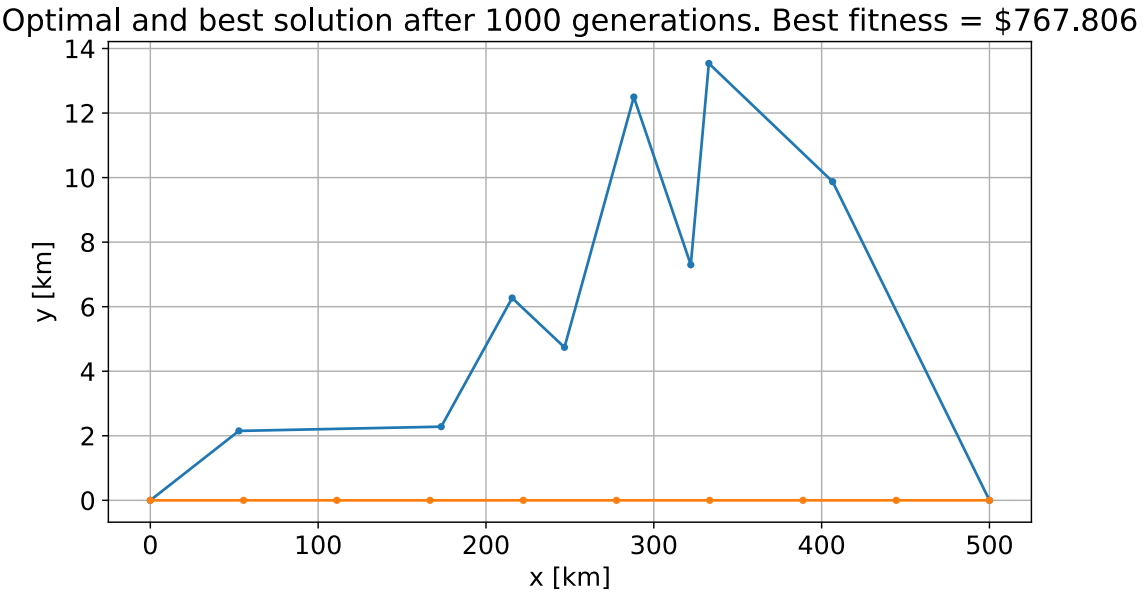

Figure 7.3: The optimal (orange) and best (blue) solutions of the final generation (1000) are presented. The solutions consist of 10 nodes. A generation consists of 100 individuals. The origin of the route is at $(0, 0)$ and the destination at $(500, 0)$. The standard deviation of the mutation is set to 30. The fitness of the best solution: $C_e = \$767.806$.

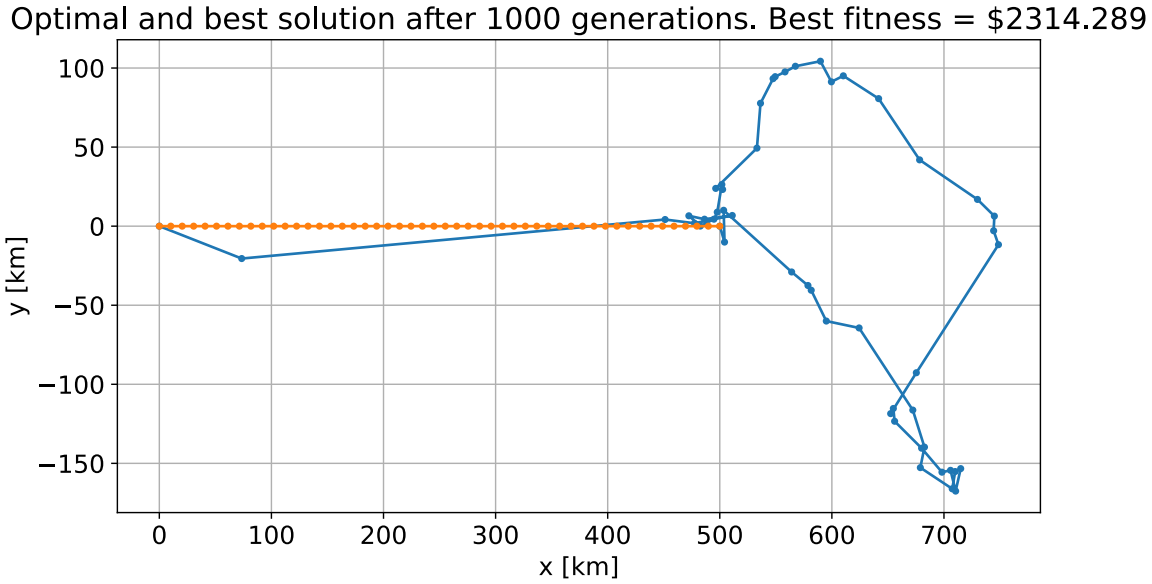

Figure 7.4: The optimal (orange) and best (blue) solutions of the final generation (1000) are presented. The solutions consist of 50 nodes. A generation consists of 100 individuals. The origin of the route is at $(0, 0)$ and the destination at $(500, 0)$. The standard deviation of the mutation in the 10 optimizations is set to 5. The fitness of the best solution: $C_e = \$2314.289$.

7.2. Discussion and Verification

It was expected that the algorithm would find a trajectory that closely represents the optimal route. However, the basic model does not perform as desired. This is especially true when the solutions consist of more nodes. The basic model could not be verified using the simple case. The algorithm should be improved and properly functioning before the additions discussed in the next chapter can be implemented. Due to time constraints, it was not possible to improve the algorithm such that it does meet the expectations. However, several potential solutions to the problem have been identified.

7.2.1. Additional Constraint

Firstly, an additional constraint regarding the heading changes of the trajectory can be imposed. In Figure 7.3, it can be seen that the proposed trajectory requires multiple extreme turns. By imposing a constraint on the number or size of the heading changes, a smoother trajectory is expected. The outcome is expected to more closely represent the optimal trajectory if these constraints are added.

7.2.2. Mutation Scheme

Secondly, the mutation should be set correctly for the chosen settings. Currently, the mutation is done according to a normal distribution with a constant standard deviation. As the model converges with an increasing number of generations, the mutation can be of a smaller scale. Currently, when many iterations have taken place, mutations affect the newly created individuals so much that most parents have better fitness than their offspring. This causes a lower improvement over the course of the generations.

This is supported by Figure 7.5. In Figure 7.5a, four individuals of the first generation of an optimization are shown. Figure 7.5b shows the four best individuals after 10 generations. In the first generation, the range of the y-values is more than $500km$. In the tenth generation, this range has decreased to approximately $40km$. It would be better to apply a different standard deviation in the mutation for the two situations.

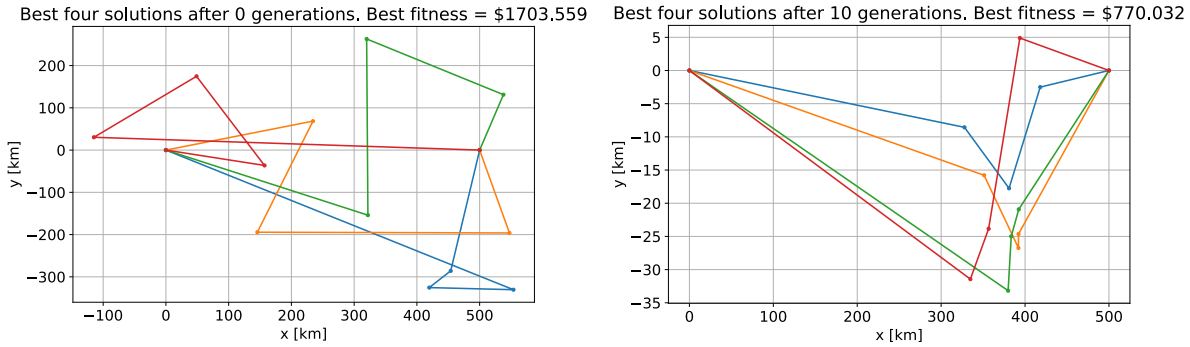

(a) The best four individuals of the first generation of an optimization. The fitness of the best solution: $C_e = \$1703.559$.

(b) The best four individuals after the optimization ran for 10 generations. The fitness of the best solution: $C_e = \$770.032$.

Figure 7.5: The four best individuals of the first and tenth generations are presented. The solutions consist of 5 nodes. A generation consists of 100 individuals. The origin of the route is at $(0, 0)$ and the destination at $(500, 0)$. The standard deviation of the mutation is set to 15.

Besides, the mutation can sometimes be too soft in earlier generations. This can be seen in Figure 7.6. It can be clearly seen that a similar route with many variations of that route are evaluated. The mutations are not large enough to get out of the local search. This results in an inaccurate result.

The slower convergence with more iterations is one of the reasons why an additional stopping criterion should also be added. This criterion should be: if the fitness of the best solution has not improved over a set number of generations, the optimization should be stopped. This is also discussed in Section 6.2.8 and Section 8.1.

7.2.3. Increased Population Size and Generations

Thirdly, the population size and the maximum number of generations can be enlarged. It has been observed that this does improve the results. However, this is up to a certain point as discussed in the previous paragraph; the convergence slows down when more generations are created. Also, it requires more computational effort, and thus time. Before this option is explored, the additional stopping criterion should be added.

First setting the population size to a large number and then letting the population size decrease with increasing generations may be beneficial. It would only require additional computing effort in the first generations and could prevent the algorithm from getting trapped into local optima. An example of the algorithm searching in local areas can be found in Figure 7.6; large patches of the search space are not searched.

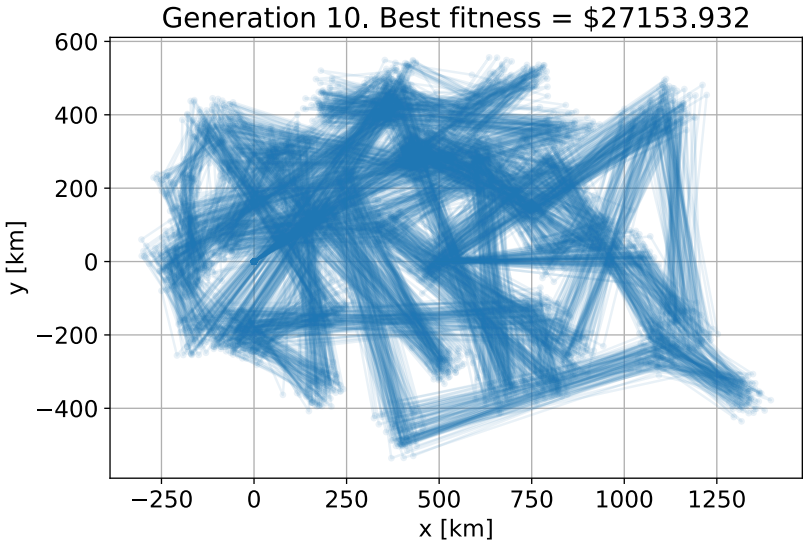

Figure 7.6: The trajectories of an optimization at generation 10 with 100 individuals. The solutions consist of 50 nodes. The origin of the route is at $(0, 0)$ and the destination at $(500, 0)$. The standard deviation of the mutation in the 10 optimizations is set to 15. The fitness of the best solution: $C_e = \$27153.932$.

With regard to the population of the generations, an option to improve the algorithm could be to add random individuals throughout the iterations. This is also done in [29]. This is an alternative to mutations. It holds the same purpose: not getting stuck in local optima. However, it is possible that inserting random individuals in a generation may not work. The reason is that the random individual is likely to have lower fitness than the other, already existing individuals. Nonetheless, it can be worth it to explore this solution.

7.2.4. Multiple Optimizations

The final solution proposed to the problem at hand is to run multiple optimizations with the same settings and different initial guesses. This could work because the random individuals in the first generation affect the resulting best solution. This is shown in Figure 7.7. The best solutions of 10 optimizations with the same settings are presented. There is a clear difference between the outcomes.

An additional optimization can be run with the best solutions found in the performed optimizations. This optimization is then conducted with high-scoring individuals, which is thought to lead to an even better solution.

An attempt has been made to try the latter option. An example of the result is given in Figure 7.8. First, 10 optimizations were run with 100 individuals for 100 generations. Of which the results are shown in Figure 7.7. Then, the best solution for each of the 10 optimizations was taken and used as the initial guess for final optimization. The final optimization was done with a smaller value for the standard deviation because the initial guesses are more converged than the random individuals in the other optimizations. The resulting best solution for the final optimization is presented in Figure 7.8.

Comparing the outcome to Figure 7.2, it can be determined that a better result is found using this approach while the number of computed generations does not differ much. For the optimization in Figure 7.2, 1000 generations were computed. For the optimizations in Figure 7.7, each optimization was run for 100 generations. The final optimization also ran for 100 generations, totaling the number of generations to 1100. The functionality of this improvement most likely has to do with the fact that the convergence is largest in the first generations. More generations do not necessarily lead to an improved result. It is thought that this solution is promising, especially in combination with an extra stopping criterion and an improved usage of the mutation rates.

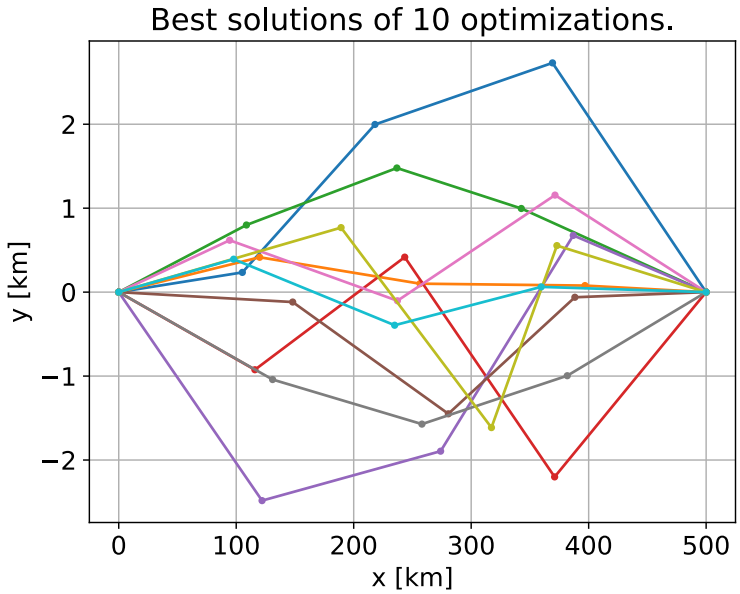

Figure 7.7: The best solutions of 10 optimizations after 100 generations are presented. The solutions consist of 5 nodes. A generation consists of 100 individuals. The origin of the route is at $(0, 0)$ and the destination at $(500, 0)$. The standard deviation of the mutation in the 10 optimizations is set to 15.

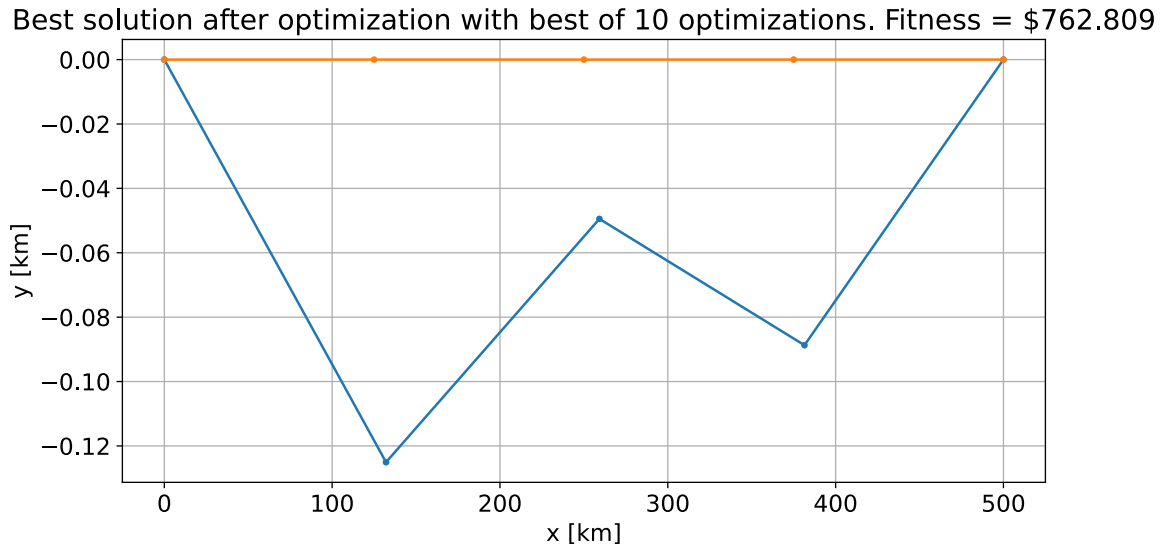

Figure 7.8: The optimal and best solution after an optimization with the best solutions of 10 optimizations. The 10 best solutions are found in Figure 7.7. The best solution is found after 100 generations. The solutions consist of 5 nodes. A generation consists of 10 individuals. The origin of the route is at $(0, 0)$ and the destination at $(500, 0)$. The standard deviation of the mutation in the final optimization is set to 0.5. The fitness of the best solution: $C_e = \$762.809$.

8

Future Plans

To answer the main research question as posed in Chapter 3 the subquestions should be answered. Questions 1a and b, 2a and e, and 3a, b, and c have been answered previously. Six subquestions remain unanswered. The goal of the remaining time for this research thesis is to answer these. Ultimately, formulating an answer to the main research question.

In this chapter, a description of the approach to answer all questions is given. In Section 8.1, the planned extensions of the optimization model are presented. A description of the proposed case study and sensitivity analysis is provided in Section 8.2. This section also includes information on the data that are required to perform these experiments and the results that are desired.

8.1. Model Extensions

When the basic model is performing as desired, the model can be expanded. This section presents a discussion on what the additions to the basic model are and how they are thought to be implemented. An overview of the constraints that will be imposed can be found in Section 8.1.6. An approach for the verification and validation of the model is also given.

8.1.1. Mass Constraint and Assumption

In the basic model, the mass of the aircraft is constrained by its initial value at 80% of the MTOW. In the final model, this initial value should depend on whether the aircraft is departing from or arriving at the airport. This affects the assumption that can be made on the initial mass. Also, a final boundary constraint should be included. It should be checked whether the mass does not fall below the operational empty weight (OEW). Ideally, it should be larger than the OEW as reserve fuel is required. The implementation of a variable mass will answer question 2d.

The course of the mass can be calculated using Equation 6.6 as described in Section 6.2.3. This is an iterative calculation and cannot be achieved through NumPy vectorization. It thus requires more computational steps. To simplify this, a constant mass flow will be assumed throughout the flight trajectory. Only for the best solution found at the end of the optimization, the accurate values of the mass at the nodes will be calculated. This simplification is expected to not influence the outcome of the model and is expected to decrease computation time. However, this should be ensured by verifying it with a simple case.

8.1.2. Variable Altitude and Velocity

As discussed in Chapter 6, the altitude and velocity of the flight are currently kept at a constant value. This way, the basic model could be verified easier.

The altitude will be allowed to vary just like the x and y values are. The standard deviation and mutation rate that are to be used in the mutation step for z will have to be determined.

Velocity is not a state that defines an individual. The combination of the positional values and Δt provides the velocity. See Equations 6.2 and 6.3 for the exact relationship. The velocity (both in

horizontal and vertical direction) in the basic model has a constant value; the value of Δt is varied such that the velocity stays the same.
In the complete model, Δt is allowed to vary completely. Question 2c will be answered with this implementation: in the generation of the first individuals, it will be assigned random values. Thus, the velocity over each segment will be different. The boundary values of Δt will have to be determined such that the aircraft will not stall or exceed its maximum velocity. Also, as is the case for z, a sufficient value for the standard deviation in the mutation step will have to be found.

8.1.3. Air Traffic Control Regulations

To complete the case study and to keep the model realistic, the regulations of ATC have to be implemented in the model. As described in Section 2.3, aircraft have to follow predetermined routes when departing from or arriving at an airport. These SID/STARs are to be added to the model.

The information on the waypoints of the routes will be included. When an aircraft is to follow a route, the trajectory will be forced to fly over the waypoints; path constraints will be employed. At most waypoints, the aircraft is required to comply with velocity and altitude constraints as well. These are also considered path constraints.

Additionally, a piece of airspace is sometimes considered a restricted area for aircraft. For instance, if military activities take place, commercial aircraft are not allowed to fly close by. It could also be that certain regions should be tried to be avoided. This could for example be following noise abatement procedures. Densely populated areas can be steered away from to limit noise nuisance. The model should include an option to include both cases.

The area that is to be avoided can be stored in the model. It should be checked whether a solution flies through this area. If this is the case, the solution should be assigned a penalty. This will result in a worse fitness, and should eventually lead to a near-optimal flight trajectory that complies with the path constraints. If this implementation functions, question 2e is answered.

8.1.4. Wind

In Section 2.2.3, a discussion on the implementation of wind in flight trajectory optimization of the literature is presented. As the wind can have a prominent effect on what is an optimal flight path, it should be included in this model. This was also suggested in question 2a. Multiple sources can be used to understand how to consider wind in the problem. These include [17, 29, 34, 45].

Currently, the plan is to assume a static atmosphere; the wind conditions will be taken at one point in time and will remain constant for the remainder of the optimization. This choice is made because a dynamic atmosphere is thought to become too complex. The static atmosphere is expected to still approach a realistic situation with a limited number of computations.

8.1.5. Variable Settings

As shown in Figure 6.5, the only stopping criterion currently included is that of a maximum number of generations. As suggested in the previous chapter, in the extension of the model, a criterion will be added that will stop the iteration when the best solution does not improve over a number of generations. After how many 'no improvement'-generations the optimization should stop should be determined through trial and error. This additional criterion will ensure that the optimization does not take longer than necessary.

An additional feature of the model should be a varying mutation rate. As described in Section 7.2, the developed model does not behave as expected. This is assumed to be in part caused by the mutation phase. Implementing a mutation rate that can decrease throughout the optimization should improve the performance of the model. Besides, the appropriate values of the mutation per state should be found.

One of the objectives of the research is to develop a customizable model. It can be beneficial for others and their purpose to easily adjust the settings and variables of the model. One of the options that should be adjustable is the airport which is evaluated. This influences the calculations concerning the CRS transformations and the search space.

Besides, the objective function should be customizable. For this research, the cost of emissions as established by Grobler et al. [1] is used. However, others may be interested in the mass of the emitted

species or another metric. Several options for the objective function should be included. Regarding the emission costs used currently, the costs are available for cruise and the landing and take-off cycle. These could be linearly interpolated to find the costs at the altitudes between these to more accurately calculate the cost of emissions.

At this time, the model can already allow different aircraft types in the model. This is, however, limited to the types available in OpenAP. As mentioned before, these include most commercial aircraft. The distance between nodes can also be altered. This allows the user to set a resolution on the flight trajectory. A trade-off is that a higher resolution results in a larger amount of time for the algorithm to finish.

8.1.6. Overview Constraints

This section provides a brief overview of the constraints that are to be included in the extended model.

Boundary constraints are imposed on all states. As is already implemented, the position of the first and final nodes are set to the origin and destination locations. For Δt, the initial value is always set to $0s$. The reason is that it describes the time it took to cover the past segment. The first node has no past segment, and therefore, its value should equate $0s$. The final value is not constrained. An additional constraint is imposed on the mass of the aircraft; the initial mass is set to a value and the final mass should be larger than the OEW.

The path constraints are imposed because of the ATC regulations as described in Section 8.1.3. If a given route is to be followed, the positions are constrained. The velocity, and thus Δt, can also be forced to a certain value at the waypoints. Besides, the path should not travel through restricted areas. Path constraints are imposed on the three positional states. As proposed in Section 7.2.1, a constraint regarding the heading of the flight path should also be added.

Additionally, dynamic constraints are imposed. These are present to guarantee that the flight path is achievable in terms of the aircraft's dynamics. As mentioned in Section 8.1.2, the velocity of the aircraft should not exceed its limit or be below its stall speed. This is also the case for the flight path angle. An increased flight path angle is caused by the increased vertical component of the velocity. The vertical speed should remain between certain boundaries as well. The reasoning is twofold: the aircraft should be able to perform the trajectory and the passengers inside should not experience an uncomfortable flight. The value of these boundaries should be explored in the literature before the constraints are implemented.

To ultimately determine the best flight trajectory in which all constraints are complied with, the individuals who violate any should be penalized. A penalty score should be added to the fitness of the individual. This will result in a lower probability of reproduction for individuals that do not comply with the constraints. The appropriate penalty score should be determined per constraint. This can be done using the found literature ([46]) on penalties in GAs.

8.1.7. Verification and Validation

The verification of the basic model can be done using the simple case presented in Chapter 7. After that, the extensions of the model will also have to be verified and validated. This is to ensure that the results are representative and useful. When the verification and validation proposed in this section are completed, questions 3d and e are answered.

The verification of the previously discussed elements that will be implemented can be done through unit tests. After each addition to the model, the intermediate results must be analyzed. This can be done by running the model with a small n_{pop} for a few generations. The results can be printed and/or visualized and checked. For example, for the restrictions of certain geographical areas, the trajectories and the restricted area can be visualized. It can then be checked if the model behaves as anticipated.

As mentioned before, the model can be partly verified through a comparison of the model and previously conducted studies. This is also how Yamashita et al. [45] verify their model. The model can be set up with similar conditions as other flight trajectory optimization studies. The results of this can be compared and analyzed. The conditions must be possible with the model. Contrails are for example not taken into account in this research. Thus, comparing the results with studies that do include contrails may provide a skewed perspective. For this form of verification, appropriate studies should be found.

Regarding validation, for the calculation of the emission cost, ideally, the results of a flight test are compared to those of the model. However, it is not deemed possible to find the exact flow of emissions during a flight. Besides, validating the complete model is considered to be impossible. It would require aircraft to fly all possible trajectories in the same conditions to determine which of these is environmentally optimal. This is not realistic.

8.2. Experiments

The research question can be answered by conducting an experiment in the form of a case study. This case study will test the capabilities of the final model. It will also determine whether it is possible to minimize the environmental impact during the climb and descent phase through trajectory optimization. The proposed experiment is described in Section 8.2.1.

Additionally, it has been identified in Chapter 2 that many uncertainties apply to the quantification of the environmental effects. To study this, a sensitivity analysis is suggested. This is explained in more detail in Section 8.2.2.

In Section 8.2.3, the information required to execute the experiments is described. It is stated where the data are expected to come from and how they may be used to find meaningful results. The latter will be discussed in Section 8.2.4. The section presents the expected results of the experiments and how they are to be visualized.

8.2.1. Case Study

During the case study, a comparison will be made between the performance of actual routes and optimized ones in terms of the environmental cost. The case study will be conducted for a single airport during a specified time interval. The airport and period have not been decided upon yet.

In the decision-making process, the complexity of the airport and its airspace have to be considered. To conduct the experiment in the allotted time, it is beneficial to choose an airport that does not have many runways and predetermined routes. Additionally, all information required on the airport for the experiment will have to be available. The necessary information is discussed in Section 8.2.3.

To determine the time interval of the experiment, it is also of utmost importance to possess the required data. This includes flight and wind information. For the results to represent a realistic image, no extreme events should take place in the time interval. These include among others storms and a reduced number of flights due to a pandemic. The period should be representative to show on average what reduction in environmental effects is achievable.

It should also be chosen what the search space of the case study is. There is a tendency toward a circle with the selected airport as the center. The radius will have to be determined. Possibly, the same search space as described in Section 6.2 can be employed. For departing aircraft, the trajectory will be analyzed from the airport to the point where the aircraft leaves the search space. For arriving aircraft, the trajectory is analyzed from the point where the aircraft enters the search space until arrival at the airport. Aircraft that fly within the search space, but do not depart from or arrive at the airport will not be considered. These aircraft do not climb or descent, but are merely flying in the cruise phase. They do not fall within the scope of this research.

To compare actual and optimal flight trajectories, the environmental effects of both should be determined. For the real flights, the flown trajectory should be represented by nodes as in the optimization model. This way, the same methodology can be used to determine the cost of emissions. To optimize the real flights, the origin and destination within the search space have to be defined. Between these points, possibly following the specified SID/STARs, the trajectory should be optimized. This results in a near-optimal cost of emissions for the flight. This should be repeated for all flights in the time interval. A sum can be taken over all flights such that the resulting cost of emissions for the near-optimal routes can then be compared to that of the real flights. From this analysis, the mitigation potential for environmental effects can be determined.

8.2.2. Sensitivity Analysis

One of the scientific gaps identified by Simorgh et al. [18] in a review on climate trajectory optimization is a missing study on uncertainties. It would be interesting to find the effect of the uncertainty in the climate metric on the resulting best solution of the model. A sensitivity analysis can be employed to

bridge part of the identified gap.

A simulation for a single trajectory with constant conditions and variables, except for a varying emission cost, should be run many times. The cost of emissions is allowed to vary according to its distribution. According to Grobler et al. [1], the emission costs are subject to large uncertainties. Data are available on these uncertainties of the specific species. It is expected that the near-optimal solution of the model changes with different costs of emissions. Also, its total cost of emissions will be altered. By running the optimization a large number of times, a distribution of the total cost of emissions of the trajectory should be identifiable.

8.2.3. Data

To execute the previously discussed experiments, several forms of data are required. This includes data on real flight trajectories, aircraft performance, wind, and air traffic regulations.

Real flight trajectory data are required and could be obtained from The OpenSky Network [1]. This information will be used to perform the case study and to compare the current situation to the optimized one. An appropriate choice should be made for the size and inclusion of data in the dataset. This has been discussed in Section 8.2.1. In conducted research, the use of The OpenSky Network for this purpose has been shown to work. For instance, Sun and Dedoussi [19] use data from the network to evaluate aviation emissions in Europe. The authors make use of Python packages pyopensky [53] and traffic [54]. To aid the process of the experiment, this could be done as well.

Also, data on the performance of aircraft are required. This will be available in OpenAP and includes information on the fuel usage and emission of gasses. The use of OpenAP has been discussed in Section 6.1. The data are available for many commercial aircraft types for different conditions like thrust setting and weight. It may be necessary to filter the real flight data on the available aircraft types in OpenAP.

Data on wind strength and direction are required as well; an adequate source for the wind data should be found. This depends on the location and date and time of the real flight trajectory data.

Lastly, information on air traffic regulations, such as airspace structure and the usage of SID/STARs, should be known for the location chosen. This information is often available from the country's air navigation service provider.

8.2.4. Desired Results

A final extension to the basic model is a meaningful visualization of the problem at hand. In this section, the desired results of the model and the experiments are presented. Visuals can aid in bringing across the message of the results.

For the model in general, the trajectories should be visualized with an actual map in the background. Currently, the individuals are simply displayed in an empty figure as nodes with connecting lines. The package Cartopy [51] can be used to better visualize the trajectories. An airport can be taken as the center of the graph and the flight trajectories can be displayed on top of the map. The visuals of the trajectories over the map could also include the restrictions imposed by ATC; the waypoints and the route to be followed can be shown.

Additionally, it could be beneficial to display the course of aircraft performance parameters. This could among others be the velocity (horizontal and/or vertical), flight path angle, and the mass of the aircraft. In these plots, the constraints described in Section 8.1.6 can also be visualized.

For the case study, it would be useful to display one or more real flight trajectories and the optimized version. This way, the trajectories can easily be compared. This is, however, not possible for all flights considered in the study. Thus, a boxplot or other statistical graphic can be used to demonstrate the effect of trajectory optimization on the total cost of emissions. Additionally, other differences can be presented. These can include, but are not limited to, the fuel usage and time flown.

The results of the sensitivity analysis should also be visually presented. This would be a figure that displays the distribution of total emission costs found in the analysis. The variation in these costs are

[1] `https://opensky-network.org`. Visited on Mar. 18, 2022.

due to the uncertainties present in the unit emission costs of Grobler et al. [1]. Besides, if a variety of near-optimal trajectories is found due to the variance in emission costs, this should be visualized. It could show a few of these different trajectories on top of a map.

9 Conclusion

Over the last years, an increase in literature on flight trajectory optimization for environmental objectives has occurred [7]. This is in line with the growing necessity of the aviation industry to become more sustainable [2]. This report explicated a research proposal and has demonstrated the potential of a model to answer the research question:

> How can flight trajectories be optimized to minimize the environmental impact of aviation during the climb and descent phase?

To answer this question, several subquestions have also been formulated. Throughout the research, these should be answered to formulate an answer to the main question. The subquestions are divided into three categories: environmental impact, flight trajectory, and optimization. The questions can be found in Chapter 3.

Some of the subquestions have been addressed in this report. These include decisions on the environmental effect and optimization methodology used in the research. The answers have been formed through the extensive literature study that is discussed in Chapter 2. The research will focus on minimizing the environmental costs of emissions. The emission costs of Grobler et al. [1] are used. These have been chosen because they encompass not only the climate effects of the emissions but also the societal effects. It comprises the environmental effect in the largest sense.

An optimization model will be employed to determine whether it is possible to minimize the environmental effect in the climb and descent phases of a flight. Therefore, both the lateral and vertical flight paths will be considered. A plan is proposed to implement wind, varying speed and mass, and the restrictions of ATC, such as SIDs and STARs, in the model. The research framework and planning are laid out in Chapter 4. How the features of the model will be added is discussed in Chapter 8.

The methodology that is used for the optimization model is a genetic algorithm. It has been chosen because it is intuitive and popular in sustainable flight trajectory optimization [18]. It is based on the evolution theory of Darwin [29]; the process entails the creation of a set of flight trajectories, evaluation of their fitness, crossover, and mutation of new trajectories, and an iteration of the last two phases. This should result in finding a near-optimal trajectory. The theory is further explained in Chapter 5.

A first, basic version of the model has been developed. The trajectory is only allowed to vary in the lateral direction and is flown at a constant speed. The implementation is described in more detail in Chapter 6, The basic model is not developed enough to be verified using a simple case. This is because the genetic algorithm does not converge (quickly) to the near-optimal solution.

In Chapter 7, the preliminary results are presented and suggestions are made for the improvement of the model. These recommendations include a correct implementation of the mutation phase and running multiple optimizations in parallel. The improvements have to be made before any features are added to the model.

When the extended model functions as expected, and is verified and validated, a case study and sensitivity analysis may be conducted. The experiments focus on finding an answer to the research question. In the proposed case study, the departing and arriving flights at one airport will be compared to the op-

timized flight trajectories to find out if and by how much the environmental footprint can be reduced. Realizing an open platform, in which such a trajectory optimization can be accessed by interested parties, can help accelerate the sustainability of aviation.

References

[1] C. Grobler et al. “Marginal climate and air quality costs of aviation emissions”. In: *Environmental Research Letters* 14.11 (Nov. 2019), p. 114031. DOI: 10.1088/1748-9326/ab4942.

[2] T. Ryley, S. Baumeister, and L. Coulter. “Climate change influences on aviation: A literature review”. In: *Transport Policy* 92 (June 2020), pp. 55–64. DOI: 10.1016/j.tranpol.2020.04.010.

[3] S.H.L. Yim et al. “Global, regional and local health impacts of civil aviation emissions”. In: *Environmental Research Letters* 10.3 (Feb. 2015), p. 034001. DOI: 10.1088/1748-9326/10/3/034001.

[4] L.E. Teoh and H.L. Khoo. “Green air transport system: An overview of issues, strategies and challenges”. In: *KSCE Journal of Civil Engineering* 20.3 (Apr. 2016), pp. 1040–1052. DOI: 10.1007/s12205-016-1670-3.

[5] EASA. *Updated analysis of the non-CO2 climate impacts of aviation and potential policy measures pursuant to EU Emissions Trading System Directive Article 30(4)*. Tech. rep. 1. Sept. 2020, pp. 6–116. URL: https://www.easa.europa.eu (visited on Feb. 22, 2022).

[6] C.G. Corlu et al. “Optimizing energy consumption in transportation: Literature review, insights, and research opportunities”. In: *Energies* 13.5 (Mar. 2020), p. 1115. DOI: 10.3390/en13051115.

[7] A.W.A. Hammad et al. “Mathematical optimization in enhancing the sustainability of aircraft trajectory: A review”. In: *International Journal of Sustainable Transportation* 14.6 (2020), pp. 413–436. DOI: 10.1080/15568318.2019.1570403.

[8] J. Ma et al. “Integrated optimization of terminal maneuvering area and airport”. In: *Sixth SESAR Innovation Days* (Delft, The Netherlands). Nov. 2016, p. 8. URL: https://www.sesarju.eu (visited on Feb. 16, 2022).

[9] Y. Cao et al. “Evaluation of fuel benefits depending on continuous descent approach procedures”. In: *Air Traffic Control Quarterly* 22.3 (July 2014), pp. 251–275. DOI: 10.2514/atcq.22.3.251.

[10] J.S. Fuglestvedt et al. “Transport impacts on atmosphere and climate: Metrics”. In: *Atmospheric Environment* 44.37 (Dec. 2010), pp. 4648–4677. DOI: 10.1016/j.atmosenv.2009.04.044.

[11] D.S. Lee et al. “The contribution of global aviation to anthropogenic climate forcing for 2000 to 2018”. In: *Atmospheric Environment* 244 (Jan. 2021), p. 117834. DOI: 10.1016/j.atmosenv.2020.117834.

[12] F.D.A. Quadros, M. Snellen, and I.C. Dedoussi. “Regional sensitivities of air quality and human health impacts to aviation emissions”. In: *Environmental Research Letters* 15.10 (Oct. 2020), p. 105013. DOI: 10.1088/1748-9326/abb2c5.

[13] G.P. Brasseur et al. “Impact of aviation on climate: FAA’s Aviation Climate Change Research Initiative (ACCRI) Phase II”. In: *Bulletin of the American Meteorological Society* 97.4 (Apr. 2016), pp. 561–583. DOI: 10.1175/BAMS-D-13-00089.1.

[14] S. Matthes et al. “Mitigation of non-CO2 aviation’s climate impact by changing cruise altitudes”. In: *Aerospace* 8.2 (Jan. 2021), p. 36. DOI: 10.3390/aerospace8020036.

[15] M.T. Lund et al. “Emission metrics for quantifying regional climate impacts of aviation”. In: *Earth System Dynamics* 8.3 (July 2017), pp. 547–563. DOI: 10.5194/esd-8-547-2017.

[16] S. Matthes et al. “Climate-optimized trajectories and robust mitigation potential: Flying ATM4E”. In: *Aerospace* 7.11 (Oct. 2020), p. 156. DOI: 10.3390/aerospace7110156.

[17] A. Gardi, R. Sabatini, and S. Ramasamy. “Multi-objective optimisation of aircraft flight trajectories in the ATM and avionics context”. In: *Progress in Aerospace Sciences* 83 (May 2016), pp. 1–36. DOI: 10.1016/j.paerosci.2015.11.006.

[18] A. Simorgh et al. “A comprehensive survey on climate optimal aircraft trajectory planning”. In: *Aerospace* 9.3 (Mar. 2022), p. 146. DOI: 10.3390/aerospace9030146.

[19] J. Sun and I. Dedoussi. “Evaluation of aviation emissions and environmental costs in Europe using OpenSky and OpenAP”. In: *Engineering Proceedings* 13.1 (Dec. 2021), p. 5. DOI: 10.3390/engproc2021013005.

[20] K.M. Bendtsen et al. “A review of health effects associated with exposure to jet engine emissions in and around airports”. In: *Environmental Health* 20.1 (Dec. 2021), p. 10. DOI: 10.1186/s12940-020-00690-y.

[21] J. Rosenow and H. Fricke. “Individual condensation trails in aircraft trajectory optimization”. In: *Sustainability* 11.21 (Nov. 2019), p. 6082. DOI: 10.3390/su11216082.

[22] WHO Regional office for Europe. *Environmental noise guidelines for the European Region*. 2018. URL: https://www.euro.who.int (visited on Feb. 23, 2022).

[23] V. Sparrow et al. “Aviation noise impacts white paper”. In: *2019 Environmental Report*. ICAO. 2019. Chap. 2, pp. 44–61. URL: https://www.icao.int (visited on Feb. 23, 2022).

[24] S. Stansfeld and C. Clark. “Health effects of noise exposure in children”. In: *Current Environmental Health Reports* 2.2 (Mar. 2015), pp. 171–178. DOI: 10.1007/s40572-015-0044-1.

[25] V. Grewe and K. Dahlmann. “How ambiguous are climate metrics? And are we prepared to assess and compare the climate impact of new air traffic technologies?” In: *Atmospheric Environment* 106 (Apr. 2015), pp. 373–374. DOI: 10.1016/j.atmosenv.2015.02.039.

[26] Y. Tian et al. “Cruise flight performance optimization for minimizing green direct operating cost”. In: *Sustainability* 11.14 (July 2019), p. 3899. DOI: 10.3390/su11143899.

[27] M. Zhang and A. Filippone. “Optimum problems in environmental emissions of aircraft arrivals”. In: *Aerospace Science and Technology* 123 (Apr. 2022), p. 107502. DOI: 10.1016/j.ast.2022.107502.

[28] H. Yamashita et al. “Newly developed aircraft routing options for air traffic simulation in the chemistry–climate model EMAC 2.53: AirTraf 2.0”. In: *Geoscientific Model Development* 13.10 (Oct. 2020), pp. 4869–4890. DOI: 10.5194/gmd-13-4869-2020.

[29] R.S.F. Patrón and R.M. Botez. “Flight trajectory optimization through genetic algorithms for lateral and vertical integrated navigation”. In: *Journal of Aerospace Information Systems* 12.8 (Aug. 2015), pp. 533–544. DOI: 10.2514/1.I010348.

[30] H.G. Visser and S. Hartjes. “Economic and environmental optimization of flight trajectories connecting a city-pair”. In: *Proceedings of the Institution of Mechanical Engineers, Part G: Journal of Aerospace Engineering* 228.6 (May 2014), pp. 980–993. DOI: 10.1177/0954410013485348.

[31] B. Kim et al. *Environmental optimization of Aaircraft departures: fuel burn, emissions, and noise*. Tech. rep. Pages: 22565. National Academies of Sciences, Engineering, Medicine, and Airport Cooperative Research Program, June 2013. DOI: 10.17226/22565.

[32] A.V. Rao. “A survey of numerical methods for optimal control”. In: *Advances in the Astronautical Sciences* 135 (Jan. 2010), p. 33.

[33] J. Zhou et al. “Optimization of arrival and departure routes in terminal maneuvering area”. In: *Sixth International Conference on Research in Air Traffic Management* (Istanbul, Turkey). May 2014, p. 4. URL: https://www.icrat.org/ (visited on Feb. 15, 2022).

[34] A. Franco, D. Rivas, and A. Valenzuela. “Optimal aircraft path planning in a structured airspace using ensemble weather forecasts”. In: *Eight SESAR Innovation Days* (Salzburg, Austria). Dec. 2018. URL: https://www.sesarju.eu (visited on Feb. 15, 2022).

[35] R. Dalmau. “Optimal trajectory management for aircraft descent operations subject to time constraints”. PhD thesis. Technical University of Catalonia, May 2019. URL: https://www.tdx.cat (visited on Apr. 16, 2022).

[36] J. Rosenow et al. “Impact of multi-critica optimized trajectories on European air traffic density, efficiency and the environment”. In: *Twelfth USA/Europe Air Traffic Management Research and Development Seminar 2017* (Seattle, Washington, USA). June 2017. URL: https://www.atmseminar.org (visited on Feb. 14, 2022).

[37] S.G. Park and J.P. Clarke. “Vertical trajectory optimization to minimize environmental impact in the presence of wind”. In: *Journal of Aircraft* 53.3 (May 2016), pp. 725–737. DOI: 10.2514/1.C032974.

[38] K. Riley et al. “A systematic review of the impact of commercial aircraft activity on air quality near airports”. In: *City and Environment Interactions* 11 (Aug. 2021), p. 100066. DOI: 10.1016/j.cacint.2021.100066.

[39] J.-P. Clarke et al. “Optimized profile descent arrivals at Los Angeles International Airport”. In: *Journal of Aircraft* 50.2 (Mar. 2013), pp. 360–369. DOI: 10.2514/1.C031529.

[40] ICAO. *Noise abatement procedures: review of research, development and implementation projects - discussion of survey results*. 1st ed. 9888. Montreal: ICAO, 2010. ISBN: 978-92-9231-665-5. URL: https://www.icao.int/ (visited on May 11, 2022).

[41] R. Dalmau and X. Prats. “How much fuel can be saved in a perfect flight?” en. In: *Sixth International Conference on Research in Air Traffic Management* (Istanbul, Turkey). May 2014, p. 8. URL: https://www.icrat.org/ (visited on Feb. 15, 2022).

[42] *Continuous Climb Operations (CCO) manual*. International Civil Aviation Organization (ICAO). Montréal, Quebec, Canada, 2013. ISBN: 9789292492557.

[43] M. Soler et al. “Framework for aircraft trajectory planning toward an efficient Air Traffic Management”. In: *Journal of Aircraft* 49.1 (Jan. 2012), pp. 341–348. DOI: 10.2514/1.C031490.

[44] K. White et al. “Noise annoyance caused by continuous descent approaches compared to regular descent procedures”. In: *Applied Acoustics* 125 (Oct. 2017), pp. 194–198. DOI: 10.1016/j.apacoust.2017.04.008.

[45] H. Yamashita et al. “Air traffic simulation in chemistry-climate model EMAC 2.41: AirTraf 1.0”. In: *Geoscientific Model Development* 9.9 (Sept. 2016), pp. 3363–3392. DOI: 10.5194/gmd-9-3363-2016.

[46] P. Nanakorn and K. Meesomklin. “An adaptive penalty function in genetic algorithms for structural design optimization”. In: *Computers & Structures* 79.29-30 (Nov. 2001), pp. 2527–2539. DOI: 10.1016/S0045-7949(01)00137-7.

[47] C.R. Harris et al. “Array programming with NumPy”. In: *Nature* 585.7825 (Sept. 2020), pp. 357–362. DOI: 10.1038/s41586-020-2649-2.

[48] J. D. Hunter. “Matplotlib: A 2D graphics environment”. In: *Computing in Science & Engineering* 9.3 (2007), pp. 90–95. DOI: 10.1109/MCSE.2007.55.

[49] J. Sun, J.M. Hoekstra, and J. Ellerbroek. “OpenAP: An open-source aircraft performance model for air transportation studies and simulations”. In: *Aerospace* 7.8 (July 2020), p. 104. DOI: 10.3390/aerospace7080104.

[50] PROJ contributors. *PROJ coordinate transformation software library*. Open Source Geospatial Foundation. 2022. DOI: 10.5281/zenodo.5884394.

[51] Met Office. *Cartopy: a cartographic python library with a matplotlib interface*. Exeter, Devon, 2015. URL: http://scitools.org.uk/cartopy.

[52] T. Blickle and L. Thiele. “A comparison of selection schemes used in genetic algorithms”. In: (1995), p. 67. DOI: 10.1162/evco.1996.4.4.361.

[53] J. Sun et al. “pyModeS: decoding Mode-S surveillance data for open air transportation research”. In: *IEEE Transactions on Intelligent Transportation Systems* (2019). DOI: 10.1109/TITS.2019.2914770.

[54] X. Olive. “traffic, a toolbox for processing and analysing air traffic data”. In: *Journal of Open Source Software* 4 (2019), p. 1518. DOI: 10.21105/joss.01518.

[55] *Sixth International Conference on Research in Air Traffic Management* (Istanbul, Turkey). May 2014.

A

Gantt Chart

The planning of the project can be found in the Gantt chart on the following pages. It is described in detail in Section 4.2. Note that the literature phase and the months leading up to this report are not included as these tasks have been completed. A template from Vertex42 [1] was used.

[1] https://www.vertex42.com. Accessed on 16 February 2022.

Project Start Date: 10-01-2022 1
Project Lead: Leanne van Dam

WBS	TASK	START	END	% DONE	WORK DAYS
2	**Modelling and programming**		-		-
2.1	Familiarize with programs	ma 14-03	zo 27-03	100%	10
2.2	Develop basic model	ma 21-03	vr 03-06	100%	55
2.2.1	Formulate problem	ma 21-03	vr 08-04	100%	15
2.2.2	Define problem in program	ma 11-04	vr 03-06	100%	40
2.2.3	Verify model	do 31-03	wo 06-04	100%	5
2.3	Extend and develop heuristic model	ma 11-07	vr 19-08	0%	20
2.3.1	Improve basic model	ma 20-06	vr 24-06	0%	5
2.3.2	Include wind	ma 11-07	zo 24-07	0%	6
2.3.2.1	Find and organize wind data	ma 11-07	di 12-07	0%	2
2.3.2.2	Implement wind	wo 13-07	zo 24-07	0%	3
2.3.3	Include variable speed	ma 25-07	di 26-07	0%	2
2.3.4	Include variable mass	wo 27-07	wo 27-07	0%	1
2.3.5	Include ATC regulations	do 28-07	vr 29-07	0%	2
2.3.6	Finalize model	ma 08-08	za 13-08	0%	5
2.3.7	Write model manual	ma 20-06	za 13-08	0%	25
2.3.8	Uncertainties/delays	ma 15-08	vr 19-08	0%	5
2.4	Verification	ma 11-07	za 13-08	0%	20
2.5	Validation	ma 11-07	za 13-08	0%	20
3	**Results and discussion**		-		-
3.1	Execute case study	ma 22-08	za 03-09	0%	10
3.1.1	Define case study	ma 22-08	di 23-08	0%	2
3.1.2	Find real flight trajectory data	wo 24-08	vr 26-08	0%	3
3.1.3	Execute case study	ma 29-08	za 03-09	0%	5
3.2	Execute sensitivity analysis	ma 05-09	vr 09-09	0%	5
3.2.1	Find uncertainty data	ma 05-09	di 06-09	0%	2
3.2.2	Execute sensitivity analysis	wo 07-09	vr 09-09	0%	3
3.3	Create meaningful results	ma 12-09	wo 14-09	0%	3
3.4	Analyze results	do 15-09	vr 16-09	0%	2
4	**Documentation**		-		-
4.1	Project plan	ma 14-02	zo 13-03	100%	20
4.1.1	Write project plan	ma 14-02	zo 13-03	100%	20
4.1.2	Plan thesis project	ma 14-02	za 26-02	100%	10
4.1.2.1	Determine project steps	ma 14-02	vr 18-02	100%	5
4.1.2.2	Create Gantt chart	do 17-02	za 26-02	100%	7
4.1.3	Implement feedback of peer review/supervisor	ma 21-03	di 22-03	100%	2
4.2	Preliminary (literature) study report	ma 14-03	do 16-06	100%	62
4.2.1	Write literature part	ma 14-03	ma 16-05	100%	40
4.2.2	Write model part	ma 11-04	do 16-06	100%	41
4.3	Preliminary meeting	do 23-06	do 23-06	0%	1
4.3.1	Prepare preliminary meeting	vr 17-06	wo 22-06	0%	4
4.3.2	Implement feedback of preliminary meeting	ma 11-07	do 14-07	0%	3
4.4	Thesis	ma 11-07	zo 23-10	0%	70
4.4.1	Write draft thesis	ma 11-07	vr 23-09	0%	50
4.4.2	Green light review	ma 10-10	ma 10-10	0%	1
4.4.2.1	Prepare green light review	ma 26-09	zo 09-10	0%	10
4.4.2.2	Implement feedback of green light review	di 11-10	zo 23-10	0%	9
4.4.3	Write final thesis	di 11-10	zo 23-10	0%	9
4.5	Defence	ma 07-11	ma 07-11	0%	1
4.5.1	Prepare presentation	ma 24-10	zo 06-11	0%	10
4.5.1.1	Prepare defence	ma 24-10	zo 06-11	0%	10
	Holidays		-		-
	Skiing + COVID infection	ma 31-01	vr 11-02	100%	10
	Florida	wo 27-04	wo 04-05	100%	6
	Biking	ma 27-06	zo 10-07	0%	10
	Drenthe	ma 01-08	zo 07-08	0%	5